

ABSTRACT

Title of Dissertation: **STRUCTURAL CHARACTERIZATION OF INTERACTION OF K11 AND K63 MIXED-LINKAGE POLYUBIQUITIN CHAINS WITH THE TANDEM UIMs OF EPSIN1**

Tanuja R. Kashyap, Doctor of Philosophy, 2016

Dissertation Directed By: Prof. David Fushman
Department of Chemistry and Biochemistry

Ubiquitylation or covalent attachment of ubiquitin (Ub) to a variety of substrate proteins in cells is a versatile post-translational modification involved in the regulation of numerous cellular processes. The distinct messages that polyubiquitylation encodes are attributed to the multitude of conformations possible through attachment of ubiquitin monomers within a polyubiquitin chain via a specific lysine residue. Thus the hypothesis is that linkage defines polyubiquitin conformation which in turn determines specific recognition by cellular receptors. Ubiquitylation of membrane surface receptor proteins plays a very important role in regulating receptor-mediated endocytosis as well as endosomal sorting for lysosomal degradation. Epsin1 is an endocytic adaptor protein with three tandem UIMs (Ubiquitin Interacting Motifs) which are responsible for the highly specific interaction between epsin and ubiquitylated receptors. Epsin1 is also an oncogenic protein and its expression is upregulated in some types of cancer. Recently it has been shown that novel K11 and K63 mixed-linkage polyubiquitin chains serve as internalization signal for MHC I (Major Histocompatibility Complex I) molecule through their association with the tUIMs of epsin1. However the molecular mode of

action and structural details of the interaction between polyubiquitin chains on receptors and tUIMs of epsin1 is yet to be determined. This information is crucial for the development of anticancer therapeutics targeting epsin1.

The molecular basis for the linkage-specific recognition of K11 and K63 mixed-linkage polyubiquitin chains by the tandem UIMs of the endocytic adaptor protein epsin1 is investigated using a combination of NMR methods. This study illustrates that branched K11 and K63 mixed-linkage polyubiquitin chains retain the structural properties of their K11 and K63 components. Epsin1 tUIMs bind monoubiquitin very weakly and they exhibit preferential binding to chains of different linkages, with the strongest affinity for K63-Ub₂ (K63-linked diubiquitin) followed by K11-Ub₂ and lastly K48-Ub₂. Epsin1 tUIM pair 23 binds avidly with a domain-specific orientation across K63-Ub₂, while epsin1 tUIM pair 12 binds both K11-Ub₂ and K63-Ub₂ with similar affinities. The linker region between the tUIMs is critical for linkage-dependent polyubiquitin recognition. Our results support the hypothesis that in addition to the length of the tUIM linker region, its composition also determines the selective recognition of K63-Ub₂. Epsin1 tUIMs do not distinguish between mixed-linkage branched and unbranched polyubiquitin chains. Our NMR binding studies carried out in the absence and presence of NaCl, revealed that in addition to the canonical hydrophobic patch residues of ubiquitin, electrostatic interactions play a major role in the molecular recognition of polyubiquitin by the tUIMs of epsin1. These results provide the first glimpse of the mechanism behind specific recognition of complex mixed polyubiquitin signals by a multivalent receptor with three tandem UIMs.

STRUCTURAL CHARACTERIZATION OF INTERACTION OF K11 AND K63
MIXED-LINKAGE POLYUBIQUITIN CHAINS WITH THE TANDEM UIMs OF
EPSIN1

By

Tanuja R. Kashyap

Dissertation submitted to the Faculty of the Graduate School of the
University of Maryland, College Park, in partial fulfillment
of the requirements for the degree of
Doctor of Philosophy
2016

Advisory Committee:
Professor David Fushman, Chair
Professor Douglas Julin
Professor George Lorimer
Professor Kwaku Dayie
Professor Sergei Sukharev, Dean's Representative

© Copyright by
Tanuja R. Kashyap
2016

Preface

The Ubiquitin Proteasome System (UPS) serves a critical role in regulating protein turnover in mammalian cells. The system is tightly regulated and any defects lead to the manifestation of pathogenesis. The crucial role of UPS in biology has been recognized by awarding the 2004 Nobel Prize in chemistry jointly to Aaron Ciechanover, Avram Herskho and Irwin Rose “for the discovery of ubiquitin-mediated protein degradation”. The UPS regulates a broad range of cellular processes covering all aspects of cellular function from cell cycle to host cell response to pathogens. There are two major roles of the UPS comprising attachment of mono or polyubiquitin chains to substrate proteins and their subsequent degradation in the 26S proteasome. Polyubiquitin is not only associated with protein degradation and antigen-peptide generation but also with non-degradative roles including DNA repair and endocytosis. This diversity in polyubiquitin signaling is attributed to the multitude of conformations that arise based on the linkage type between monomers in a chain.

This work is focused on investigating the dynamics of protein structure-function relationship in ubiquitin biology. A major part of this dissertation is aimed at understanding the molecular basis for the linkage-specific recognition of K11 and K63 mixed-linkage polyubiquitin chains by the tandem UIMs of the endocytic adaptor protein epsin1. Other chapters include the structural studies of K11-linked diubiquitin using NMR spectroscopy which revealed its unique interdomain interface that differs from the canonical K48 and K63-linked diubiquitins. Our attempts to

understand the molecular interactions between the anti-oncogenic protein ARF and the oncogenic protein Mdm2 revealed the complexity involved in the expression and purification of the zinc finger containing mammalian protein Mdm2 from *E.coli*. Studies using the redox protein thioredoxin as a model system to investigate substrate associated structural/ functional changes brought about by ubiquitylation, revealed a novel and unexpected high affinity interaction between thioredoxin and the E2 (ubiquitin conjugating enzyme) Cdc34b, suggesting cross-talk between two major signaling pathways in the cell- the ubiquitin proteasome system and redox regulation.

Acknowledgements

I express my sincere gratitude to my advisor Professor David Fushman for his guidance over the past few years. I thank him for his valuable inputs and for being very supportive throughout.

I thank my dissertation committee members for their helpful suggestions and review of my work. I thank my collaborators Dr. Allan Weissman, NCI and Dr. Ventzislava Hristova for their support with the Mdm2 project. I thank the NCI-UMD Partnership for Integrative Cancer Research for awarding me the CRTA pre-doctoral visiting fellowship that supported my research on Mdm2.

During my stay in the Fushman lab, I have had the opportunity to work with very good people. I convey my heartfelt thanks to Dr. Carlos Castaneda, for being my initial mentor and teaching me enzymatic polyubiquitin synthesis. I thank Dr. Rajesh Singh, for his helpful suggestions with my various projects as well as for sharing his cloning and crystallography expertise. I thank Dr. Daoning Zhang for his help with the resonance assignment of the tandem UIMs of epsin1. I thank Dr. Ming Yih-Lai for introducing me to some of the commonly used software in the lab. I thank Dr. Mark Nakasone for his resourcefulness and help with HADDOCK modeling. I thank Karina Herrera-Guzman for her generous help with collecting mass spectrometry data. I thank Dr. Urszula Nowicka, Apurva Chaturvedi and Adithya Sundar for their help with my various projects. I thank all of the past and present members of the Fushman lab especially, Dulith Abeycoon for the kind co-operation. I thank Dr. Maithili Saoji for her advice on cloning and crystallography.

I thank my husband Raghunath for making this journey possible for me and keeping my spirits up always. I appreciate all the encouragement from my family and friends, especially my parents for their enthusiasm. Special thanks to my son Arjun for his cheerfulness.

Table of Contents

Preface.....	ii
Acknowledgements	iv
List of Tables	viii
List of Figures.....	ix
List of Abbreviations	xi
Chapter 1: Introduction and specific aims	1
1.1 Ubiquitylation	1
1.1.1 The different topologies of ubiquitylation	2
1.2 Consequences of Ubiquitylation	6
1.2.1 Protein degradation/ recycling	6
1.3 Ubiquitin binding	11
1.4 Relevance of present work.....	15
Chapter 2: Structural characterization of interaction of K11 and K63 mixed-linkage polyubiquitin chains with the tandem UIMs of epsin1	20
2.1 Objectives	20
2.2 Solution NMR characterization of branched K11 and K63 mixed-linkage polyubiquitin chains.....	20
2.3 Epsin1 tUIMs bind monoubiquitin very weakly.....	22
2.4 Epsin1 tUIMs exhibit linkage-specific binding	26
2.5 Epsin1 tUIM- 23 binds avidly across K63-Ub ₂	30
2.6 Epsin1 tUIM-23 exhibits domain-specific binding across K63-Ub ₂	31
2.7 Epsin1 tUIM-12 binds both K11-Ub ₂ and K63-Ub ₂ with a similar affinity	34
2.8 The linker sequence between the UIMs is critical for linkage-dependent recognition of polyubiquitin	37
2.9 Epsin1 tUIMs do not directly interact with the isopeptide linker but they exhibit linkage-specific avidity	41
2.10 Epsin1 tUIMs do not distinguish between branched and unbranched mixed-linkage polyubiquitin chains	41
2.11 Electrostatic interactions play a major role in defining the interaction between epsin1 tUIMs and ubiquitin	44
2.12 Structural studies of epsin1 tUIMs	46
2.13 Summary	47
Chapter 3: Structural studies of K11-linked polyubiquitin chains	49
3.1 Background and Objective.....	49
3.2 Solution NMR characterization of K11-linked polyubiquitin chains	49
3.3 K11-Ub ₂ structure verification using site-directed spin labeling.....	51
3.4 Summary	52
Chapter 4: An attempt to understand the molecular interaction between the anti-oncogenic protein ARF and the oncoprotein Mdm2	54
4.1 Background and Objective.....	54
4.2 Interaction of UbcH5b with ubiquitin.....	55
4.3 Attempts to obtain stable Mdm2/MdmX RING proteins for solution NMR....	57
4.4 Cloning and expression of ARF.....	60
4.5 Summary	61

Chapter 5: Thioredoxin and ubiquitin proteasome system	63
5.1 Background and objective.....	63
5.2 Thioredoxin in solution.....	64
5.3 Invitro ubiquitination of thioredoxin using an E3 ligase- SlrP	64
5.4 Interaction of thioredoxin with Cdc34b	66
5.5 Summary	69
Chapter 6: Summary and scope for future studies.....	70
6.1 Structural characterization of interaction of K11 and K63 mixed-linkage polyubiquitin chains with the tandem UIMs of epsin1	70
6.2 Structural studies of K11-linked polyubiquitin chains	72
6.3 An attempt to understand the molecular interaction between the anti-oncogenic protein ARF and the oncoprotein Mdm2	73
6.4 Thioredoxin and ubiquitin proteasome system	74
Chapter 7: Methods and materials.....	76
7.1 Protein expression and purification	76
7.2 Synthesis of polyubiquitin chains	79
7.3 Chemical shift perturbation mapping.....	80
7.4 Determination of K_d by NMR titration experiments.....	80
7.5 Site-directed MTSL spin labeling experiments	81
Appendix.....	82
References.....	83

List of Tables

1.1 Physiological significance of the different linkage types of polyubiquitin	7
2.1 Dissociation constants for monoubiquitin binding to tUIMs of epsin1	24
2.2 Dissociation constants for diubiquitin binding to tUIMs of epsin1	26
2.3 Dissociation constants for diubiquitin binding to epsin1 tUIM-23	30
2.4 Dissociation constants for diubiquitin binding to epsin1 tUIM-12	35
2.5 Dissociation constants for diubiquitin binding to epsin1 tUIM-13	38
2.6 Dissociation constants for branched and unbranched K11 and K63 mixed-linkage triubiquitin binding to epsin1 tUIMs	42
2.7 Dissociation constants for ubiquitin binding to epsin1 tUIMs in the presence and absence of NaCl.	45
4.1 Plasmid constructs of human Mdm2 and MdmX used in the study	59
7.1 Protein constructs used in this work	77
i Dissociation constants of various ubiquitin chains for epsin1 tUIMs	82

List of Figures

1.1 The different topologies of Ubiquitin	3
1.2 Ubiquitylation Cycle.....	5
1.3 Ubiquitin hydrophobic patch	12
1.4 Domain organization of Epsin1	18
1.5 Epsin1 mediated endocytosis of MHC I	19
2.1 Chemical shift perturbation plots for distal domains in branched triubiquitin	22
2.2 Amino acid sequences for the different constructs of epsin1 tUIMs.....	24
2.3 Titration curves and CSP plots for monoubiquitin	25
2.4 Monoubiquitin binding to epsin1 tUIMs	26
2.5 Titration curves and CSP plots for diubiquitin	28
2.6 Diubiquitin binding to epsin1 tUIMs.....	29
2.7 Titration curves and CSP plots for diubiquitin	31
2.8 Effect of spin-labeling of epsin1 tUIM-23 on proximal and distal Ub in K63-Ub ₂	33
2.9 Sequence alignment of human RAP80 tUIM (80-124) and human epsin1 tUIM (183-252).....	34
2.10 Similar binding mode across K63-linked Ub ₂	34
2.11 Titration curves and CSP plots for different linkages of diubiquitin.....	35
2.12 Effect of spin-labeling of epsin1 tUIM-12 on proximal and distal Ub in K11-Ub ₂	37
2.13 Amino acid sequences for the different constructs of epsin1 tUIM-13	38
2.14 Titration curves and CSP plots for diubiquitin binding to epsin1 tUIM-13	39
2.15 Titration curves and CSP plots for K11 and K63 mixed-linkage triubiquitin binding to epsin1 tUIMs	43

2.16 K11 and K63 mixed-linkage triubiquitin binding to epsin1 tUIMs.....	44
2.17 Putative residues involved in ubiquitin-epsin1 tUIMs electrostatics.....	45
2.18 Promising conditions for optimization of crystallization of epsin1 tUIMs:K63-Ub ₂ complex.....	47
3.1 CSP plots for K11-Ub ₂	50
3.2 PRE effects from MTSL attached to I36C.....	52
4.1 NMR studies with UbcH5b.....	56
4.2 Binding surface for ubiquitin on UbcH5b	57
4.3 Schematic representation of Mdm2 domain organization	58
4.4 ¹ H- ¹⁵ N SOFAST-HMQC spectra of Mdm2.....	60
5.1 Mass chromatograms for thioredoxin	65
5.2 Ubiquitination of thioredoxin	66
5.3 Titration curves and CSP plot* for thioredoxin binding to Cdc34b	68
5.4 ¹ H- ¹⁵ N HMQC SOFAST spectra of thioredoxin binding to Cdc34b.....	68
7.1 Amino acid sequences of various epsin1 tUIM constructs.....	77
i CD spectrum of epsin1 tUIMs	82

List of Abbreviations

μg	micro gram
μM	micro molar
ADP	adenosine diphosphate
ATP	adenosine-5'-triphosphate
CD	circular dichroism
CP	core particle
CSP	chemical shift perturbation
CUE	coupling of ubiquitin conjugation to ER degradation
D ₂ O	deuterium oxide (heavy water)
Da	dalton (mass unit)
Ddi1	DNA damage inducible protein 1
DNA	deoxyribonucleic acid
DTT	dithiothreitol
DUB	deubiquitinase / deubiquitinating enzyme
<i>E. coli</i>	Escherichia coli
EGFR	epidermal growth factor receptor
ESCRT	endosomal sorting complex required for transport
H ₂ O	water
HECT E3	homologous to the E6-AP carboxyl terminus E3 ligase
HEPES	4-(2-hydroxyethyl)-1-piperazineethanesulfonic acid
HMQC	heteronuclear multiple quantum coherence
HSQC	heteronuclear single quantum coherence
JAMM/MPN+	JAB1/MPN/MOV34 metalloenzymes
K	lysine
K _d	equilibrium dissociation constant
kDa	kilodalton
LB	Luria broth
LUBAC	linear ubiquitin chain assembly complex
Lys	lysine
MBP	maltose-binding protein
MDa	megadalton
Mdm2	mouse double minute 2 homolog
mM	millimolar
MS	mass spectrometry
MTSL	1-oxyl-2,2,5,5-tetramethyl-3-pyrroline-3-methyl methanesulfonate
MWCO	molecular weight cut off
NEMO	NF-kappa-B essential modulator / IKK-γ

NF- κ B	nuclear factor- κ B
nm	nano meter
NMR	nuclear magnetic resonance
PAGE	polyacrylamide gel electrophoresis
PBS	phosphate buffered saline
PDB	protein data bank
PEG	polyethylene glycol
PMSF	phenylmethanesulfonylfluoride or phenylmethanesulfonyl fluoride
ppm	parts per million
PRE	paramagnetic relaxation enhancement
Pru	pleckstrin-like receptor for ubiquitin
RAP80	receptor associated protein 80
RING E3	really interesting new gene E3 ligase
RP	regulatory particle
rpm	revolutions per minute
RTK	receptor tyrosine kinase
SANS	small angle neutron scattering
SDS	sodium dodecyl sulfate
SOFAST	selective optimized-flip-angle short transient
SUMO	small ubiquitin-like modifier
TCEP	tris (2-carboxyethyl)phosphine
TLCK	tosyl lysine chloromethyl ketone hydrochloride
TOCSY	total correlation spectroscopy
Tris	2-amino-2-hydroxymethyl-propane-1,3-diol
tRNA	transfer RNA
Ub	ubiquitin
UBA	ubiquitin-associated domain
UBD	ubiquitin binding domain
UBL	ubiquitin like
tUIM	tandem ubiquitin interacting motif
UPS	ubiquitin proteasome system
USP	ubiquitin specific protease
WT	wild type

Chapter 1: Introduction and specific aims

1.1 Ubiquitylation

The essence of molecular biology is to understand the mechanisms underlying complex biological processes. Upon oversimplification, the eukaryotic cell can be thought of as a repository of signaling networks, molecular machines and organelles organized within the confines of a cellular skeleton and its surrounding plasma membrane¹. While the blueprint for this complex cellular organization is held in its relatively small genome, the vast proteome is the master architect. Post-translational modifications assist in bridging the gap between the genome and proteome. Post-translational modifications are chemical modification of a protein after ribosomal synthesis. Ubiquitylation refers to the attachment of a small, 76 amino acid, highly conserved protein called ubiquitin to substrate proteins². This process is one among several post-translational modifications occurring in eukaryotic cells including acetylation, phosphorylation, methylation, glycosylation, nitrosylation, lipidation etc. that regulate cell signaling and protein turnover³. It is one of the most versatile mechanisms resulting in a wide array of outcomes depending on the nature of attachment of ubiquitin to the substrate lysine residue^{4,5}. The attachment is usually via an isopeptide bond between the C-terminus of ubiquitin and ϵ -amino group of a lysine residue on the target protein. Both unanchored and substrate-anchored ubiquitin/polyubiquitin chains have signaling roles in the cell. The “canonical” polyubiquitin chains are K48- and K63-linked chains that have well-defined roles in targeting substrates for proteasomal proteolysis and signaling DNA repair, respectively⁴.

1.1.1 The different topologies of ubiquitylation

Polyubiquitin chains comprise 2 or more ubiquitin monomers, linked via an isopeptide bond between C-terminal glycine (G76) residue of one ubiquitin and ϵ -amino group of a lysine residue on another ubiquitin molecule. This highly stable protein has 7 lysine residues- K6, K11, K27, K29, K33, K48, and K63. Ubiquitin can also be attached to the N-terminus (Met1-) of another ubiquitin moiety to form linear chains or to other proteins as N-terminal ubiquitin fusions. Conventionally, the Ub moiety in unanchored polyubiquitin chains with free C-terminus is called the proximal domain (referring to its proximity while on the substrate) and the ubiquitin moiety that is attached to the lysine residue on another ubiquitin via its C-terminus, is referred to as the distal domain. Polyubiquitin chains formed via elongation through the same lysine residue are referred to as being homogeneous. However, if different linkages alternate at succeeding positions within a polyubiquitin chain, such chain is referred to as having mixed topology ⁶. Polyubiquitin chains comprising a single ubiquitin moiety with multiple lysine modifications are referred to as branched chains (figure 1.1). Polyubiquitin chains of all linkage types have been observed to occur *in vivo* at varying amounts based on the cell type and organism^{7,8,9}. The functional outcome of polyubiquitylation is linkage-specific ⁴ (table 1.1). The molecular basis for structural recognition of the polyubiquitin signals by cellular receptors is believed to be determined by the conformations polyubiquitin chains adopt^{4, 10}.

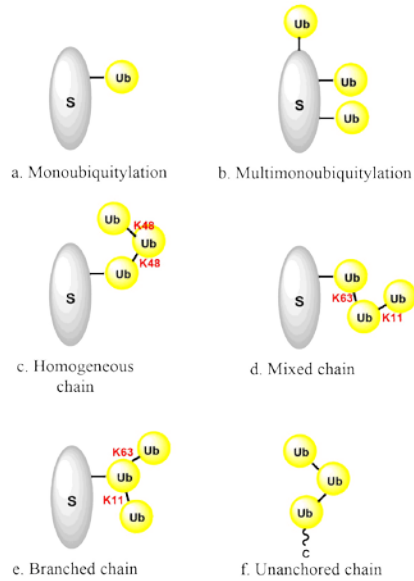


Figure 1.1 The different topologies of Ubiquitin

a) Monoubiquitylation, b) Multiple monoubiquitylation, c) Homogeneous ubiquitin chain, d) Unbranched mixed ubiquitin chain, e) Branched ubiquitin chain, f) Unanchored ubiquitin chain (adapted from⁶)

1.1.2 Ubiquitylation cycle

Ubiquitylation involves the concerted action of three different enzymes namely E1 ubiquitin-activating enzyme, E2 ubiquitin-conjugating enzymes, and E3 ubiquitin-protein ligases¹¹(figure 1.2). Ubiquitin is activated by E1 in an ATP-dependent reaction resulting in thioester formation at ubiquitin C-terminus. The Ubiquitin thioester is then transferred to the E2 active site cysteine. The E3 ligase associates with the E2~Ub thioester and the substrate, ultimately catalyzing the transfer of ubiquitin onto the substrate protein. The E2 enzyme is responsible for determining length, topology and processivity of polyubiquitin chains during assembly¹². Active E2s comprise a Ubiquitin-Conjugating (UBC) domain with a catalytic cysteine. E3 determines substrate specificity¹³. The human genome encodes 2 E1s, ~38 E2s and nearly 600-1000 E3 enzymes^{12,14}. The large number of E3s stems

from the need to specifically ubiquitylate a diverse array of substrates. Consequently E3s are implicated in numerous pathophysiological conditions¹⁵. There are 3 different classes of E3s characterized by conserved domains and mechanism of ubiquitin transfer to substrate¹⁶. RING (Really Interesting New Gene) family E3s bind simultaneously to both the E2~Ub and substrate and catalyze the direct transfer of ubiquitin onto the substrate¹⁴. HECT (Homology to E6AP C Terminus) and RBR (RING-between-RING) E3s catalyze a 2-step ubiquitin transfer reaction that involves transfer of ubiquitin from E2 onto an active site cysteine on E3 and then from E3 to the substrate^{17,18}.

Ubiquitylation is a dynamic and reversible process. De-Ubiquitylating enzymes (DUBs) cleave ubiquitin from proteins, proteasome-associated peptides, polymeric ubiquitin chains, fusion proteins and also process ubiquitin precursor polypeptides to maintain ubiquitin homeostasis in cells^{2,19}. DUBs are mostly cysteine proteases or metalloproteases. They are classified into five groups namely Ubiquitin C-terminal Hydrolases (UCHs), Ubiquitin-Specific Proteases (USPs), Ovarian Tumor proteases (OTUs), Josephins, and JAB1/MPN/Mov34 Metalloenzymes (JAMMs or MPN+)¹⁹. Some DUBS exhibit recognition and cleavage of ubiquitin chains with a particular linkage. Since they are implicated in an array of regulatory processes, they are good targets for drug therapy.

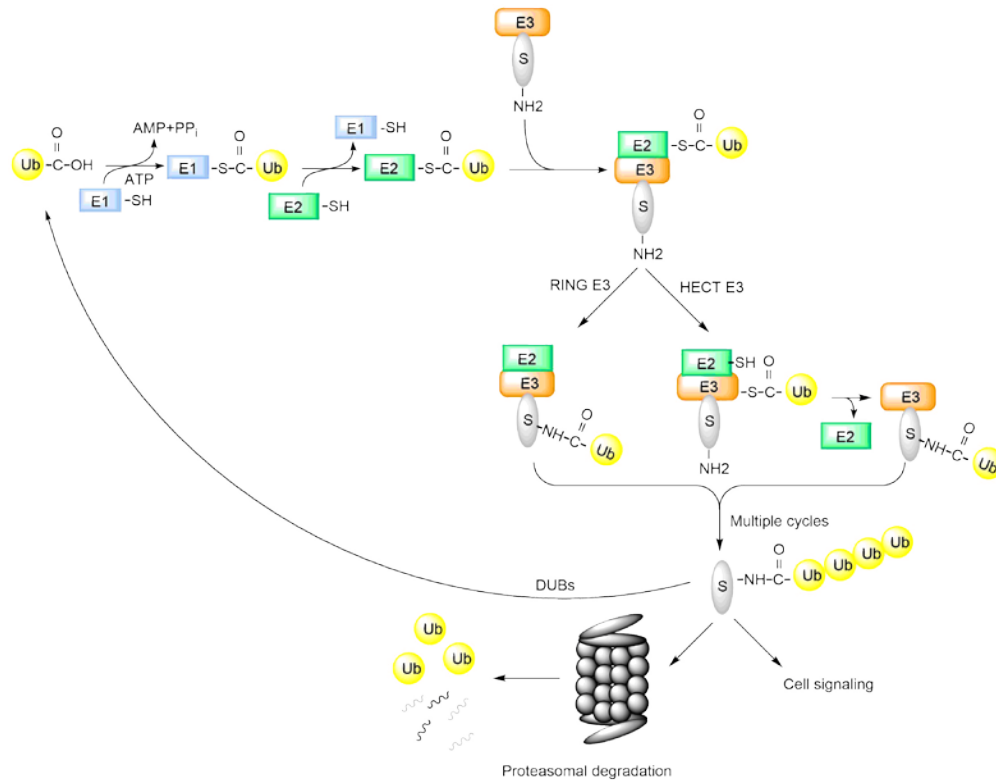


Figure 1.2 Ubiquitylation Cycle

Substrate proteins are ubiquitylated in a cascade of events involving ATP dependent activation of ubiquitin by an E1- Ub activating enzyme, followed by transfer to active site of E2- Ub conjugating enzyme and finally an E3 ligase mediates transfer of ubiquitin from E2 to substrate; The fate of the ubiquitylated substrate depends on the nature of the ubiquitin tag; DUBs play an important role in maintaining ubiquitin homeostasis in cells.

A class of proteins called ubiquitin-like proteins (UBLs) also utilize a similar enzymatic cascade (E1-E2-E3) resulting in post-translational modification of substrate proteins. The most well characterized UBLs are SUMO (Small Ubiquitin-like Modifier) and NEDD8 (Neuronal precursor cell Expressed Developmentally Downregulated protein-8). Most UBL attachments are transient. For instance, SUMO-specific proteases bring about desumoylation. Sumoylation is a key regulatory mechanism involved in virtually all cellular processes including chromatin organization, DNA repair, macromolecular assembly, protein homeostasis, trafficking

and signal transduction²⁰. NEDD8 is also not directly associated with proteolysis but it regulates E3 ubiquitin-protein ligases and covalently binds to Cullin family of E3 complexes²¹. UBL-protein modification seems to have evolved from prokaryotic systems²². Currently, ten distinct UBLs including ubiquitin have been demonstrated to covalently modify other macromolecules and several others are suspected to have a similar role²².

1.2 Consequences of Ubiquitylation

The ubiquitin proteasome system (UPS) comprises both substrate recruiting and degradation machinery. Although a major function of UPS revolves around protein turnover in cells, it also plays a crucial role in DNA repair, regulation of transcription, membrane trafficking, chromatin dynamics and protein kinase activation²¹ (table 1.1).

1.2.1 Protein degradation/ recycling

The majority of proteolysis occurring in cells is non-lysosomal and occurs by ATP dependent degradation through the UPS. The crucial component of the UPS is the 2.5 MDa protein complex- the proteasome, which is very abundant and stable. The proteasome complex comprises a 28 subunit core particle (CP, 20S proteasome) and the 19 subunit regulatory particle (RP, 19S proteasome). The 20S proteasome is a barrel-like structure made up of four stacked seven-membered rings, with the subunit stoichiometry $\alpha_{1-7}\beta_{1-7}\beta_{1-7}\alpha_{1-7}$ ²³.

Ubiquitin	Biological role
Monoubiquitylation	endocytosis ²⁴ , subcellular protein localization and trafficking ²⁵ , chromatin remodeling ²⁶
Multiple monoubiquitylation	receptor tyrosine kinase endocytosis and degradation ²⁵
Unanchored chains	activation of protein kinases ²⁷ , innate immune response to viral RNA ²⁸
K6 polyubiquitin chains	DNA repair (BRCA1 foci) ²⁹
K11 polyubiquitin chains	proteasomal degradation ³⁰ , misfolded proteins ⁸ , ERAD pathway ³¹
K27 polyubiquitin chains	innate immune response ³² , mediates mitophagy ³³
K29 polyubiquitin chains	UFD pathway ^{34,35} , inhibits wnt/ β -catenin signaling ³⁶ , regulation of mRNA stability ³⁷
K33 polyubiquitin chains	regulation of T-cell receptor activation ³⁸ , protein kinase regulation ³⁹ , protein trafficking ^{40,41}
K48 polyubiquitin chains	proteasomal degradation ^{42,43}
K63 polyubiquitin chains	DNA repair ⁴⁴ , inflammatory response (IKK, NF κ B) ⁴⁵ , protein trafficking (EGFR, MHC class I, TrkA), ribosomal protein synthesis (L28) ⁴⁶
Linear chains	NF κ B regulation ⁴⁷
Mixed chains	cell signaling ⁴⁸ , membrane trafficking ⁴⁹ and DNA damage response
Branched chains	improved signal for proteasomal degradation ⁵⁰
N-terminal ubiquitin fusion	proteasomal degradation ⁵¹

Table 1.1- Physiological significance of the different linkage types of polyubiquitin

The catalytic subunits of the 20S proteasome degrade proteins into a heterogeneous mixture of peptides⁵². The proteolytic active sites are located on the two inner β rings. The different β subunits of the 20S proteasome have unique catalytic roles. The $\beta 1$ subunit has caspase-like activity and cleaves peptide bonds after acidic residues. The $\beta 2$ subunit has trypsin-like activity and cleaves after basic residues. The $\beta 5$ subunit has chymotrypsin-like activity and cleaves after large hydrophobic residues²³.

The 19S regulatory particle is attached to either one or both ends of the 20S core particle, resulting in the 26S proteasome complex. The 19S particle can be further distinguished into the base and the lid. The base is composed of six AAA ATPase subunits (ATPases Associated with diverse cellular Activities, Rpt1-6 in *S.Cerevisiae*) and two large organizing subunits, Rpn1 and Rpn2; and two well-known ubiquitin receptors, Rpn10 and Rpn13. The lid comprises of a deubiquitinating enzyme Rpn11, its homologous non-catalytic binding partner Rpn8 and seven scaffolding subunits (Rpn 3, 5, 6, 7, 9, 12 and 15, also known as sem1)⁵³. The scaffolding subunits (except for sem1) contain protein-protein interaction motifs called PCI (Proteasome-CSN-eIF3) domains⁵³.

Entry of substrates into the 20S proteasome is regulated by the 19S proteasome, Rpn10, Rpn13 subunits and three proteasome-associated proteins-Rad23, Dsk2 and Ddi1(in yeast) that serve as ubiquitin receptors that shuttle ubiquitinated proteins to the proteasome (they are also known as UBL/UBA shuttle proteins due to their ubiquitin-like (UBL) and ubiquitin-associated (UBA) domains). Before substrate degradation, ubiquitin has to be removed and the substrate protein

has to be unfolded. De-ubiquitylation is brought about by Rpn11 in yeast (POH1 in humans) along with Ubp6 (Usp14 in mammals) and Uch37⁵⁴. Substrate unfolding and translocation is thought to be brought about by the six ATPases at the base of the 19S regulatory particle⁵⁴. In addition to several regulatory proteins such as cyclins, CDK (Cyclin-Dependent Kinase) inhibitors, IκB and p53 that are key substrates for the proteasome, misfolded and aberrant proteins are also proteasomal substrates. Protein degradation by the UPS is a tightly regulated process in normal cells.

K48 residue has long been recognized as the only essential lysine of yeast ubiquitin⁵⁵. Consequently the role of targeting proteins for proteasomal degradation was first assigned to K48-linked chains⁴². Several proteomic studies have indicated that K48 linkages are the most abundant type of ubiquitin chains in cells^{7,8}. Some examples for E3s synthesizing K48 linkages are SCF, gp78, E6AP etc.

K11-linked ubiquitin chains bind proteasomal receptors and target cell cycle regulators for proteasomal degradation during mitosis. The APC/C (Anaphase Promoting Complex) is the E3 responsible for the synthesis of K11-linked chains^{56,57}. Inhibition of APC/C halts the formation of K11-linked chains on its substrates resulting in cell cycle arrest⁵⁸. A recent study demonstrated that APC/C also generates branched polyubiquitin signals with multiple K11-linked segments, and these signals enhance substrate recognition by the proteasome⁵⁰. Thus K11-linked chains play a very important role in cell cycle progression.

K63-linked ubiquitin chains or even mixed chains have also been implicated to trigger proteasomal degradation⁵⁹⁻⁶¹. K29-linked ubiquitin chains are responsible for proteasomal degradation of substrates in the UFD (Ubiquitin Fusion Degradation)

pathway³⁵. The diversity in recognizing different chain topologies of ubiquitin chains on substrate proteins is due to the plasticity of the proteasomal subunits Rpn10 (S5a in humans) and Rpn13^{6,62,63}. However proteins targeted for proteasomal degradation are more frequently tagged with K48- or K11-linked ubiquitin chains. This could be due to either the transient nature of the other ubiquitin modifications through the action of DUBs, the efficient association of the specific E3s namely SCF (K48-linked chains) or APC/C (K11-linked chains) with the proteasome or that these chain types are less likely to introduce ubiquitin chain branching⁶.

1.2.2 Protein signaling

Apart from targeting proteins for proteasomal degradation, ubiquitylation of substrate proteins has a myriad of other roles in the cell (table 1.1).

Regulation of lysosomal degradation- Ubiquitylation is also implicated in regulation of protein degradation by lysosomes. Plasma membrane proteins are frequently monoubiquitylated or modified with K63-linked chains that promote endocytosis followed by lysosomal degradation⁶⁴. Ubiquitylated membrane proteins are recognized by ESCRT (Endosomal Sorting Complexes Required for Transport) complexes which also recognize the coat of endocytic vesicle, suggesting that colocalization of substrates and effectors determine the consequences of ubiquitylation⁶.

Regulation of protein-protein interactions- Monoubiquitylation of PCNA (Proliferating Cell Nuclear Antigen, a processivity factor for DNA polymerases) helps recruit Y family polymerases facilitating translesion synthesis⁶⁵. Modification of PCNA with K63-linked ubiquitin chain renders error-free DNA repair⁶⁶. K63 ubiquitin chains are essential for Double Strand Break (DSB) repair. These chains are

assembled in conjunction with the E2 complex MMS2 (Methyl Methane Sulfonate 2)-UBC13 complex and the E3 ligase Rad5 in yeast (RNF8 and RNF168 in humans), which further help recruit DNA damage bypass factors to enable replication past DNA lesions⁶⁶. K63 ubiquitin chains at sites of DNA repair are also recognized by Rap80 (Receptor Associated Protein 80) through its Ubiquitin Interacting Motifs (UIMs). Rap80 recruits BRCA1-A complex (consisting of Breast Cancer Associated Tumor suppressor BRCA1, Rap80, Abraxas, BRCC36, BRE and NBA1) thereby facilitating DSB repair⁶⁷⁻⁶⁹. Unanchored K63 chains are involved in activation of TAK1, IKK kinases²⁷ and eliciting innate immune response²⁸.

Regulation of protein activity- K48-linked polyubiquitylation of IκB (Inhibitor of NF-κB) by the E3 ligase SCF^{β-TRCP} targets it for proteasomal degradation thereby activating the transcription factor NF-κB⁷⁰. The UPS also functions in the regulated processing of peptides as seen in the case of p105 peptide required for activation of NF-κB⁷¹.

Regulation of protein localization- Monoubiquitylation can determine the intracellular localization of proteins as seen with the E2s UbcH6 and UBE2E2⁷². In case of the transcription factor p53, multimonoubiquitylation leads to nuclear export⁷³.

Thus ubiquitin serves as a versatile cellular signal involved in the regulation of a wide variety of processes.

1.3 Ubiquitin binding

Ubiquitin has a prominent hydrophobic patch comprising residues Leu8, Val70 and I44⁷⁴ (figure 1.3). This hydrophobic patch along with the flexible C-

terminal tail and the electrostatic potential caused by positive charges surrounding the hydrophobic patch (Lys6, Arg42, Lys48, His68 and Arg72) is very important for interaction with multiple cellular factors⁴. Polyubiquitin chains linked through different lysine residues serve as distinct signals in the cell and this is partially determined by the Ubiquitin Binding Domains (UBDs) or ubiquitin receptors that interact selectively to decipher the message⁷⁵. UBDs interact noncovalently with ubiquitin monomer or chains. Most of the UBDs bind at the hydrophobic patch on ubiquitin centered on Ile44. Additionally, there are two alternative patches on ubiquitin comprising hydrophobic residues Ile36, Leu71 and Leu73 and also Gln2, Phe4 and Thr12, which are very important in yeast^{55,75}. UBDs can be grouped into several subfamilies characterized based on their domain architecture.

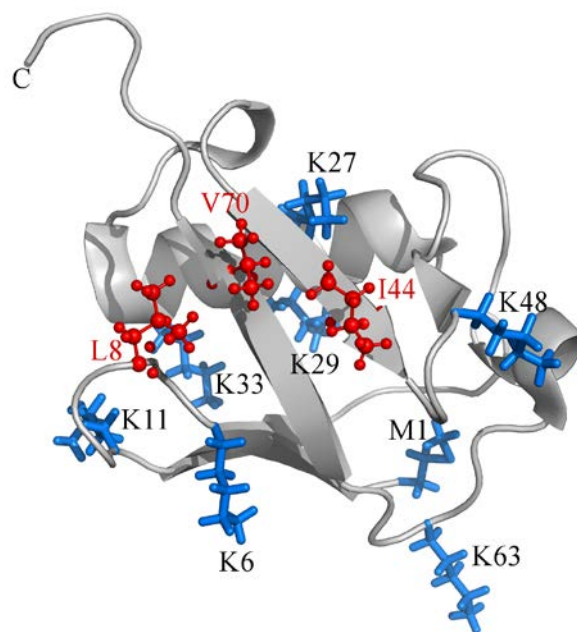


Figure 1.3 Ubiquitin hydrophobic patch

The canonical hydrophobic patch on ubiquitin is centered on Leu8, Ile44 and Val70 (figure generated from PDB entry 1D3Z, adapted from⁴)

UBDs with α -helices include the three-helix bundle containing UBA (Ubiquitin Associated Domains, example-Ddi), single α -helix containing UIM, often present in tandem (Ubiquitin Interacting Motif, example- Epsin1, Rap80, etc.), superhelix of eight α -helices- VHS (Vps27/Hrs/STAM) all of which interact with the canonical hydrophobic patch on ubiquitin⁷⁵.

UBDs with zinc fingers include NZF (Nuclear protein localization 4 Zinc Finger, example- HOIP, HOIL-1 Interacting Protein), ZnF UBP (Zinc Finger containing Ubiquitin Binding Protein, example USP5- Ubiquitin Specific Protease 5), etc.⁷⁵

Other examples for UBDs include those with a Pleckstrin Homology (PH) fold like the PRU (Pleckstrin-like Receptor for Ubiquitin, example Rpn13), UBC (Ubiquitin Conjugating) domains like UbcH5C, WD40 repeat β -propeller like Doa1, SH3 domains in amphiphysin, UBAN which is a parallel coiled-coil dimer present in NEMO⁷⁵, UBL (Ubiquitin Like domain) of Ddi1⁷⁶. Few characteristic mechanisms by means of which UBDs decode ubiquitin signals are discussed below.

Avidity and complex formation- It has been observed that the binding affinities for interaction between UBDs and ubiquitin is generally low (examples- yeast CUE2-1 (Coupling of Ubiquitin to ER degradation) and ubiquitin have a K_d of $155 \pm 9 \mu M$ ⁷⁷, Stam1 and Stam2 UIM and ubiquitin have a K_d of $\sim 200 \mu M$ ⁷⁸, the NZF domains in Npl4, Vps36-1, Vps36-2 and TAB2 bind to ubiquitin with a K_d of $\sim 100-400 \mu M$ ⁷⁹), which falls in line with the intracellular ubiquitin concentration ($\sim 85 \mu M$)^{75,80}. UBDs typically function together with additional localization and recognition signals that

help to recruit and retain ubiquitylated proteins in the appropriate biological pathway, and with effector domains that perform specific biological functions⁸¹. Many endocytic proteins contain multiple UIMs including epsins, Eps15⁸², Vps27 and STAM (Signal-Transducing Adaptor Molecule) and they associate with each other bringing their UBDs in close proximity thus enhancing complex formation. Epsin1 and Eps15 are adaptor proteins essential for receptor endocytosis and they have been shown to interact through their UIMs to facilitate internalization⁸³. Despite weak binding between the UIMs and monoubiquitin, polyubiquitin or oligomerization of ubiquitylated proteins and their receptors leads to high-avidity interactions⁷⁵. This has been observed with K63-linked polyubiquitin and Rap80⁸⁴. Different structural variations of UIM architecture (tUIMs-tandem UIMs, DUIM, MIU/ IUIM-inverted UIM) have been utilized in evolution to broaden the binding spectrum to diverse ubiquitin signals⁷⁵.

Activity modulation - As an example for this mechanism, we could consider the yeast transcription activator protein called Met4⁷⁵. This protein makes use of a combination of different UBDs including UIM and UIM-like domains, which stabilize Met4 with K48-linked chains⁸⁵. The UBDs regulate the length of the polyubiquitin modification such that instead of being targeted for proteasomal degradation, its ability to interact with promoters is lost⁸⁶.

Linkage selectivity- There are at least two modes of linkage-specific interaction between UBDs and polyubiquitin. Some show specificity towards the linkage between the ubiquitin monomers and interact directly with this segment, while others are specific to the spatial orientation of the two domains in ubiquitin

dimer. This linkage sensitivity leads to the diverse outcomes associated with ubiquitylation⁸⁷. HHR23A (Human Homologue of the yeast Rad23- Radiation Sensitivity Abnormal 23) UBA2 has binding preference for K48-linked chains over K63, K29-linked ubiquitin chains and monoubiquitin. The UBA2 binds to the canonical Ile44-centered hydrophobic patch on each ubiquitin along with the isopeptide bond connecting the individual ubiquitin monomers⁸⁸.

Rap80 has two tandem UIMs that interact selectively with K63-linked chains to recruit BRCA1 to sites of DNA double strand breaks. The short linker region between the two UIMs promotes interaction with K63-linked chains by positioning the UIMs for efficient avid binding. This type of recognition is termed linkage-specific avidity and it does not necessarily involve interaction with the isopeptide bond connecting the individual ubiquitin monomers⁸⁴.

However more structural analysis is needed to understand how ubiquitin receptors bind and decode ubiquitin chains in cells. This information will help address pathological conditions where the ubiquitin system is impaired.

1.4 Relevance of present work

This work is part of an attempt to understand the role of ubiquitylation in receptor endocytosis. More specifically it is targeted at gaining information regarding structural and mechanistic details of the interaction between polyubiquitin signals and the three tandem UIMs of the adaptor protein Epsin1.

Endocytosis is a regulatory mechanism for several membrane surface receptors. Ligand binding to membrane receptors triggers a cascade of signaling events which mediate several important cellular processes including proliferation,

differentiation, migration and survival⁸⁹. After signal initiation, receptors are mostly internalized and are routed to endosomes⁹⁰. Some receptors undergo clathrin-mediated endocytosis while others opt for clathrin-independent mechanisms⁹¹. Receptors can continue to signal in early endosomes and they are either recycled back to the plasma membrane or integrated into intraluminal vesicles (ILVs) of multivesicular endosomes (MVEs). MVEs target the enclosed receptors for lysosomal degradation resulting in signal termination⁹². The specificity of this process is important for regulating receptor signaling duration and to maintain cellular homeostasis in order to avoid prolonged or excessive activation of processes downstream of the receptor which could contribute to pathologies like cancer⁹¹.

Ubiquitylation of receptor proteins plays a very important role in regulating receptor endocytosis as well as endosomal sorting for degradation. Based on current understanding, the fate of receptors is determined depending on ligand concentration and the extent of ubiquitylation⁹¹. In case of the EGFR (Epidermal Growth Factor Receptor), low EGF concentrations leads to clathrin-mediated endocytosis of EGFR resulting in receptor recycling. Whereas, at high ligand concentrations, EGFR is ubiquitylated and this leads to clathrin-independent endocytosis followed by endosomal sorting into ILVs of MVEs, en route to lysosomal degradation⁸³. Several endocytic proteins involved in the regulation of early steps in endocytosis have UBDs including EPS15 (EGFR substrate 15), epsin1 (EPN1, EPS15 interacting Protein 1) and epsin2 (EPN2). They interact with the clathrin adaptor AP-2 complex at the plasma membrane to assemble clathrin-coated vesicles⁹¹. It has been observed that the functions of Eps15 and epsin1 are redundant in clathrin-independent endocytosis⁸³.

The ESCRT (Endosomal Sorting Complex Required for Transport) machinery plays a crucial role in sorting ubiquitylated receptors into MVEs and in MVE biogenesis⁹³. The ESCRT complex consists of four different subcomplexes (0, I, II and III) made up of several proteins with UBDs that allow the ESCRT machinery to capture and sort ubiquitylated receptors into MVEs.

Epsins are an evolutionarily conserved class of proteins, with ubiquitous expression of mammalian epsins 1 and 2 while epsin 3 is spatially and temporally expressed in migrating keratinocytes of the epidermis and parietal cells of the stomach⁹⁴. Epsins are multivalent proteins made up of several different interaction motifs (figure 1.4) that function cooperatively to target epsins to the plasma membrane and enable them to interact with and recruit cell surface receptors into clathrin-coated pits. Epsins have a highly conserved N-terminal domain- ENTH (Epsin N-terminal Homology) made up of α -helices which interact specifically with phosphatidyl-inositol (4,5) biphosphate. This interaction recruits epsin to the inner leaflet of the plasma membrane facilitating membrane curvature necessary for clathrin-coated pit formation⁹⁴. The clathrin-, AP2- and EH (EPS15 Homology)-binding domains are all unstructured and assist in routing epsin and ubiquitinated cargo to clathrin-coated pits for internalization. Epsin1 has three tandem UIMs, each 20 amino acids in length, predicted to have α -helical structure, with two linker regions (comprising five amino acids each) in between the dual tandem UIMs which are thought to be responsible for the highly specific interaction between epsin and ubiquitylated receptors. Epsins are also involved in regulating the activation of GTPases⁹⁵.

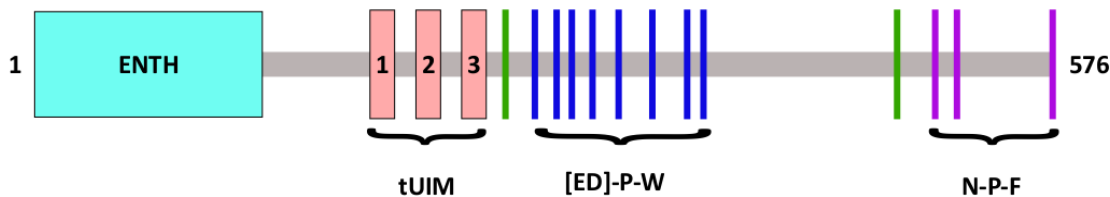


Figure 1.4 Domain organization of Epsin1

The schematic illustration shows the location of the different Epsin1 motifs including an ENTH (Epsin N-terminal Homology) domain (12-144), tUIMs (tandem Ubiquitin Interacting Motifs, UIM-1: 183-202, UIM-2: 208-227, UIM-3: 233-252), AP-2-binding Glu/Asp-Pro-Trp ([ED]-P-W) sequences (blue bars), clathrin-binding sequences (green bars) and EH domain-binding Asn-Pro-Phe (N-P-F) triplets (pink bars) (adapted from ⁹⁶)

Epsin expression is upregulated in several types of cancer suggesting its role as an oncogenic protein⁹⁷. Epsins have been implicated in tumor cell proliferation, tumor cell migration and tumor angiogenesis⁹⁴. In the context that epsins have been reported to alter seemingly different signaling cascades, it is important to note the specificity with which they operate during internalization of ligand-dependent ubiquitinated receptors. Therefore epsins may serve as a favorable target for future anticancer therapeutic development⁹⁴.

Recently it has been shown that novel K11 and K63 mixed-linkage polyubiquitin chains serve as internalization signal for MHC I (Major Histocompatibility Complex I) molecule through their association with the UIMs of epsin1^{49,98} (figure 1.5). However the molecular mode of action and structural details of the interaction between polyubiquitin chains on receptors and tUIMs of epsin1 is yet to be determined⁹¹. This information is crucial for the development of anticancer therapeutics.

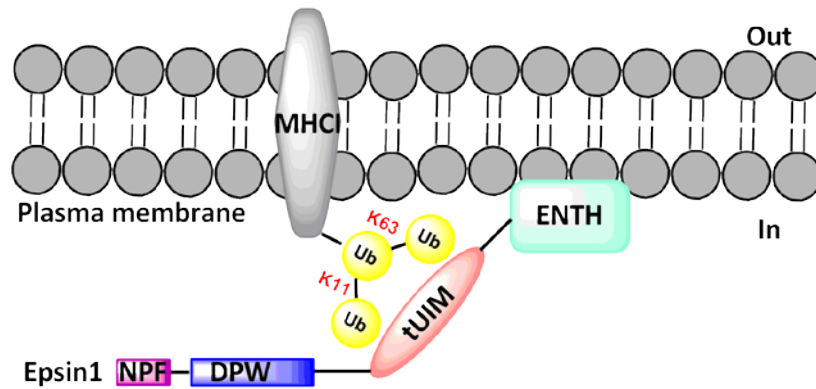


Figure 1.5 Epsin1 mediated endocytosis of MHC I

The immunoreceptor MHC I (Major Histocompatibility Complex I) is internalized upon ubiquitylation with a unique K11 and K63 mixed-linkage polyubiquitin chain which associates with the tandem UIMs of the adaptor protein Epsin1. ENTH- Epsin N-terminal Homology domain; UIM- Ubiquitin Interacting Motif; DPW- Aspartate-Proline-Tryptophan containing central region housing clathrin- and AP-2-binding domains; NPF- Asparagine-Proline-Phenylalanine containing C-terminal region housing Eps15 Homology (EH) protein binding domains; Ub- ubiquitin (adapted from⁹⁴)

The objective of this work is to understand the role of complex mixed polyubiquitin signals in endocytosis. The molecular basis for the linkage-specific recognition of K11 and K63 mixed-linkage polyubiquitin chains by the tandem UIMs of the endocytic adaptor protein epsin1 is investigated.

Chapter 2: Structural characterization of interaction of K11 and K63 mixed-linkage polyubiquitin chains with the tandem UIMs of epsin1

2.1 Objectives

This study aims to address the following questions:

1. Does K11 and K63 mixed-linkage polyubiquitin chain confer a unique physiological conformation that is different from either homogeneously K11 or K63-linked polyubiquitin chains?
2. What is the mode of interaction between epsin1 tUIMs and K11 and K63 mixed-linkage polyubiquitin chains?
3. Do the epsin1 tUIMs distinguish K11- from K63-linkage within a polyubiquitin chain and how?

2.2 Solution NMR characterization of branched K11 and K63 mixed-linkage polyubiquitin chains

It is widely accepted that diversity in polyubiquitin chain function is due to the differential recognition of differently linked chains in the cell⁹⁹. Currently, complex polyubiquitin signals including mixed chains with ubiquitin monomers linked heterogeneously are poorly understood. Nevertheless evidence for the existence of complex polyubiquitin signals *in vivo* has been mounting^{49,61,98,100,101}. It has been established using quantitative mass spectrometry that efficient internalization of MHC I molecules is dependent on K11 and K63 mixed-linkage polyubiquitin chains^{49,98}.

Recently, it has been illustrated that mixed-linkage chains retain the signaling properties of their K48 and K63 components and these multiple signals can be recognized by multiple linkage-specific receptors¹⁰⁰. In this context, it is of interest to determine whether branched K11 and K63 mixed-linkage polyubiquitin chains adopt distinct conformations in solution in comparison with K11 or K63-linked components.

Branched K11 and K63 mixed-linkage triubiquitin was generated enzymatically incorporating selective ¹⁵N isotope labeling on one ubiquitin domain at a time, generating each linkage in a stepwise manner^{102,103}. Chemical shift mapping using NMR was used to identify whether there were deviations in the mixed trimer with respect to K11 or K63-Ub₂. Chemical shifts for the amide backbone residues were compared between the corresponding ¹⁵N enriched K11 and K63 segment in the mixed-linkage trimer and ¹⁵N labeled K11-Ub₂, and K63-Ub₂ respectively, under identical NMR experimental conditions (20 mM sodium phosphate, 130 mM NaCl, pH 6.8 at 310 K). The ¹⁵N enriched ubiquitin domain in the polyubiquitin schematic is shown in red while the unlabeled ubiquitin domain is shown in yellow here (figure 2.1) and throughout the document. No significant perturbations were observed for both K11 and K63-linked segments in the trimer in comparison with the respective Ub₂. This suggests that the relative conformation of the K11 and K63-linked segments in the branched mixed-linkage trimer do not differ from K11-Ub₂ and K63-Ub₂ respectively. Also it means that the two distal domains do not interact with each other.

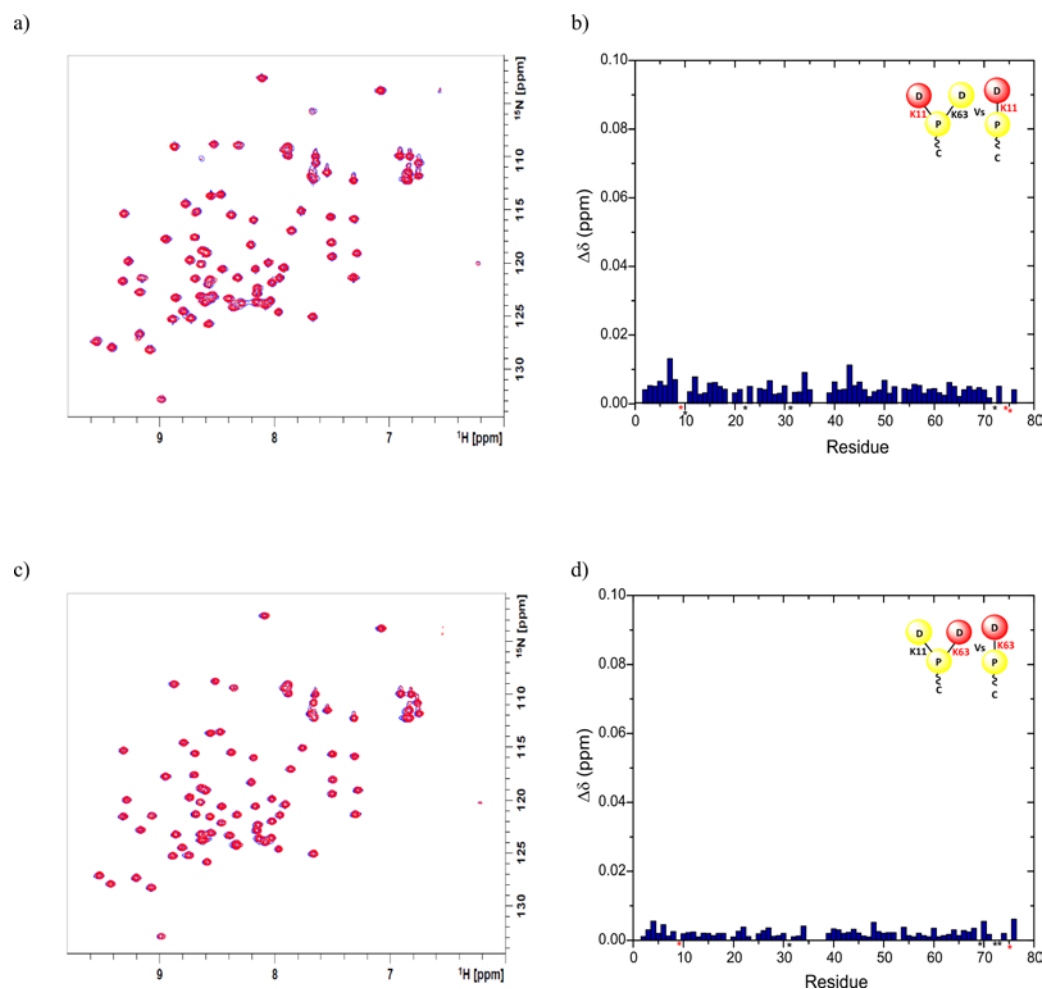


Figure 2.1 Chemical shift perturbation plots for distal domains in branched triubiquitin

a) Overlay of spectra for the distal domain linked via K11-linkage in branched K11 and K63 mixed-linkage triubiquitin (blue) with respect to K11-Ub₂ (red) and the corresponding CSP plot in b; c) overlay of spectra for the distal domain linked via K63-linkage in branched K11 and K63 mixed-linkage triubiquitin (blue) with respect to K63-Ub₂ (red) and the corresponding CSP plot in d. Overall the CSPs are insignificant as illustrated by the spectral overlays, indicating no deviation in the 3D conformation with respect to Ub₂. * Overlapping residues; * residues with weak/no signal intensity.

2.3 Epsin1 tUIMs bind monoubiquitin very weakly

The relative importance of mono- versus polyubiquitination and the role of specific types of polyubiquitin linkages in endocytic trafficking remain controversial¹⁰⁴. In order to investigate the possibility of recognition of monoubiquitin by the tUIMs of epsin1, ¹⁵N labeled K11RK63R monoubiquitin

mutant was utilized (since this mutant constitutes the distal monomeric Ub unit utilized in the enzymatic synthesis of the branched trimer; evidence from our earlier studies indicate that the mutation does not alter the conformational properties of polyubiquitin chains¹⁰⁵). NMR titration experiments were performed and the average K_d (apparent dissociation constant) derived using a 1:1 stoichiometry binding model was determined to be $320 \pm 53 \mu\text{M}$ in the absence of NaCl (figure 2.3-a,b) and $3700 \pm 775 \mu\text{M}$ in the presence of 130 mM NaCl (figure 2.3-c,d), from chemical shift perturbations in monoubiquitin. This is in agreement with the weak dissociation constants previously reported for other UIMs^{84,106}.

In order to dissect which of the epsin1 tUIMs specifically recognize the different linkage types in K11 and K63 mixed-linkage polyubiquitin chains, deletion mutants of epsin1 tUIMs were designed, deleting one UIM at a time. The two deletion mutants of epsin1 tUIMs were also assessed for their affinity for monoubiquitin. The average K_d of the binding event between ¹⁵N labeled K11RK63R monoubiquitin and epsin1 tUIM-12 (UIM-3 deleted, figure 2.2b) was determined to be $4546 \pm 490 \mu\text{M}$ (figure 2.3-e,f). The apparent K_d for monoubiquitin binding to epsin1 tUIM-23 (UIM-1 deleted, figure 2.2c) was found to be $2558 \pm 350 \mu\text{M}$ using a 1:1 binding model (figure 2.3-g,h).

These results agree with previous reports^{96,107} that there is extremely poor affinity of epsin1 tUIMs for monoubiquitin (table 2.1) and indicate that monoubiquitination of receptor proteins may not serve as a signal for receptor internalization through epsin1. Another important effect to be noted is the abolition of

monoubiquitin binding in the presence of 130 mM NaCl (figure 2.4), suggesting an essential role for electrostatic interactions between the tUIMs and ubiquitin.

Protein	Ligand	NaCl (mM)	K _d (μM)*
¹⁵ N K11RK63R Ub	epsin1 tUIMs	0	320 ± 53
¹⁵ N K11RK63R Ub	epsin1 tUIMs	130	3700 ± 775
¹⁵ N K11RK63R Ub	epsin1 tUIM-12	130	4546 ± 490
¹⁵ N K11RK63R Ub	epsin1 tUIM-23	130	2558 ± 350

Table 2.1- Dissociation constants for monoubiquitin binding to tUIMs of epsin1

* The errors in K_d values are the standard errors of the mean over multiple residues

a) Epsin1 tUIMs

QSSGEEELQLQLALAMSKEEADQPPSCGPEDDAQLQLALSLSREEHDKEERIRRGDDLRLQMAIEESKRETGGKEES

b) Epsin1 tUIM-12

QSSGEEELQLQLALAMSKEEADQPPSCGPEDDAQLQLALSLSREEHDKEERIRR

c) Epsin1 tUIM-23

PSCGPEDDAQLQLALSLSREEHDKEERIRRGDDLRLQMAIEESKRETGGKEES

Figure 2.2 Amino acid sequences for the different constructs of epsin1 tUIMs -UIMs are highlighted in yellow and the linker regions are in grey.

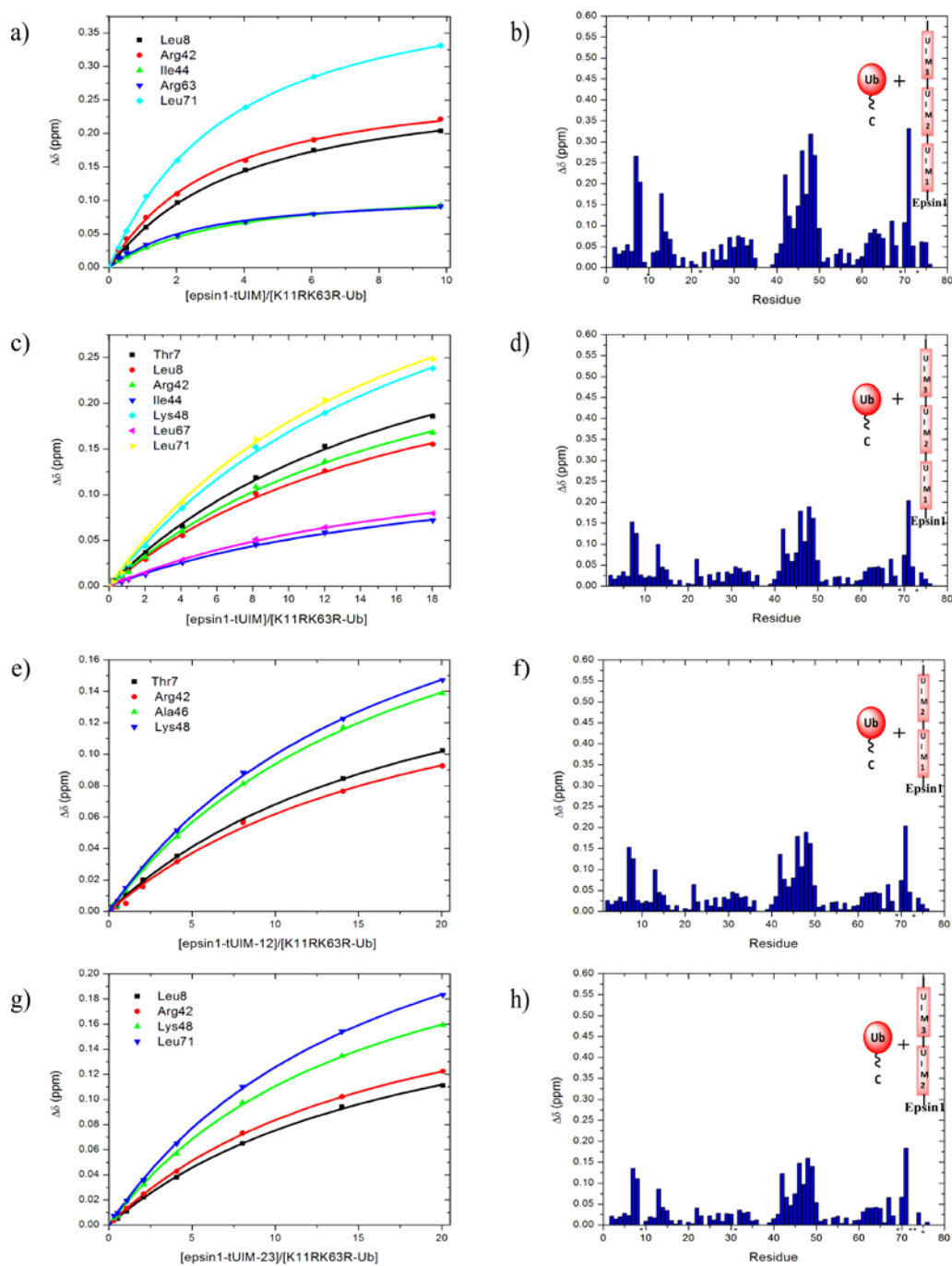


Figure 2.3 Titration curves and CSP plots for monoubiquitin binding to epsin1 tUIMs in the absence (a and b) presence of 130 mM NaCl (c and d); with epsin1 tUIM-12 (e and f) and epsin1 tUIM-23 (g and h) in the presence of 130 mM NaCl. * indicates overlapping residues or residues with weak signal intensities; protein concentration at the beginning of titration in a), c), e), g) was uniformly 100 μ M; protein concentration at the end of titration was a) 61.4 μ M, c) 66.7 μ M, e) 61.5 μ M and g) 69.6 μ M.

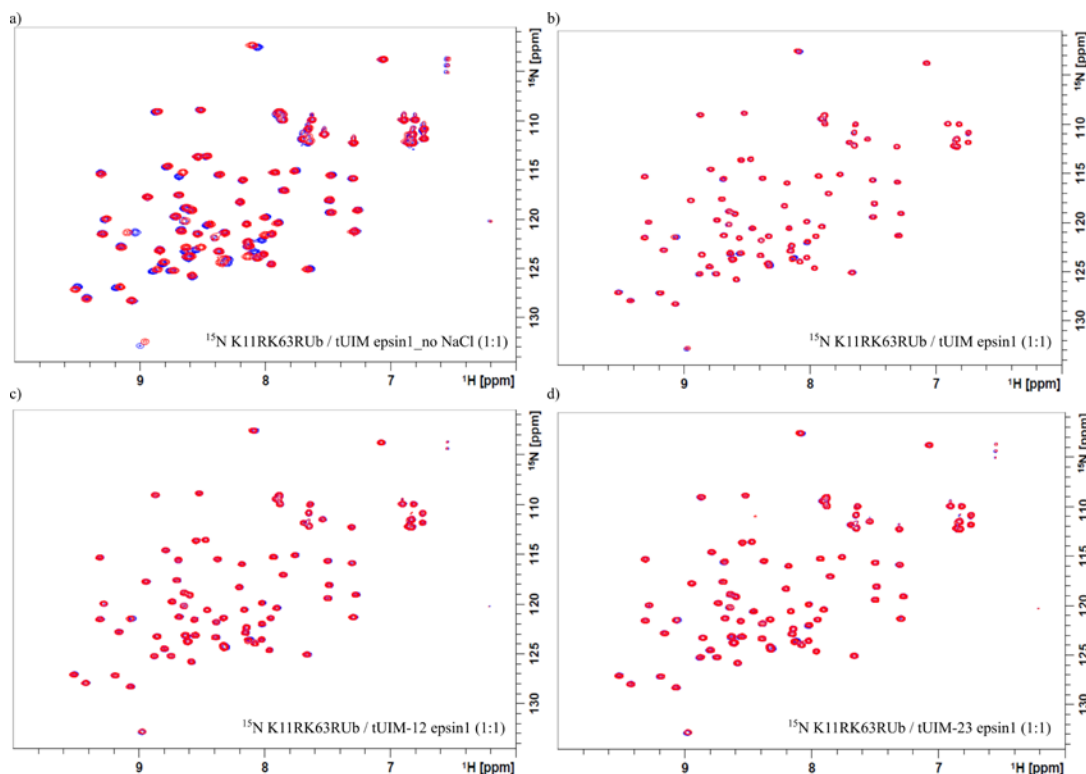


Figure 2.4 Monoubiquitin binding to epsin1 tUIMs- Overlay of monoubiquitin spectra in the absence (blue) and presence of epsin1 (red) a) tUIMs in the absence of NaCl; b) tUIMs, c) tUIM-12 and d) tUIM-23 in the presence of 130 mM NaCl.

2.4 Epsin1 tUIMs exhibit linkage-specific binding

In light of an earlier study suggesting that epsin1 tUIMs show linkage specificity to K63-Ub₂¹⁰⁸, we wanted to determine the affinity of this interaction and investigate if the tUIMs show selectivity towards either K11-Ub₂ or K48-Ub₂. We determined the affinities of K11-Ub₂, K63-Ub₂ and K48-Ub₂ for tUIMs of epsin1 from NMR titration experiments in 20 mM sodium phosphate, 130 mM NaCl, pH 6.8 at 310K.

Protein*	Ligand	NaCl (mM)	K _d (μM)	K _d (μM) [†]
¹⁵ N-D-K63 Ub ₂	epsin1 tUIMs	130	88 ± 17	89
¹⁵ N-D-K11 Ub ₂	epsin1 tUIMs	130	411 ± 87	294
¹⁵ N-D-K48 Ub ₂	epsin1 tUIMs	130	803 ± 98	835

Table 2.2- Dissociation constants for diubiquitin binding to tUIMs of epsin1

*¹⁵N-D indicates ¹⁵N-enriched distal Ub in Ub₂; [†] K_d determined using Kdfit global analysis

The apparent K_d for different diubiquitins binding to tUIMs of epsin1 determined based on a 1:1 binding model (figure 2.5) is listed in table 2.2. The affinity for K63-Ub₂ is by far the strongest interaction among other diubiquitins tested and reiterates the linkage selectivity exhibited by epsin1 tUIMs (similar to RAP80 tUIM^{84,108}) for this chain type. The affinity for K11-Ub₂ is intermediate between that for K63-Ub₂ and K48-Ub₂ (figure 2.6). The K_d value for K48-Ub₂ is similar to that for monoubiquitin binding to the tUIMs (table 2.1), indicating that K48-Ub₂ utilizes only one UIM and therefore the interaction is not avid. However, the smaller K_d values for both K63-Ub₂ and K11-Ub₂ in comparison to that of monoubiquitin (table 2.1) suggests an avid interaction, involving the simultaneous binding of both domains to tUIMs. The avid interaction with K63 and K11-Ub₂ falls in line with recent findings indicating that K11 and K63 mixed-linkage polyubiquitin chains interact with tUIMs of epsin1 during MHC I internalization^{49,98}. It is interesting to note the correlation with RAP80 tUIM. RAP80 tUIM also binds preferentially to K63-Ub₂ ($K_d = 22 \mu\text{M}$) tighter than K48-Ub₂ ($K_d = 157 \mu\text{M}$)⁸⁴. The affinity for distal domain of K11-Ub₂ is $134 \mu\text{M}$, while the affinity for the proximal domain is $68 \mu\text{M}$ ¹⁰⁵. Overall, both RAP80 tUIM and epsin1 tUIMs exhibit similarity in their binding preferences.

We further investigated the structural basis for the linkage-specific interaction of epsin1 tUIMs with K63 and K11-Ub₂ as described in the sections below.

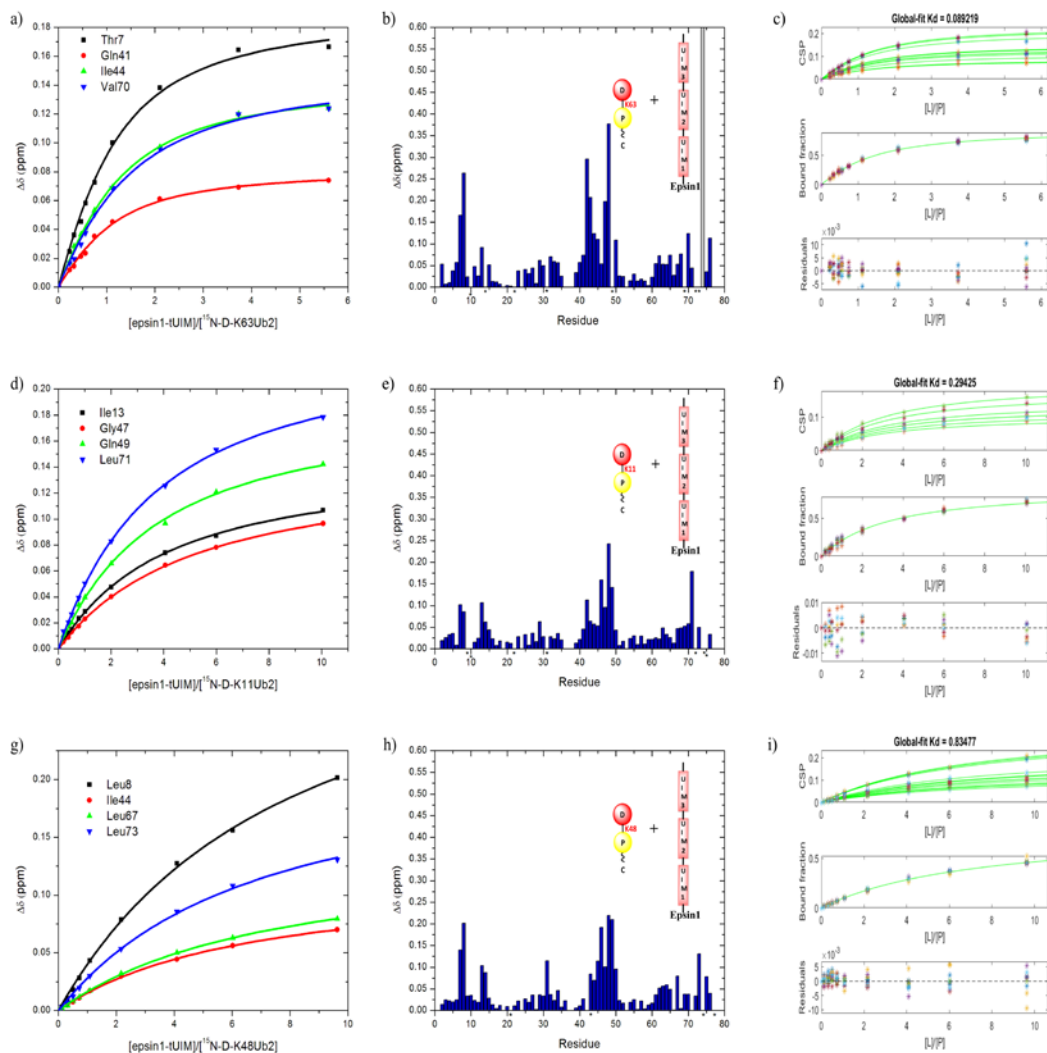


Figure 2.5 Titration curves and CSP plots for diubiquitin binding to epsin1 tUIMs in the presence of 130 mM NaCl; (a,b,c) ^{15}N -D-K63 Ub₂, (d,e,f) ^{15}N -D-K11 Ub₂, (g,h,i) ^{15}N -D-48 Ub₂; * indicates overlapping residues or residues with weak signal intensities. Grey bar indicates signal attenuation arising due to binding. Protein concentration at the beginning of titration in a), d) and g) was uniformly 100 μM ; protein concentration at the end of titration was a) 69.2 μM , d) 74.3 μM and g) 79 μM ; panels c,f and i show titration curves and residuals obtained from K_d analysis using global fit.

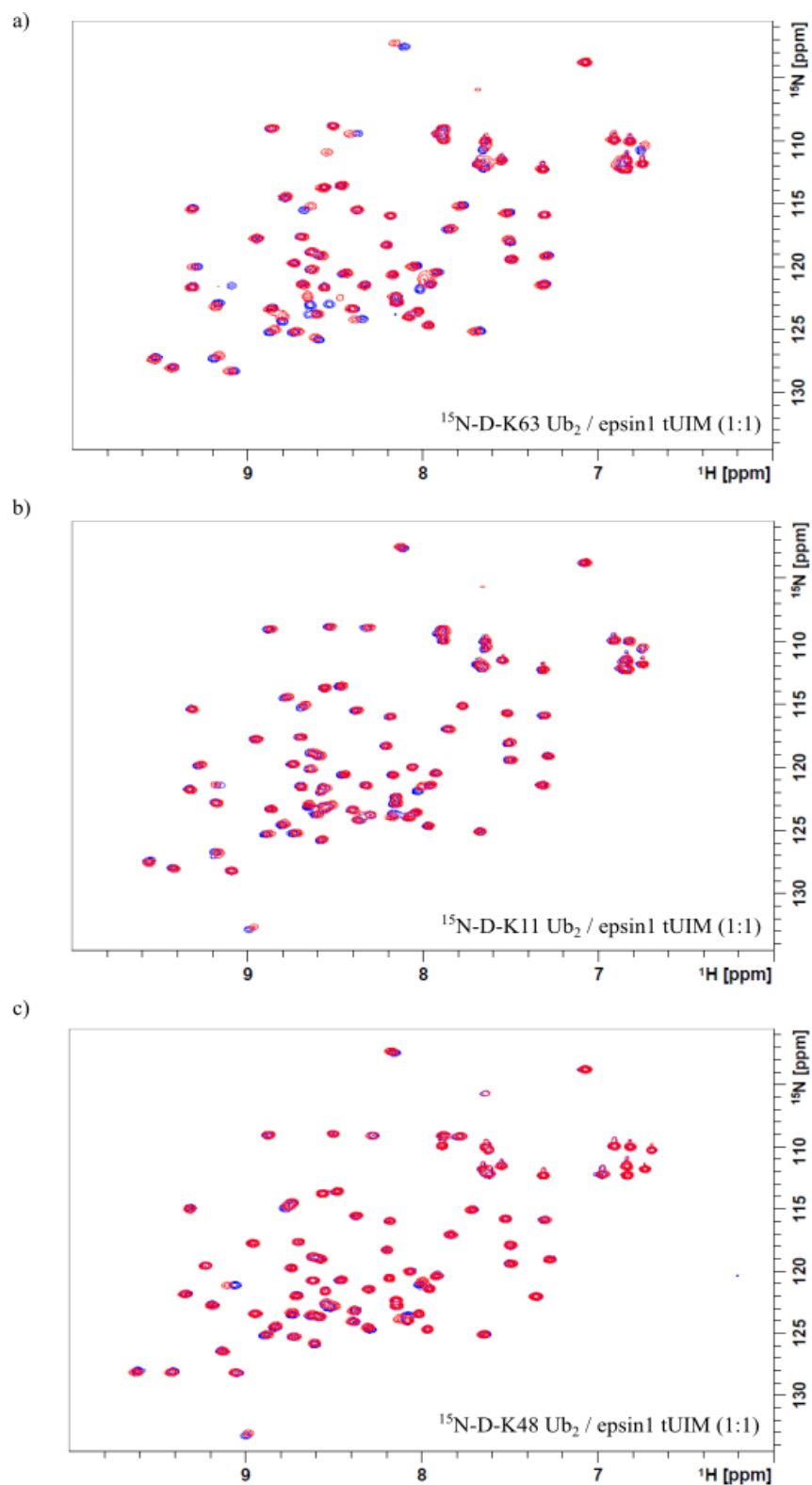


Figure 2.6 Diubiquitin binding to epsin1 tUIMs- Overlay of diubiquitin spectra in the absence (blue) and presence of epsin1 tUIMs (red) in 20 mM sodium phosphate, 130 mM NaCl, pH 6.8 a) $^{15}\text{N-D-K63 Ub}_2$; b) $^{15}\text{N-D-K11 Ub}_2$, c) $^{15}\text{N-D-K48 Ub}_2$

2.5 Epsin1 tUIM- 23 binds avidly across K63-Ub₂

In order to dissect which of the epsin1 tUIMs specifically recognize the different linkage types in K11 and K63 mixed-linkage polyubiquitin chains, deletion mutants of epsin1 tUIMs were designed, deleting one UIM at a time. The epsin1 tUIM pairs were then tested for their affinity for K11-Ub₂ and K63-Ub₂ by NMR titration experiments carried out at near physiological conditions (in 20 mM sodium phosphate, 130 mM NaCl, pH 6.8, 310 K) (table 2.3).

Protein	Ligand	NaCl (mM)	K_d (μM)
¹⁵ N-D-K63 Ub ₂	epsin1 tUIM-23	130	216 ± 25
¹⁵ N-D-K11 Ub ₂	epsin1 tUIM-23	130	1197 ± 146

Table 2.3- Dissociation constants for diubiquitin binding to epsin1 tUIM-23

The average K_d for ¹⁵N-distal labeled K63-Ub₂ and epsin1 tUIM-23 was determined to be 216 ± 25 μM, from a 1:1 binding model, whereas the K_d for ¹⁵N-distal labeled K11-Ub₂ and epsin1 tUIM-23 was found to be 1197 ± 146 μM (figure 2.7). Thus epsin1 tUIM-23 exhibits a six-fold preference for binding to K63-Ub₂ over K11-Ub₂, indicating that this tUIM pair selectively interacts with the K63-Ub₂ segment in K11 and K63 mixed-linkage polyubiquitin chains. Epsin1 tUIM-23 also shows a twelve-fold preference for binding to K63-Ub₂ over monoubiquitin (K_d= 2558 ± 350 μM, table 2.1). These data demonstrate a relatively high-affinity interaction between tUIM-23 and K63-Ub₂, which depends on both UIMs 2 and 3 suggesting that the interaction is avid and involves the simultaneous binding of both ubiquitin domains similar to the mechanism observed with RAP80 tUIMs and K63-Ub₂⁸⁴.

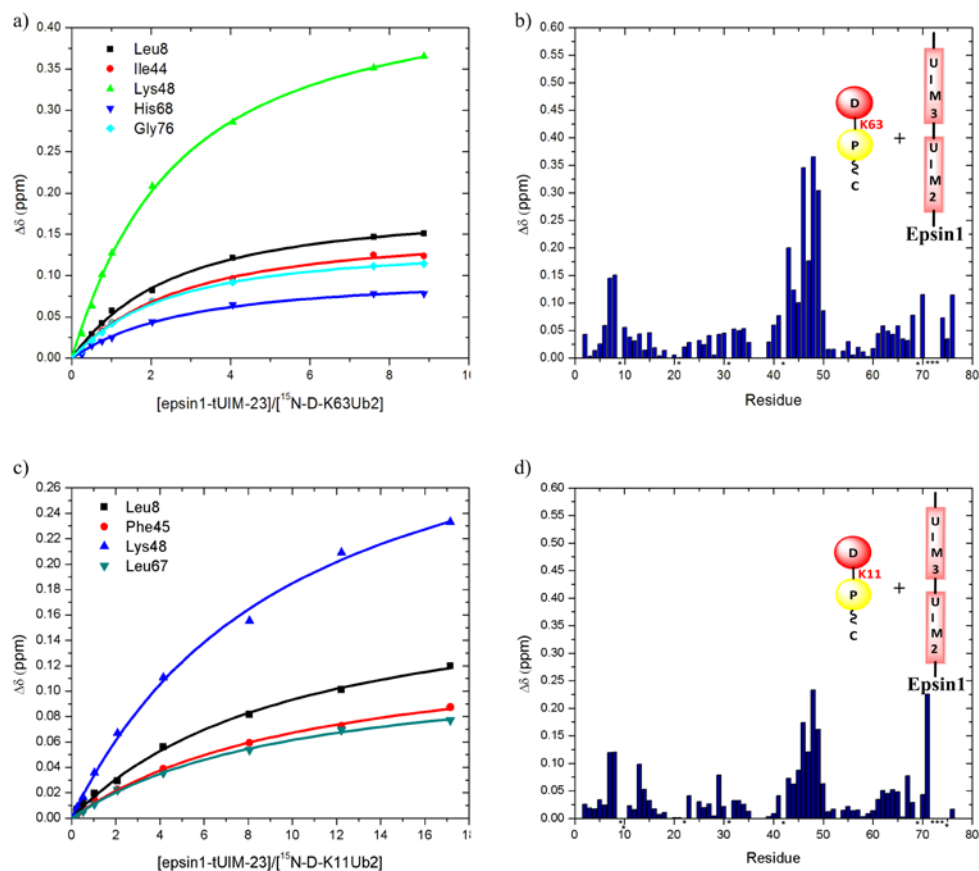


Figure 2.7 Titration curves and CSP plots for diubiquitin binding to epsin1 tUIM-23 in the presence of 130 mM NaCl; (a and b) ^{15}N -D-K63 Ub₂, (c and d) ^{15}N -D-K11 Ub₂; * indicates overlapping residues or residues with weak signal intensities. Protein concentration at the beginning of titration in a) and c) was uniformly 100 μM ; protein concentration at the end of titration was a) 68.2 μM and c) 69.4 μM .

2.6 Epsin1 tUIM-23 exhibits domain-specific binding across K63-Ub₂

In order to determine whether the binding of epsin1 tUIM-23 across K63-Ub₂ is domain-specific, site-specific spin labeling experiments were carried out. The paramagnetic spin label 1-oxyl-2,2,5,5-tetramethyl-3-pyrroline-3-methyl methanesulfonate (MTSL) was covalently attached to a single native cysteine residue in the linker region N-terminal to epsin1 UIM-2 and the effect of paramagnetic relaxation rate enhancement (PRE) was measured on both proximal and distal

ubiquitin domains of K63-Ub₂ in (1:2):(K63-Ub₂:epsin1 tUIM-23) NMR sample. The residues in the domain that comes in close proximity to the modified Cys experience signal attenuation due to PRE. The attenuations were calculated as the ratio of signal intensities in the presence of oxidized and reduced MTSL. Significant attenuations in signal intensities were observed in the ¹⁵N-proximal K63-Ub₂ spectra, indicating the close proximity of the proximal domain to the Cys-MTSL near UIM-2 on epsin1 tUIM-23. However, no such effect was observed in ¹⁵N-distal K63-Ub₂ in the presence of the spin-labeled epsin1 tUIM-23. This suggests that epsin1 UIM-2 interacts with the proximal domain of K63-Ub₂. The attenuations were converted to distance constraints using SLfit¹⁰⁹ and the position of the MTSL's unpaired electron was determined. The back-calculated PRE attenuation profile is in good agreement with experiment (figure 2.8 a).

In a complementary experiment, MTSL was covalently attached to a single cysteine residue inserted in the linker region C-terminal to UIM-3 and the effect of PRE on the proximal and distal domains of K63-Ub₂ in (1:1):(K63-Ub₂:epsin1 tUIM-23) sample was measured. Significant attenuations in signal intensities were observed in the ¹⁵N-distal K63-Ub₂ spectra, indicating the close proximity of the distal domain to the Cys-MTSL near UIM-3 on epsin1 tUIM-23, while no such effect was observed for ¹⁵N-proximal K63-Ub₂ in the presence of the spin labeled epsin1 tUIM-23. This suggests that epsin1 UIM-3 interacts with the distal domain of K63-Ub₂. Again, the back-calculated PRE attenuation profile is in good agreement with experiment (figure 2.8 e).

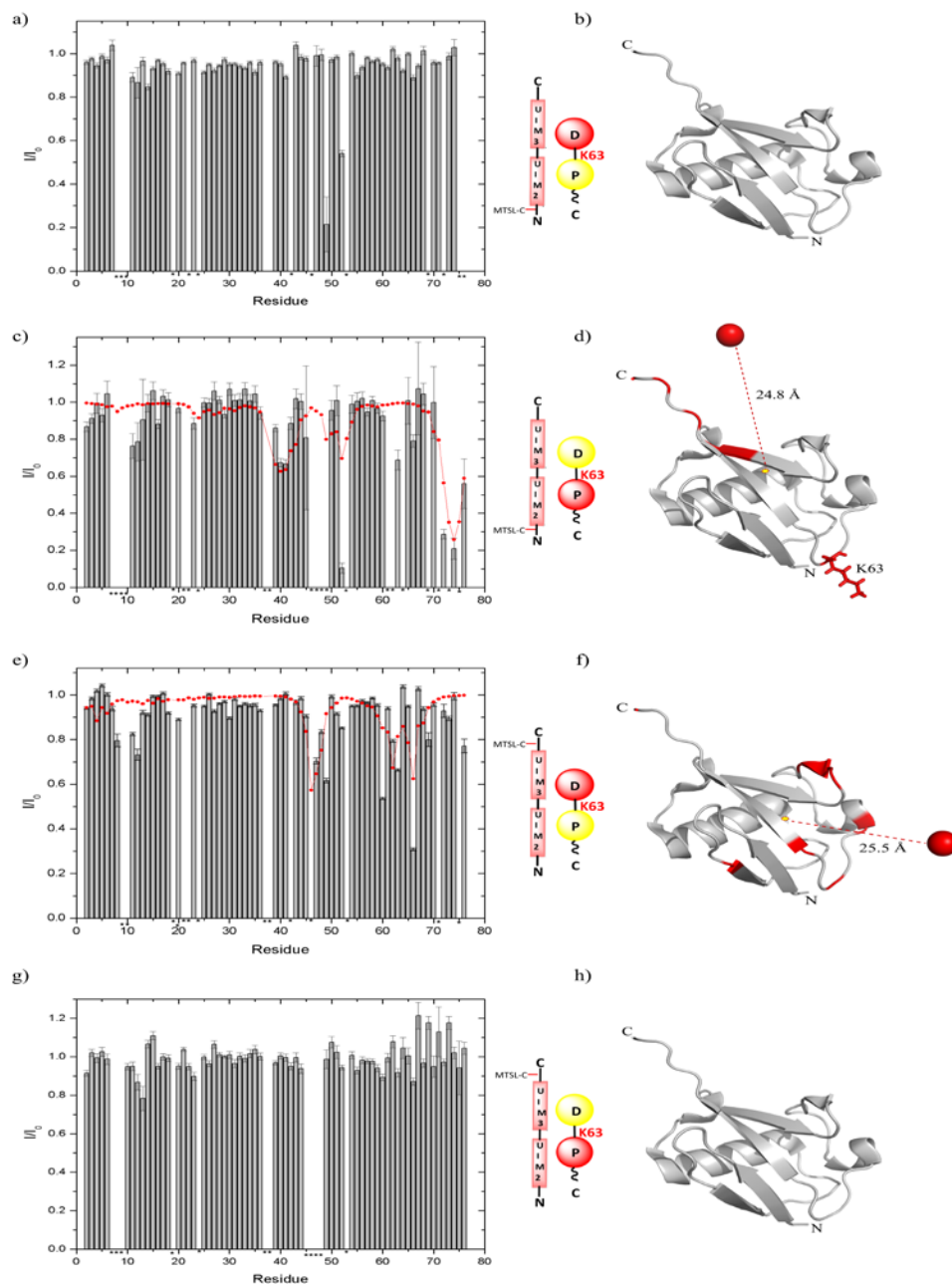


Figure 2.8 Effect of spin-labeling of epsin1 tUIM-23 on proximal and distal Ub in K63-Ub₂

Signal attenuations observed in the presence of MTSL attached to a Cys residue at the N-terminus of epsin1 tUIM-23 on a,b) the distal domain of K63-Ub₂; c,d) the proximal domain of K63-Ub₂; Signal attenuations observed in the presence of MTSL attached to a Cys residue at the C-terminus of epsin1 tUIM-23 on e,f) the distal domain of K63-Ub₂; g,h) the proximal domain of K63-Ub₂; The attenuations are calculated as the ratio of signal intensities in the presence of oxidized and reduced MTSL. Residues with an intensity ratio ≤ 0.7 are colored red on the structure of ubiquitin monomer and the red sphere indicates the location of the unpaired electron of MTSL. The distance indicated represents the distance between the spin label and the geometric center of ubiquitin structure in 1D3Z. * indicates residues that are not visible or overlapping.

RAP80_tUIM	1	TEEEQFALALKMSEQEAREVNSQEEEEEELLRK-----A-----I
epsin1_tUIM	1	EEELQLQLALAMSKEADQPPSCGPEDDAQQLALSLSLREEHDKEERIRRQDDLRLQMAI
RAP80_tUIM	36	AE SL NSCRPS
epsin1_tUIM	61	EE SK RETGGK

Figure 2.9 Sequence alignment of human RAP80 tUIM (80-124) and human epsin1 tUIM (183-252)- Alignment obtained from T-Coffee¹¹⁰ and output generated using Boxshade

It is interesting to note that despite significant differences in the UIM sequences between epsin1 tUIM-23 and that of RAP80 tUIM (figure 2.9), the binding mode across K63-Ub₂ is somewhat similar, with the N-termini of both proteins in close proximity to the proximal domain of K63-Ub₂ while the C-termini face the distal domain (figure 2.10).

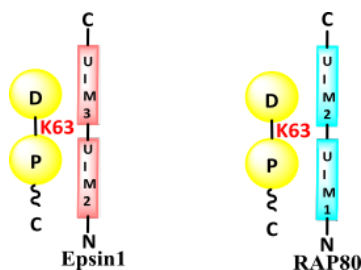


Figure 2.10 Similar binding mode across K63-linked Ub₂- Both epsin1 tUIM-23 and RAP80 tUIM-12 bind with their C-termini close to the proximal moiety in K63-linked Ub₂

2.7 Epsin1 tUIM-12 binds both K11-Ub₂ and K63-Ub₂ with a similar affinity

Epsin1 tUIMs have been reported to interact with K11 and K63 mixed-linkage polyubiquitin chains^{49,98}. Since we had determined that tUIM-23 selectively binds across K63-Ub₂ but not K11-Ub₂ (table 2.3), the logical step was to examine whether tUIM-12 shows linkage specificity to K11-Ub₂. The deletion mutant epsin1 tUIM-12 (with UIM-3 deleted) was tested for its affinity for K11-, and K63-Ub₂ using NMR titration experiments. The average K_d for ¹⁵N-distal labeled K11-Ub₂ was determined to be $613 \pm 33 \mu\text{M}$, for a 1:1 binding model, whereas, the average K_d for ¹⁵N-distal labeled K63-Ub₂ was estimated to be $940 \pm 93 \mu\text{M}$ (figure 2.11).

Protein	Ligand	NaCl (mM)	K _d (μM)
¹⁵ N-D-K11 Ub ₂	epsin1 tUIM-12	130	613 ± 33
¹⁵ N-D-K63 Ub ₂	epsin1 tUIM-12	130	940 ± 93

Table 2.4 Dissociation constants for diubiquitin binding to epsin1 tUIM-12

Thus, epsin1 tUIM-12 shows a similar binding preference for both K11-Ub₂ and K63-Ub₂ (table 2.4). However, the affinity for monoubiquitin was found to be $4546 \pm 490 \mu\text{M}$ (table 2.1), similar to the tUIMs of epsin1. These results suggest that epsin1 tUIM-12 interacts avidly across both K11 and K63-Ub₂, involving simultaneous binding of both distal and proximal domains of the ubiquitin dimer.

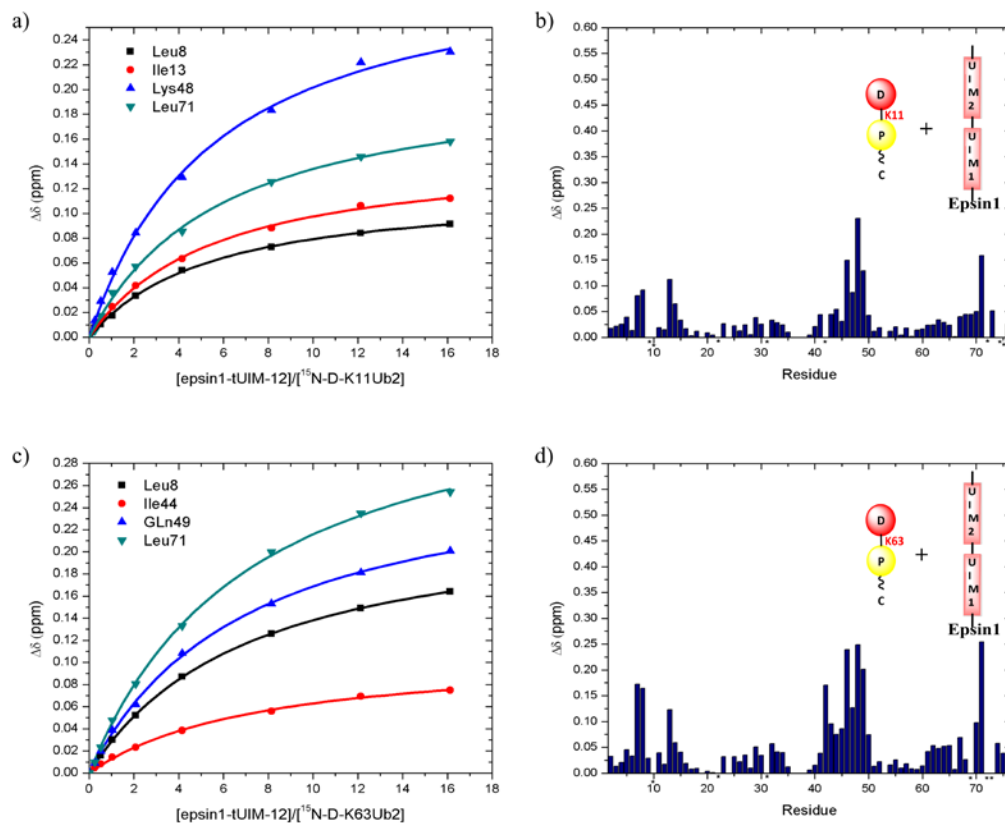


Figure 2.11 Titration curves and CSP plots for different linkages of diubiquitin and epsin1 tUIM-12 in the presence of 130 mM NaCl with ¹⁵N-D-K11 Ub₂ (a and b); with ¹⁵N-D-K63 Ub₂ (c and d); * indicates overlapping residues or residues with weak signal intensities. Protein concentration at the beginning of titration in a) and c) was 100 μM; protein concentration at the end of titration in a) and c) was 61.7 μM.

Epsin1 tUIM-12 seems to show a slight binding preference for K11-Ub₂ over K63-Ub₂ (table 2.4). In order to determine whether this segment of tUIM exhibits domain-specific binding across K11-Ub₂, site-specific spin labeling experiment was carried out. The paramagnetic spin label MTSL was covalently attached to a cysteine residue in the linker region N-terminal to epsin1 UIM-1 and the effect of paramagnetic relaxation rate enhancement was measured on both proximal and distal ubiquitins of K11-Ub₂ in a (1:2):(K11-Ub₂:epsin1 tUIM-12) NMR sample. The attenuations were calculated as the ratio of signal intensities in the presence of oxidized and reduced MTSL. Significant attenuations in signal intensities were observed both in the case of ¹⁵N-proximal and ¹⁵N-distal K11-Ub₂ spectra. The attenuations were converted to distance constraints using SLfit¹⁰⁹ and the position of the MTSL's unpaired electron was determined. The back-calculated PRE attenuation profile is in good agreement with experiment in both cases (figure 2.12). These results suggest that epsin1 tUIM-12 does not exhibit domain-specific binding across K11-Ub₂.

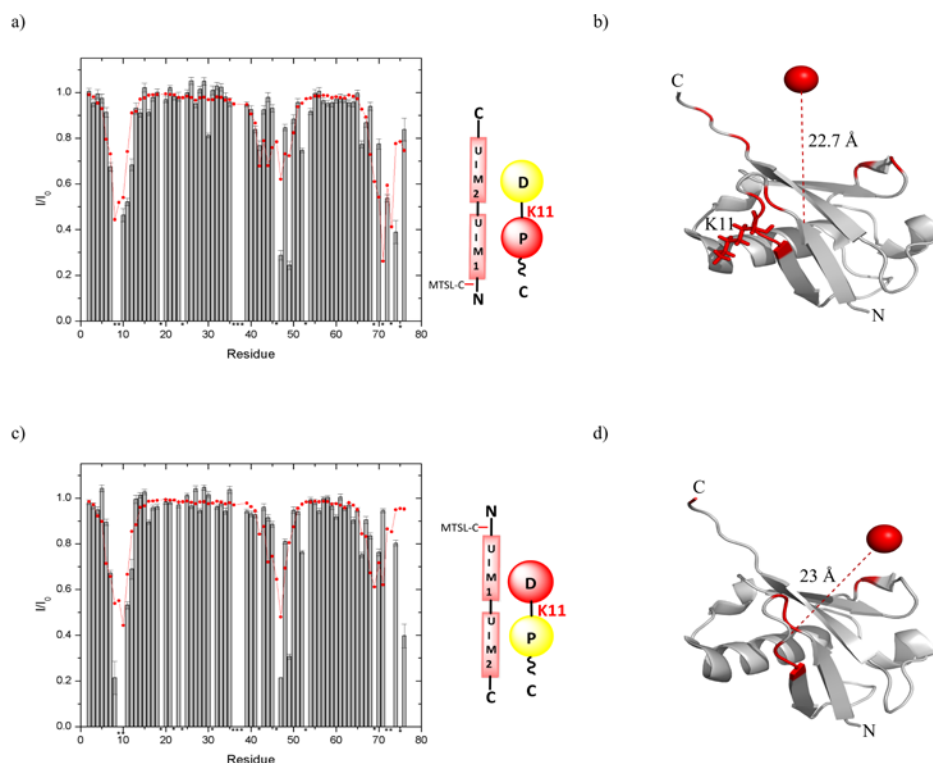


Figure 2.12 Effect of spin-labeling of epsin1 tUIM-12 on proximal and distal Ub in K11-Ub₂. Signal attenuations observed in the presence of MTSL attached to a Cys residue at the N-terminus of epsin1 tUIM-12 a,b) the proximal domain of K11-Ub₂ in; c,d) the distal domain of K11-Ub₂; The attenuations are calculated as the ratio of signal intensities in the presence of oxidized and reduced MTSL. Residues with an intensity ratio ≤ 0.7 are colored red on the structure of ubiquitin monomer and the red sphere indicates the location of the unpaired electron of MTSL. The distance indicated represents the distance between the spin label and the geometric center of ubiquitin structure in 1D3Z. * indicates residues that are not visible or overlapping.

2.8 The linker sequence between the UIMs is critical for linkage-dependent recognition of polyubiquitin

To examine the role played by the linker regions in between the dual tandem UIMs of epsin1 in determining linkage specificity to polyubiquitin, protein constructs with either of the linker sequences inserted in between UIM-1 and UIM-3 were generated (UIM-2 deleted, figure 2.13), i.e., tUIM-13-LR1 (Linker Region) and tUIM-13-LR2. Among the two constructs, the tUIM-13-LR2, which lacks UIM2 along with Pro, Ser and Gly residues in LR1, is not only a splicing variant but also a

functional protein *in vivo*¹⁰⁷, which was previously shown to interact selectively with K63-Ub₂¹⁰⁸. These constructs were then tested for their affinities for both K11-, and K63-Ub₂ using NMR titration experiments (figure 2.14).

a) Epsin1 tUIM-13-LR1

QSSGEEELQLQLALAMSKEEADQPPSCGPGDDLRLQMAIEESKRETGGKEES

b) Epsin1 tUIM-13-LR2

QSSGEEELQLQLALAMSKEEADQPERIRRGDDLRLQMAIEESKRETGGKEES

Figure 2.13 Amino acid sequences for the different constructs of epsin1 tUIM-13- UIMs are highlighted in yellow whereas the linker regions are in grey.

Protein	Ligand	NaCl (mM)	K _d (μM)
¹⁵ N-D-K11 Ub ₂	epsin1 tUIM-13-LR1	130	1365 ± 55
¹⁵ N-D-K63 Ub ₂	epsin1 tUIM-13-LR1	130	1003 ± 117
¹⁵ N-D-K11 Ub ₂	epsin1 tUIM-13-LR2	130	254 ± 87
¹⁵ N-D-K63 Ub ₂	epsin1 tUIM-13-LR2	130	145 ± 39

Table 2.5- Dissociation constants for diubiquitin binding to epsin1 tUIM-13

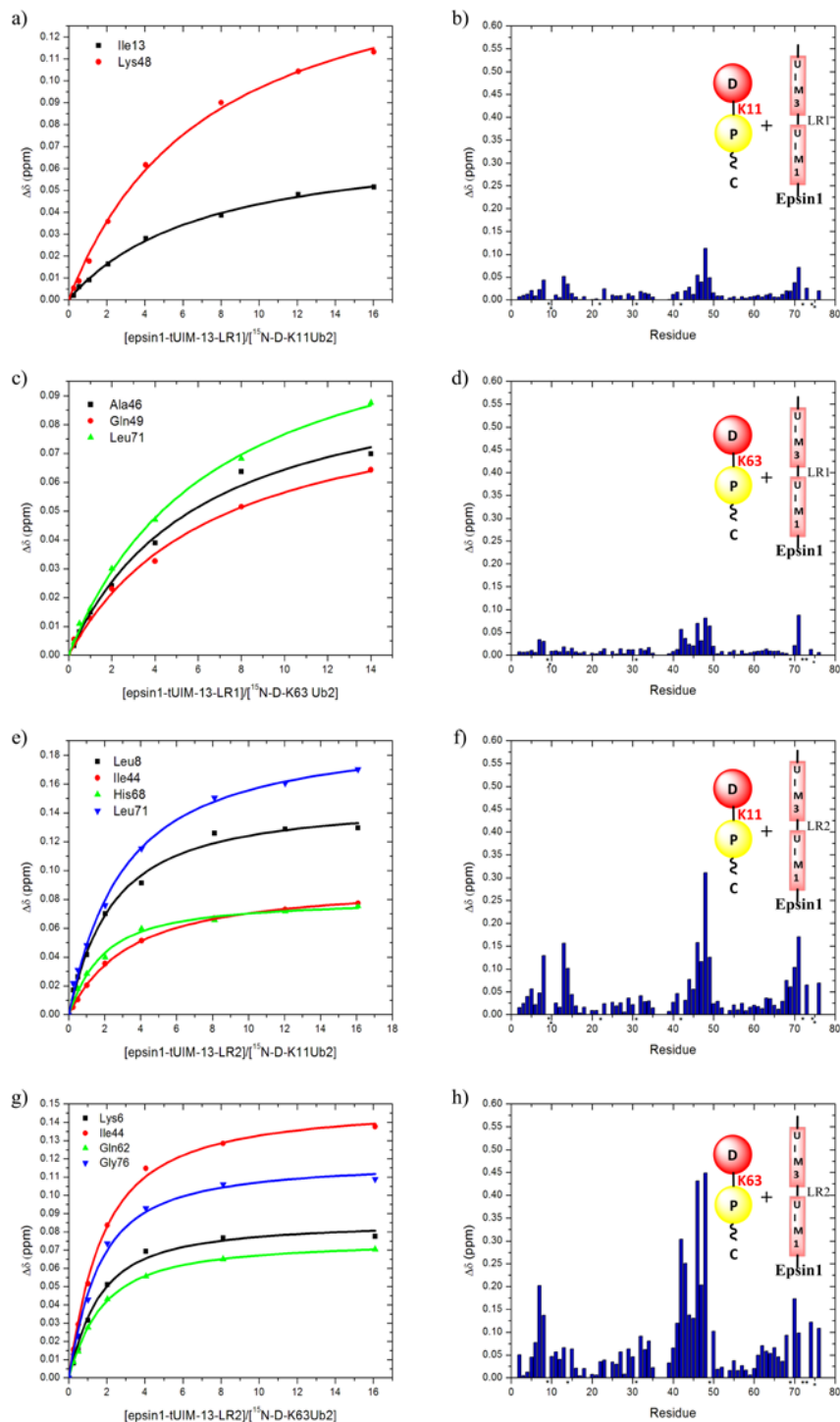


Figure 2.14 Titration curves and CSP plots for diubiquitin binding to epsin1 tUIM-13-LR1 in the presence of 130 mM NaCl with ^{15}N -D-K11 Ub₂ (a and b); with ^{15}N -D-K63 Ub₂ (c and d); and epsin1 tUIM-13-LR2 in the presence of 130 mM NaCl with ^{15}N -D-K11 Ub₂ (e and f); with ^{15}N -D-K63 Ub₂ (g and h); * indicates overlapping residues or residues with weak signal intensities. Protein concentration at the beginning of titration in a), c), e) and g) was uniformly 100 μM ; protein concentration at the end of titration was a) 45.7 μM , c) 51.7 μM , e) 54.2 μM and g) 54.2 μM .

From table 2.5, it is apparent that tUIM-13-LR1 has similar binding affinities for both K11-, and K63-Ub₂, which suggests lack of linkage specificity in these interactions. This is similar to the interaction of tUIM-12 (comprising LR1) with K11-, and K63-Ub₂ (table 2.4). However, tUIM-13-LR2 has a twofold-preference for K63-Ub₂ over K11-Ub₂. This clearly indicates linkage specificity for K63-Ub₂, similar to the mechanism observed with tUIM-23 (comprising LR-2, table 2.3). These results suggest that LR-2 determines linkage specificity for K63-Ub₂ in the interaction with epsin1 tUIMs. Besides, accounting for the differences in affinities for individual UIMs binding to ubiquitin (as observed for the UIMs of RAP80⁸⁴), and unique UIM pairs, the common theme underlying the interactions discussed involves the presence of a particular linker region and its ability to determine linkage specificity.

It is interesting to note that both the linker regions in between the dual tandem UIMs of epsin1 are of the same length consisting of five amino acid residues. However, their composition (figure 2.13) and affinities for K63-Ub₂ differ significantly (table 2.5). While linker region 2 doesn't include any residues that might distort the α -helical structure, linker region 2 comprises one serine, one glycine and three proline residues, which might prevent this segment from forming an α -helical structure¹⁰⁸. This study reaffirms that intrinsic helical propensity in the linker sequence correlates with tighter avid binding because the more ordered linkers are, more favorably they can position the second receptor binding site after the first site is bound⁸⁴.

2.9 Epsin1 tUIMs do not directly interact with the isopeptide linker but they exhibit linkage-specific avidity

The isopeptide linker in diubiquitin comprises Gly76 residue of the distal domain and the ϵ -amino group of the lysine residue on the proximal domain. Since these signals did not exhibit significant chemical shift perturbations in NMR titration experiments with different constructs of epsin1 tUIMs, it is evident that the UIMs do not directly interact with the isopeptide linker.

Epsin1 tUIMs achieve linkage selectivity through particular spatial orientation of the ubiquitin monomers in a polyubiquitin chain of a specific linkage type. The UIMs are favorably arranged to achieve optimal interaction with both domains in K63-Ub₂ and K11-Ub₂ but not in the case of K48-Ub₂ (table 2.2). Binding of the first UIM to a ubiquitin subunit positions the second UIM favorably for interaction with a nearby ubiquitin in the chain. Since the second binding event occurs between binding partners at high local concentrations, it is highly favored as evident from the K_d for monoubiquitin versus K63-, and K11-Ub₂ (table 2.2). This type of co-operative binding has previously been termed as “linkage-specific avidity” using the RAP80 tUIM and K63-Ub₂ as the model system⁸⁴.

2.10 Epsin1 tUIMs do not distinguish between branched and unbranched mixed-linkage polyubiquitin chains

After having learnt that epsin1 tUIM-23 exhibits both linkage specificity and domain-specific interaction across K63-Ub₂, while tUIM-12 does not show these traits in its interaction with K11-, and K63-Ub₂, we wanted to examine these features of the tUIMs in the context of K11 and K63 mixed-linkage polyubiquitin chains.

Since triubiquitin is the simplest unit of a mixed-linkage chain comprising two different linkages, we analyzed the binding preferences for branched and unbranched triubiquitin chains for epsin1 tUIMs using NMR titration experiments (figure 2.15 and figure 2.16).

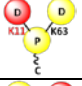
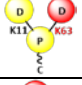
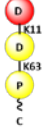
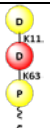
Protein*	Schematic representation	Ligand	NaCl (mM)	K _d (μM)
Ub(¹⁵ N)[Ub] ^{-11,63} Ub		epsin1 tUIMs	130	93 ± 14
Ub[Ub(¹⁵ N)] ^{-11,63} Ub		epsin1 tUIMs	130	60 ± 8
Ub(¹⁵ N) ⁻¹¹ Ub ⁻⁶³ Ub		epsin1 tUIMs	130	116 ± 42
Ub ⁻¹¹ Ub(¹⁵ N) ⁻⁶³ Ub		epsin1 tUIMs	130	58 ± 10

Table 2.6- Dissociation constants for branched and unbranched K11 and K63 mixed-linkage triubiquitin binding to epsin1 tUIMs

(*mixed polyubiquitin chain nomenclature is from ¹⁰⁰)

The similar K_d values for both branched and unbranched K11 and K63 components of the mixed-linkage chains binding to tUIMs (table 2.6), is an indication that the tUIMs do not distinguish between the two topologies. The smaller K_d values for K11 and K63 components in triubiquitin (Ub₃) versus K11-, and K63-Ub₂ respectively (table 2.2), is because the Ub₃ provides a higher local concentration that may favor rebinding to neighboring sites⁸⁴. The tUIMs bound branched and linear K11 component of the mixed-linkage Ub₃ ~three-fold tighter than K11-Ub₂ (table 2.2), indicating avid binding to Ub₃.

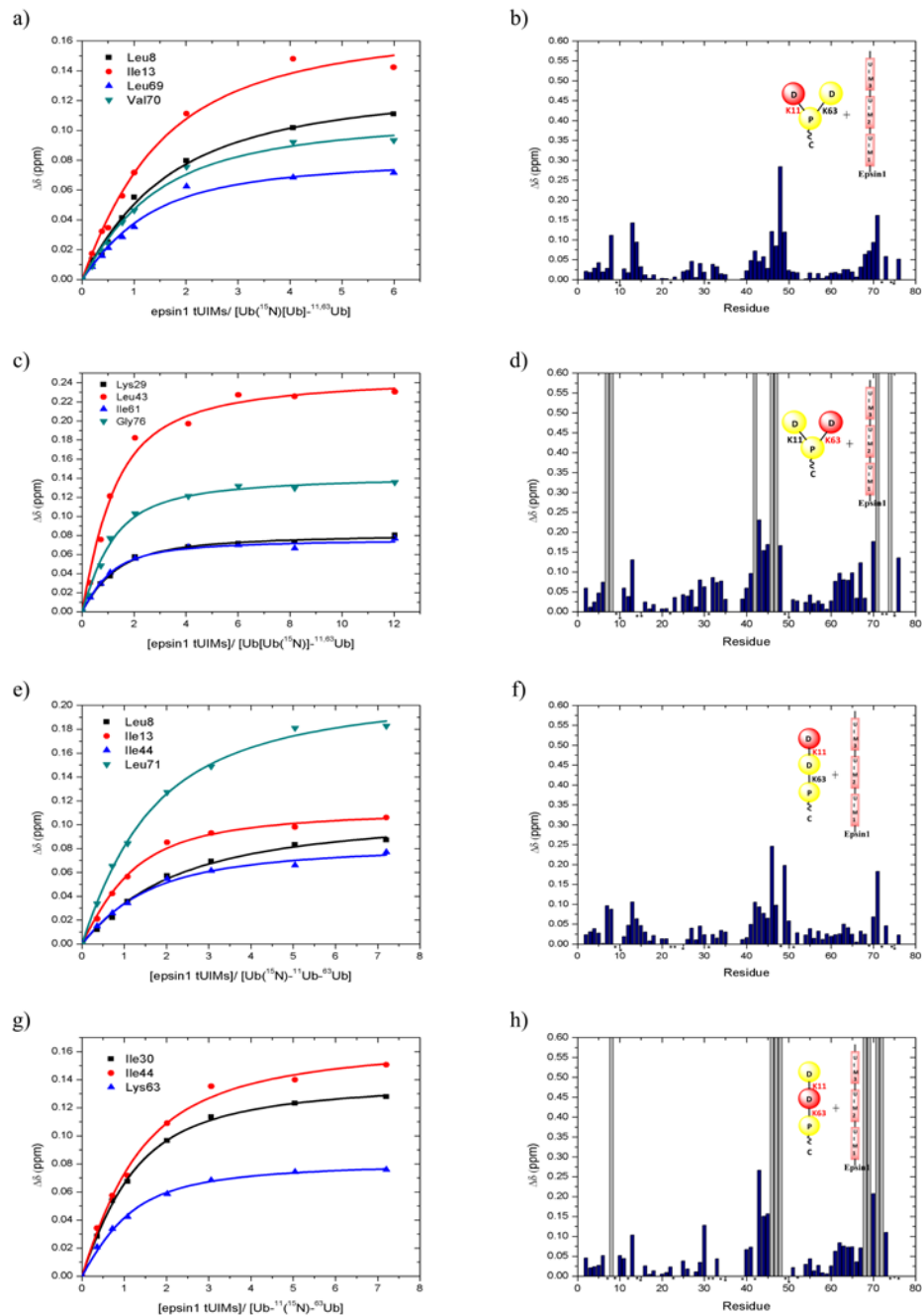


Figure 2.15 Titration curves and CSP plots for K11 and K63 mixed-linkage triubiquitin binding to epsin1 tUIMs in the presence of 130 mM NaCl a,b) Ub(^{15}N)[Ub] $^{11,63}\text{Ub}$; c,d) Ub[Ub(^{15}N)] $^{11,63}\text{Ub}$; e,f) Ub(^{15}N) ^{11}Ub ^{63}Ub ; g,h) Ub ^{11}Ub (^{15}N) ^{63}Ub * indicates overlapping residues or residues with weak signal intensities. Grey bars indicate signal attenuations arising due to binding. Protein concentration at the beginning of titration in a), c), e) and g) was uniformly 100 μM ; protein concentration at the end of titration was a) 82.9 μM , c) 75 μM , e) 88.2 μM and g) 79.4 μM .

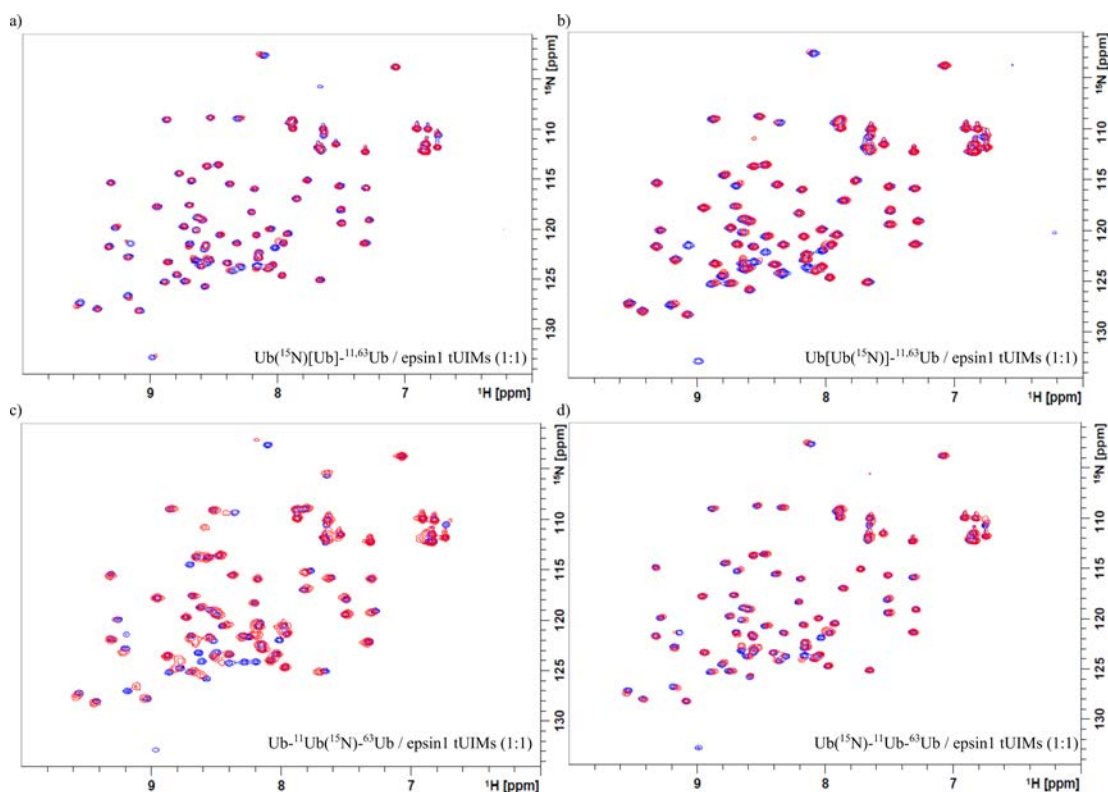


Figure 2.16 K11 and K63 mixed-linkage triubiquitin binding to epsin1 tUIMs- Overlay of K11 and K63 mixed-linkage triubiquitin spectra in the absence (blue) and presence of epsin1 tUIMs (red) tUIMs in the presence of 130 mMNaCl. a) Ub(¹⁵N)[Ub]-^{11,63}Ub; b) Ub[Ub(¹⁵N)]-^{11,63}Ub; c) Ub-¹¹Ub(¹⁵N)-⁶³Ub; d) Ub(¹⁵N)-¹¹Ub-⁶³Ub.

2.11 Electrostatic interactions play a major role in defining the interaction between epsin1 tUIMs and ubiquitin

The differences in K_d values for ubiquitin binding to epsin1 tUIMs in the presence and absence of NaCl (table 2.7) reveal the importance of electrostatics in the interaction between epsin1 tUIMs and ubiquitin. The putative participants in the strong electrostatic interactions on ubiquitin would be the positively charged Lys and Arg residues (Lys6, Arg42, Lys48 and Arg72) surrounding the canonical hydrophobic patch (figure 2.17a). A stretch of negatively charged residues including Asp and Glu alongside the ‘LALAL-motif’ comprising epsin1 tUIMs (figure 2.17c), could serve as ubiquitin counterparts.

Protein	Ligand	NaCl (mM)	K _d (μM)
¹⁵ N-K11RK63R Ub	epsin1 tUIMs	0	320 ± 53
		130	3700 ± 775
¹⁵ N-D-K63 Ub ₂	epsin1 tUIMs	0	22 ± 7
		130	88 ± 17
¹⁵ N-D-K11 Ub ₂	epsin1 tUIMs	0	166 ± 33
		130	411 ± 87
¹⁵ N-D-K11 Ub ₂	epsin1 tUIM-12	0	368 ± 93
		130	613 ± 33

Table 2.7 Dissociation constants for ubiquitin binding to epsin1 tUIMs in the presence and absence of NaCl.

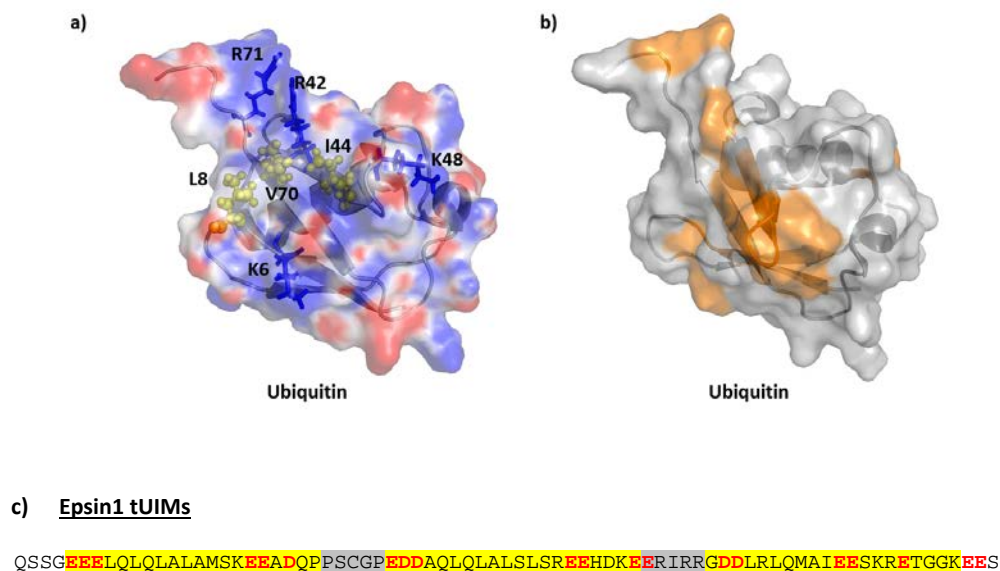


Figure 2.17 Putative residues involved in ubiquitin-epsin1 tUIMs electrostatics - a) electrostatic surface potential on ubiquitin with the hydrophobic residues (L8, I44, V70) depicted in yellow and positively charged residues in blue sticks rendered using PyMOL; b) ubiquitin surface representation with residues having CSPs > 0.05 upon binding to epsin1 tUIMs shown in orange; c) amino acid sequence of epsin1 tUIMs with negatively charged residues in red.

Electrostatic properties of proteins depend on the proportion and distribution of polar and charged residues which form short-range salt-bridges and hydrogen-bonds¹¹¹, and the ionic strength of the environment affects these interactions. While flexible parts of proteins lack these short-range interactions, the rigid parts have stronger electrostatics. Previous studies have indicated that linker sequences that

reduce the flexibility between UIMs promote high-affinity and linkage-selective interactions⁸⁴. This could be due to contribution of conformational entropy to the entropy of binding. Several examples in literature suggest that fine tuning of local and global electrostatic properties are essential for protein binding and function¹¹¹.

The persuasive arguments suggesting that the linker region (comprising residues with high helical propensity) in RAP80 tUIMs is fine-tuned for interaction with K63-Ub₂^{84,108}, is an example favoring the hypothesis that proteins are evolutionally tuned for their specific functions. In addition to this, interdomain dynamics exhibited by polyubiquitin chains of a specific-linkage type¹⁰ could determine the potential for electrostatic interactions with putative binding partners, which might partially explain the different affinities of K11-, and K63-Ub₂ observed for tUIMs of epsin1.

2.12 Structural studies of epsin1 tUIMs

To gain an in depth atomic-level understanding of the structural details of the interaction between epsin1 tUIMs and K11-Ub₂ and K63-Ub₂, sequential resonance assignment for the tUIMs of epsin1 would be useful. We collected a series of 3D triple resonance NMR experiments on ¹³C, ¹⁵N isotope enriched samples of epsin1 tUIMs, epsin1 tUIM-12 and epsin1 tUIM-23. The NMR experiments collected for resonance assignment of each of these samples included HNCO, HN(CA)CO, HNCA, HN(CA)CO, CBCA(CO)NH, HNCACB, HNCANNH and 3D TOCSY.

We also attempted to crystallize the epsin1 tUIMs: K63-Ub₂ complex for X-ray crystallography. The protein complex at a concentration of 15 mg/mL was initially screened for crystals using PEG and Index suite from Hampton research. The

phoenix protein crystallization robot was used to set up a hanging drop vapor diffusion screen. Although there were no initial hits, a few conditions that could be optimized for crystals in the Index screen were found (figure 2.18) (based on the appearance of spherulites). Optimization for obtaining diffraction-quality crystals remains to be done.

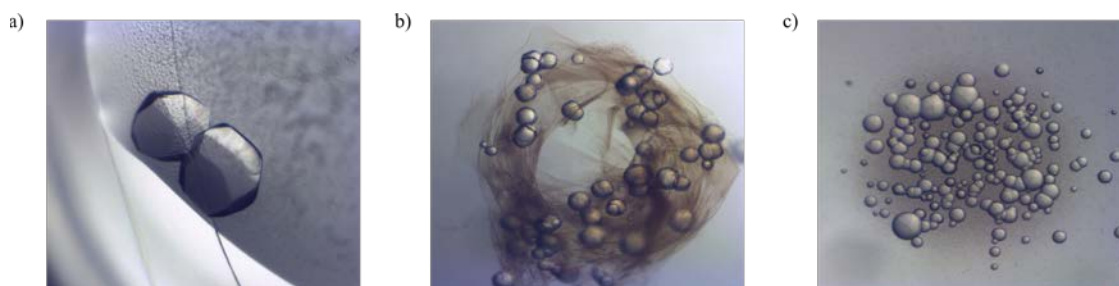


Figure 2.18 Promising conditions for optimization of crystallization of epsin1 tUIMs:K63-Ub₂ complex –Index screen initial leads a) F4-2 (protein:precipitant:1:1) / Index 64 (0.1 M HEPES, pH 7.5, 12% w/v polyethyleneglycol 3,350, 0.005 M Cobalt(II) chloride hexahydrate, 0.005 M Nickel(II) chloride hexahydrate, 0.005 M Cadmium chloride hydrate) shows promising crystals with a polygonal surface; b) F4-1 (protein:precipitant:1:3) / Index 64 shows a mix of both small polygonal crystals and spherulites along with precipitate; c) B4-3 (protein:precipitant:3:1) / Index 16 (0.1 M Tris, pH 8.5, 0.3 M Magnesium formate dihydrate) shows a cluster of small spherulites.

2.13 Summary

Our study illustrates that branched K11 and K63 mixed-linkage polyubiquitin chains retain the structural properties of their K11 and K63 components. Epsin1 tUIMs bind monoubiquitin very weakly and they exhibit preferential binding to chains of different linkages, with the strongest affinity for K63-Ub₂, followed by K11-Ub₂ and lastly K48-Ub₂. Epsin1 tUIM-23 binds avidly with a domain-specific orientation across K63-Ub₂, wherein UIM-2 interacts with the proximal domain of K63-Ub₂. Epsin1 tUIM-12 binds both K63-, and K11-Ub₂ with similar affinities with no domain-specific interaction across K11-Ub₂. The linker region between the tUIMs is critical for linkage-dependent polyubiquitin recognition. Our results support the

hypothesis that in addition to the length of the tUIM linker region, its composition also determines the selective recognition of K63-Ub₂. Epsin1 tUIMs do not distinguish between mixed-linkage branched and unbranched polyubiquitin chains. Our NMR binding studies carried out in the absence and presence of NaCl, revealed that in addition to the canonical hydrophobic patch residues of ubiquitin, electrostatic interactions play a major role in the molecular recognition of polyubiquitin by the tUIMs of epsin1. The interdomain dynamics exhibited by polyubiquitin chains of a specific-linkage type could determine the potential for electrostatic interactions with putative binding partners, which might partially explain the different affinities of K11-, and K63-Ub₂ observed for tUIMs of epsin1. These results provide the first glimpse of the mechanism behind specific recognition of complex mixed polyubiquitin signals by a multivalent receptor with three tandem UIMs.

Chapter 3: Structural studies of K11-linked polyubiquitin chains

3.1 Background and Objective

Post-translational modification of proteins through the attachment of ubiquitin on one of the substrate lysines has several outcomes. Attachment of a polyubiquitin chain linked homogeneously via K48, signals the protein for proteasomal degradation. Substrate proteins with a homogeneous polyubiquitin chain linked via K63 are predominantly involved in DNA repair. In addition to these “canonical” lysine linkages, substrates with polyubiquitin chains linked through other lysine residues (K6, K11, K27, K29 and K33) on ubiquitin have been identified to have unique roles in the cell (table 1.1). Currently the most widely accepted hypothesis suggests that linkage defines polyubiquitin conformation which determines specific recognition by cellular receptors⁴. K11-linked polyubiquitin chains have been implicated to play an important role in regulating cell cycle^{31,57}. Recently a quantitative MS study has highlighted that K11-linked polyubiquitin chains are as abundant as K48-linked polyubiquitin in the cellular milieu⁸. We set out to determine the solution structure of K11-Ub₂ (reference 105) in order to understand the structural basis for these chains to serve as unique cellular signals. My role in this project involved enzymatic protein synthesis of K11-Ub₂ for NMR studies along with chemical shift perturbation mapping and PRE data collection.

3.2 Solution NMR characterization of K11-linked polyubiquitin chains

We sought to determine the interdomain interface for K11-Ub₂ using chemical shift mapping. CSPs indicate a change in the electronic environment of the nucleus

under observation arising due to chemical modification or protein interactions or both. Chain terminating mutants of ubiquitin (K11RK63R and K63RD77) were utilized to generate segmentally isotope enriched K11-Ub₂ enzymatically using the E2 Ube2S. ¹H-¹⁵N TROSY-HSQC spectra were obtained at neutral pH for both proximal and distal K11-Ub₂. These chemical shifts were compared to the respective mutant ubiquitin monomers to generate the CSP plots. The distal domain showed small CSPs around the “canonical” hydrophobic patch residues comprising Leu8, Ile44 and Val70 (figure 3.1a). Large CSPs were observed for the C-terminal residues, which are involved in forming the isopeptide linkage with the proximal domain. The proximal domain showed significant CSPs mostly clustered around K11 (figure 3.1b). The large perturbations around K11 in the proximal domain arise mostly due to the isopeptide bond. This was confirmed by examining CSPs for a monoubiquitin variant with a Lys(Boc) in place of K11, which mimics an isopeptide bond. The CSP pattern obtained for this variant is near identical to that of the proximal domain in K11-Ub₂.

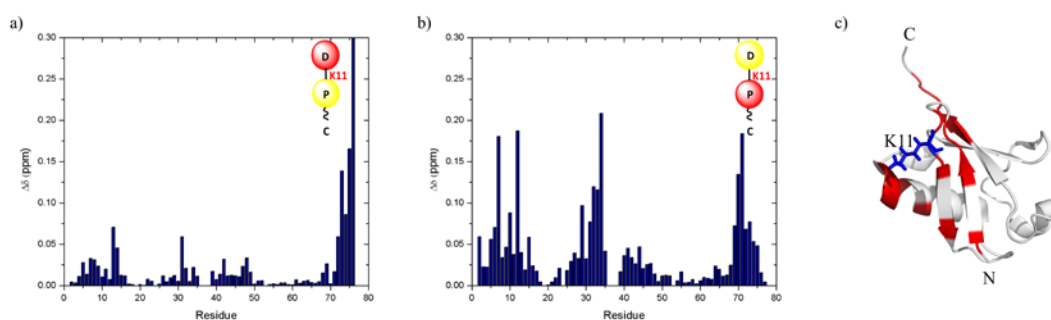


Figure 3.1 CSP plots for K11-Ub₂ - a) amide CSPs for distal K11-Ub₂ vs K11RK63R Ub; b) amide CSPs for proximal K11-Ub₂ vs K63RD77 Ub; c) proximal Ub residues with CSPs > 0.05 ppm mapped in red on the structure of ubiquitin (1D3Z).

In order to verify that the chain terminating ubiquitin mutants used to enzymatically generate K11-Ub₂ had no effect on the properties of K11-linked polyubiquitin chains, all-natural K11-linked chains were generated using nonenzymatic chain assembly¹¹². The CSP pattern observed for all-natural K11-Ub₂ is very similar to that in figure 3.1, indicating that the chain terminating mutations had no effect on the structural properties of K11-Ub₂.

3.3 K11-Ub₂ structure verification using site-directed spin labeling

We used site-directed spin labeling to independently verify the RDC-derived structures of K11-Ub₂¹⁰⁵ (figure 3.2c). The paramagnetic spin label MTSL was attached to I36C in the distal ubiquitin. The interdomain distance information from paramagnetic relaxation enhancement (PRE) effects induced in the proximal ubiquitin were obtained. The PRE attenuation profile of spin-labeled I36C monoubiquitin (used here both as control and as a mimic of MTSL on the distal ubiquitin) is shown in figure 3.2a. In the presence of the paramagnetic spin label, signals for residues 8–13, 34–42, and 69–72 were completely attenuated. By converting the attenuations into distance constraints, the position of the MTSL's unpaired electron was found to be near residue 36, as expected. The back-calculated PRE attenuation profile is in excellent agreement with experiment. When MTSL was attached to I36C of the distal ubiquitin in K11-Ub₂, a significant number of attenuations ($I/I_0 < 0.5$) were observed for signals in the proximal ubiquitin (figure 3.2b), particularly for residues 7–14, 33–41, and 69–76.

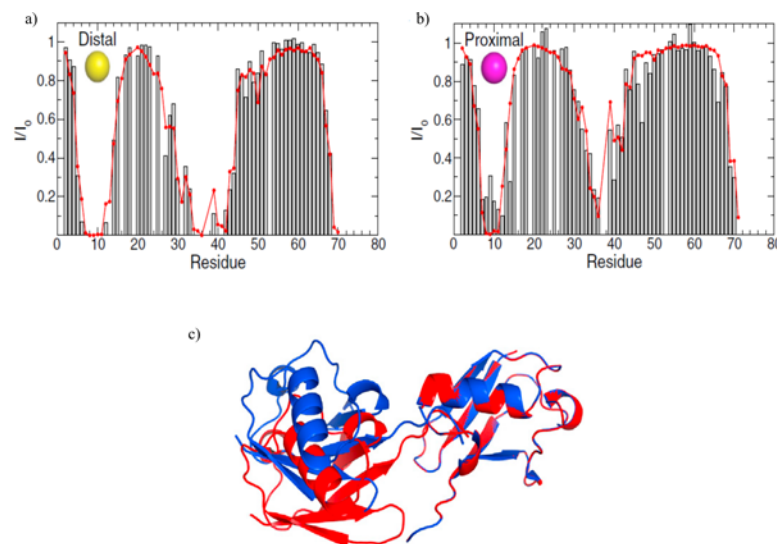


Figure 3.2 PRE effects from MTSL attached to I36C- experimental (gray bars) and back-calculated (red line) attenuation profiles for the I36C-MTSL-Ub a) distal ubiquitin; b) proximal ubiquitin; c) RDC-derived solution structures of K11-Ub2 in 0 mM (blue) and 150 mM NaCl (red) superimposed by the proximal Ub (figure from¹⁰⁵).

The PRE attenuations and the back-calculated MTSL's positions for both ubiquitin domains were mapped onto the two putative RDC-derived structures¹⁰⁵. The results indicate that of the two structures, only one complies with the distance constraints imposed by the PREs. The relative positioning of the two ubiquitin domains was optimized by translating one ubiquitin along the z axis of the alignment tensor such that the spin label positions overlapped. Using this structure and the PREs for both the distal and proximal ubiquitin taken together, the back-calculated PRE attenuation profile for K11-Ub2 is in excellent agreement with the experimental data¹⁰⁵.

3.4 Summary

We determined the three-dimensional solution structure of K11-Ub2 (figure 3.2c) using experimental data presented here namely CSPs, PREs and additionally

RDCs, ^{15}N relaxation rates and SANS¹⁰⁵. These studies revealed unique structural and dynamical properties of K11-Ub₂. There is a marked difference between the solution structure of K11-Ub₂ and the recently published crystal structures^{57,113}. The interdomain interface observed for K11-Ub₂ is unique. The small CSPs observed in the distal domain around the hydrophobic patch reflect the interaction between the two domains in K11-Ub₂. These contacts differ from K48-Ub₂, in which the hydrophobic patch residues on both domains comprise the interface¹⁰³. They also differ from K63-Ub₂ in which no interdomain contacts are present¹¹⁴. The excellent agreement between back-calculated PRE attenuation profile and experimental data along with structures derived from overall tumbling and molecular alignment suggest that these structures represent the predominant conformations for K11-Ub₂. Our solution structures and the crystal structures together depict the range of conformations possible for this linkage type under varying conditions. The diversity in biological roles observed for K11-linked polyubiquitin chains can be attributed to the range of conformations possible with this chain. However, more work needs to be done in order to understand the underlying relationship between structure and biological function. Studying these chains along with their cognate receptors may be important to understand the role of interdomain dynamics in the recognition process.

Chapter 4: An attempt to understand the molecular interaction between the anti-oncogenic protein ARF and the oncoprotein Mdm2

4.1 Background and Objective

Tight regulation of the levels of tumor suppressor protein p53 is essential for normal cellular growth and development¹¹⁵. The RING (Really Interesting New Gene) domain containing E3 ubiquitin protein ligase Mdm2 (Mouse double minute 2 homolog) is an important negative regulator of p53. Mdm2 antagonizes p53 function by various mechanisms including targeting p53 for proteasomal degradation¹¹⁶. Mdm2 forms a heterodimer with another RING finger E3 called MdmX and this complex is more efficient at regulating p53 levels¹¹⁷. However overexpression of Mdm2 causes inactivation of p53 leading to cancer. ARF (Alternative ReadinG Frame protein product of the *Ink4a* locus) blocks Mdm2 activity thereby promoting p53 stability¹¹⁸. ARF function is lost in over 75% of some tumor types¹¹⁸. An understanding of the structural details of the interaction between ARF and Mdm2 is important and has the potential for design of small molecule inhibitors of Mdm2 or ‘ARF mimetics’ for therapeutic use in ARF negative tumors¹¹⁹. We set out to study the details of the interaction between ARF and Mdm2/MdmX from a molecular and structural biology perspective.

We hypothesize that the inhibitory activity of ARF towards Mdm2 is due to inhibition of the E3 activity of Mdm2/MdmX by binding to regions N-terminal to the RING finger of Mdm2. ARF normally manifests its effects through allosteric effects on the RING finger of Mdm2, which negatively impacts critical RING finger

interactions with the ubiquitin conjugating enzyme (E2)-UbcH5b, necessary for E3 function. This inhibition impedes the activity of Mdm2/MdmX and also reveals the cryptic nucleolar localization signal in the Mdm2 RING finger, which physically separates Mdm2 from p53 within the nucleus^{120,121}. Based on the Mdm2-MdmX RING finger crystal structure¹²², we predict this cryptic signal to overlap the E2 binding site on the central α -helix of the Mdm2 RING finger.

4.2 Interaction of UbcH5b with ubiquitin

UbcH5b (a homologous member of the UbcH5 family¹²³) is one of the physiological E2s for Mdm2, which plays an important role in maintaining low levels of p53 and Mdm2 in unstressed cells¹²⁴. To set the stage for analyzing E2-E3 interactions between UbcH5b and Mdm2 using NMR spectroscopy, characterization of UbcH5b is a prerequisite. An ¹⁵N-isotope enriched GST-fused UbcH5b protein construct was expressed in *E.coli* BL21(DE3) cells and purified using affinity chromatography. The GST- tag was later cleaved using thrombin and an NMR sample was prepared at neutral pH using 20 mM Potassium phosphate, 150 mM KCl, 10 μ M ZnCl₂. ¹H-¹⁵N-HSQC spectrum (figure 4.1a) was collected with this sample that showed well resolved peaks which agreed with the BMRB entry #6277 for the solution structure of UbcH5b (PDB ID-1W4U). NMR relaxation measurements were carried out to get an idea about the overall shape and molecular tumbling. The average T1 relaxation time was determined to be 981.3 ± 13.4 ms (figure 4.1b), which is consistent with the tumbling of a compact globular molecule of 17-20 kDa^{103,125}, as expected for UbcH5b.

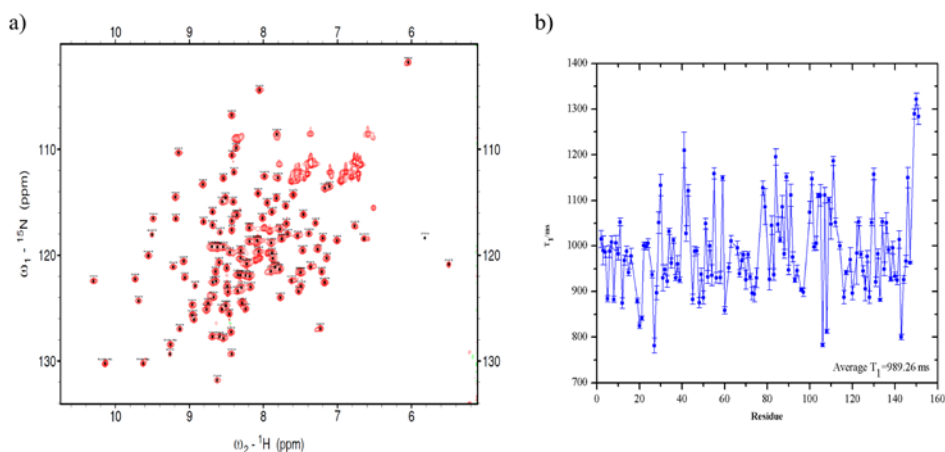


Figure 4.1 NMR studies with Ubch5b- a) ^1H - ^{15}N -HSQC spectrum of Ubch5b in 20mM Potassium phosphate, 150mM KCl, 10 μM ZnCl₂, pH 7.0; b) T1 relaxation data measured for Ubch5b

To get a generic idea of the binding surface on Ubch5b, we assessed its affinity for ubiquitin using NMR titration experiments. The average K_d for the interaction between ^{15}N -Ubch5b and ubiquitin was determined to be $120 \pm 23\mu\text{M}$, using a 1:1 stoichiometry binding model (figure 4.2b and c). This is two-fold stronger than the affinity reported for Ubch5c¹²⁶ (another homologous member of the Ubch5 family, figure 4.1a) and ubiquitin. Our study also demonstrates that the Ubch5 family of E2s bind ubiquitin at a site away from the active site¹²⁶ (figure 4.2d), and this site is away from the predicted binding surface for E3^{122,127} as illustrated in figure 4.2e. Therefore, the ubiquitin and E3 binding sites on E2 are nonoverlapping allowing both types of noncovalent interactions to occur simultaneously¹²⁶.

a)

Ubch5b	MALKRIHKELNGLARDPPAQCSAGPVGDDMFHQATIMGPNDSPYQGGVFFLTIHFPPTY	60
Ubch5c	MALKRINKELSDLARDPPAQCSAGPVGDDMFHQATIMGPNDSPYQGGVFFLTIHFPPTY	60
	*****:***:*****	
Ubch5b	PFKPPKVAFTTRIYHPNINSNGSICLDILRSQWSPALTISKVLLSICSLLCDPNPDDPLV	120
Ubch5c	PFKPPKVAFTTRIYHPNINSNGSICLDILRSQWSPALTISKVLLSICSLLCDPNPDDPLV	120
	*****:*****:*****	
Ubch5b	PEIARIYKTDREKYNRIAREWTQKYAM	147
Ubch5c	PEIARIYKTDREKYNRIAREWTQKYAM	147
	*****:*****:*****	

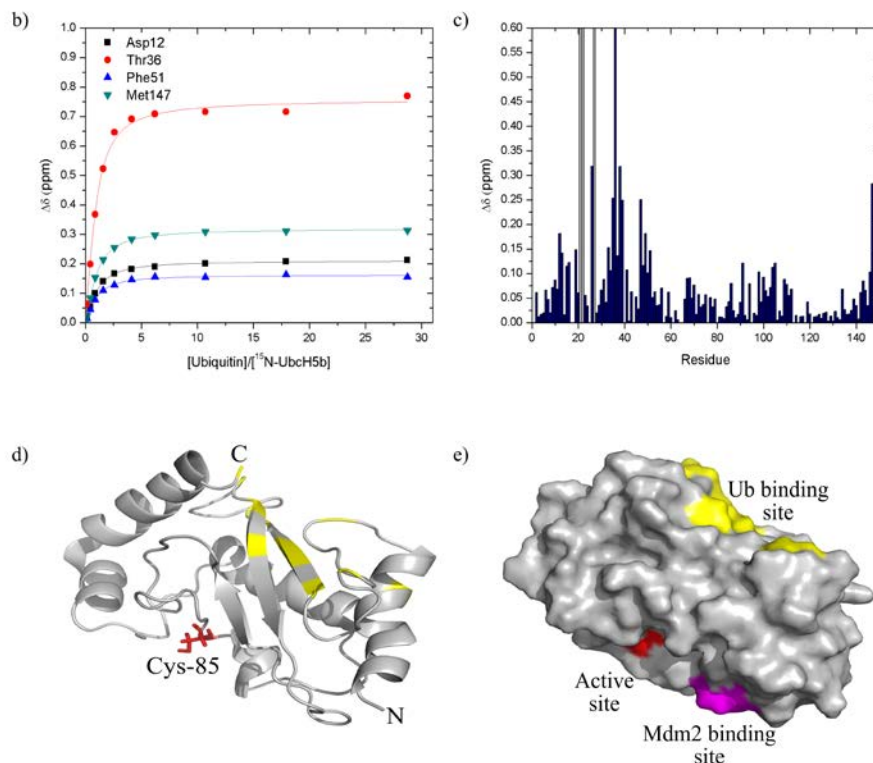


Figure 4.2 Binding surface for ubiquitin on UbcH5b a) sequence alignment for the homologous E2's UbcH5b and UbcH5c with their differences in blue, active site Cys in red. The residues on UbcH5c involved in interactions with ubiquitin are highlighted in yellow¹²⁶ while the residues on UbcH5b with CSPs > 0.15 are highlighted in green and residues with signal attenuations are highlighted in grey. b) Titration curves for ¹⁵N UbcH5b in 50 mM Tris, 120 mM NaCl, 1 mM DTT, pH 7.4 in the presence of wild type ubiquitin. c) CSP plot at the endpoint of titration for ¹⁵N UbcH5b with ubiquitin, with gray bars indicating signal attenuations. The concentration of ¹⁵N UbcH5b at the beginning and end of titration was 245 μ M and 150 μ M respectively. d) The ubiquitin binding surface for residues with CSPs > 0.15 are shown in yellow on UbcH5b (PDB ID- 1W4U). e) Surface representation of UbcH5b with the active site cysteine in magenta, ubiquitin binding surface in yellow and the predicted Mdm2 binding site in magenta.

4.3 Attempts to obtain stable Mdm2/MdmX RING proteins for solution NMR

Before assessing the allosteric effects of ARF on Mdm2 interactions with UbcH5b, we set out to characterize the E2-E3 interactions between UbcH5b and Mdm2. The human Mdm2 protein (Hdm2) is a multidomain protein (figure 4.3) comprising an N-terminal p53 binding domain, short sequences that encode the nuclear localization signal (NLS) and nuclear export signal (NES), a middle domain

composed of acidic residues which is the interaction site for ARF and ribosomal proteins, a zinc finger domain and the C-terminal ring finger domain with a nucleolar localization signal (NoLS)¹⁵. The C-terminal RING finger domain is responsible for its E3 ligase activity, ATP binding, homodimerization, heterodimerization with MdmX (also known as Mdm4 and HdmX in humans), autoubiquitination and interaction with the E2¹²⁸ UbcH5b. MdmX also has a C-terminal RING domain that does not have intrinsic E3 ligase activity and does not homodimerize¹²⁹. Mdm2 and Mdmx form heterodimers through their C-terminal RING domains with interactions occurring between β -strands in one RING domain and C-terminal residues in the other subunit¹²².

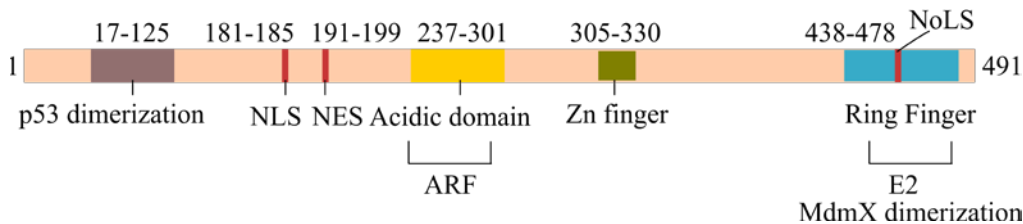


Figure 4.3 Schematic representation of Mdm2 domain organization- MdmX also has a similar domain structure except for the lack of nuclear localization signal (NLS), nuclear export signal (NES) and nucleolar localization signal (NoLS) found in Mdm2. The proteins known for interacting with specific domains are listed below them (figure adapted from¹⁵)

We utilized several fusion constructs of human Mdm2 and MdmX (table 4.1) for the bacterial expression of the mammalian proteins. Mdm2/MdmX (pGEX6p1 and pCOLA Duet-1) and UbcH5b (pGEX-KG) plasmids were provided by the Weissman lab (National Cancer Institute, NCI) and the other constructs were generated in-house. A Trp residue was inserted past the SUMO cleavage site in 6xHis-SUMO-MdmX, to enable the determination of reliable protein concentration. Overexpression of the proteins was observed for all of the Mdm2 and MdmX

constructs. The proteins were purified from cell lysates using standard protocols for affinity chromatography followed by proteolytic cleavage of the fusion tag and further purified using gel filtration chromatography. The Mdm2 constructs without a fusion tag were purified using a protocol from previous studies on Mdm2¹³⁰. ¹⁵N isotope enriched proteins were generated for solution NMR studies.

Protein	Plasmid	Affinity tag	Protease
GST-Mdm2-full length	pGEX6p1	GST	PreScission protease
GST-Mdm2 (200-300)	pGEX6p1	GST	PreScission protease
GST- Mdm2 (399-491)	pGEX6p1	GST	PreScission protease
GST- Mdm2 (417-491)	pGEX6p1	GST	PreScission protease
GST- Mdm2 (429-491)	pGEX6p1	GST	PreScission protease
GST-Mdm2 (350-443)	pGEX6p1	GST	PreScission protease
His-Ub-Mdm2 (417-491)	pET3a	6xHis-Ubiquitin	YUH1
SUMO-Mdm2 (417-491)	pET SUMO	6xHis-SUMO	ULP1
Mdm2 (411-491)	pCOLA Duet-1	-	-
GST-MdmX (421-490)	pGEX6p1	GST	PreScission protease
SUMO-MdmX- W (421-490)	pET SUMO	6xHis-SUMO	ULP1

Table 4.1- Plasmid constructs of human Mdm2 and MdmX used in the study

¹H-¹⁵N SOFAST-HMQC spectra of several of the Mdm2 proteins revealed a cluster of peaks centered around 8.3 ppm indicating a predominantly unfolded conformation (figure 4.4a). In order to ascertain whether unfolding was arising during protein purification from *E.Coli*, we carried out in-cell NMR experiments which also showed similar characteristics (figure 4.4b). Consequently, we could not detect any CSPs in the ¹H-¹⁵N SOFAST-HMQC spectra of UbH5b in the presence of Mdm2. Stepwise refolding experiments with Mdm2 after denaturation with 6 M guanidine hydrochloride did not increase the percentage of folded conformers in solution. Although MdmX overexpressed in *E.coli*, this protein was less stable than Mdm2 while handling and showed a tendency to precipitate in solution. Since Mdm2

predominantly exists as a heterodimer with MdmX *in vivo*¹¹⁷, we co-purified the two proteins from bacterial cell lysates with the intention of obtaining a stable and active complex. However we could not detect binding of the co-purified proteins to UbcH5b from NMR experiments. Expression of intact mammalian proteins in bacterial cells is not always straightforward since bacterial cells are fairly simple and may not have all of the components required for their assembly such as chaperones. The exact requirements for the intact expression of Mdm2/MdmX proteins in bacterial cells remains to be determined.

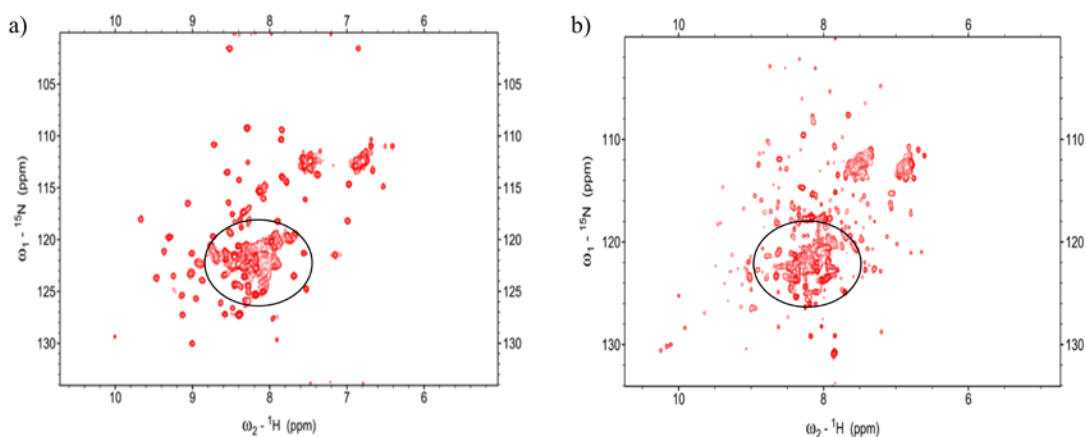


Figure 4.4 ^1H - ^{15}N SOFAST-HMQC spectra of Mdm2- a) 6xHis-SUMO-Mdm2 (417-491) in 50 mM Tris, 120 mM NaCl, 20 mM Imidazole, 1 mM TCEP, pH 7.4. The well resolved peaks that are spread out mostly belong to SUMO as verified from a SUMO-only spectrum, while the majority of clustered peaks indicated by the circle belong to Mdm2; b) GST-Mdm2 (399-491) in cell lysate with 50 mM Tris, 120 mM NaCl, 5 mM DTT, pH 7.4. Here the well resolved and spread out signals may belong to other small proteins in the cell lysate while the cluster of peaks in the center mostly belongs to Mdm2.

4.4 Cloning and expression of ARF

Full-length human ARF protein from the mammalian expression plasmid pcDNA3.1 from the Vousden lab was cloned into the *E. coli* expression plasmid pTXB1 to be expressed as a fusion protein with chitin binding domain (CBD) at the

C-terminus. The fusion protein did not express in *E.coli* BL21(DE3) cells in LB at various growth temperatures between 25-37 °C and IPTG induction from 0.05-1 mM. A SUMO fusion construct was made by inserting the human ARF protein into pET SUMO plasmid. Since it has been previously shown that the N-terminal 62 amino acid residues are sufficient for all the known functions of ARF and that the N-terminal 37 residues of ARF are sufficient for interaction with Mdm2¹²¹, we made short truncations of the SUMO fusion protein that included either the first 62 or 37 N-terminal residues of ARF. However *E.coli* cells did not express the fusion protein. The plasmid DNA sequence for ARF was later re-examined to detect the presence of rare codons that are not used frequently in *E.coli* using the rare codon calculator (RaCC) from the NIH MBI laboratory for structural genomics and proteomics. This analysis indicated the presence of 9 rare Arg codons (including one double repeat), 2 rare Leu codons, 2 rare Pro codons along with 11 other rare codons. The large number of rare codons in the ARF DNA sequence may not be recognized by the most abundant bacterial tRNAs which in turn could result in the severely diminished expression that was observed. Therefore, the plasmid DNA sequence encoding this protein has to be redesigned to include preferred bacterial codons.

4.5 Summary

We determined the K_d for UbcH5b binding to ubiquitin as $120 \pm 23 \mu\text{M}$ from a 1:1 binding model. This is twofold stronger compared to the interaction of ubiquitin with UbcH5c (a homologue of UbcH5b). The binding surface for ubiquitin on UbcH5b is away from both the active site as well as the putative Mdm2 binding site, allowing for the simultaneous interaction with both proteins. Several Mdm2/MdmX

protein variants were predominantly in an unfolded conformation after purification from bacterial cell lysates. As a result, we could not detect their interaction with UbcH5b. Expression of intact mammalian proteins in bacterial cells is not always straightforward since bacterial cells are fairly simple and may not have all of the components required for their assembly such as chaperones. The exact requirements for the intact expression of Mdm2/MdmX proteins in bacterial cells remains to be determined. Several constructs of human ARF protein did not overexpress in bacterial cells. Careful examination of the DNA sequence encoding the protein revealed the presence of a large number of rare codons that cannot be recognized by *E.Coli* tRNAs. Therefore, the plasmid DNA sequence encoding this protein has to be redesigned to include preferred bacterial codons. The structural details of the vital interaction between human UbcH5b, Mdm2/MdmX and ARF proteins remains to be elucidated.

Chapter 5: Thioredoxin and ubiquitin proteasome system

5.1 Background and objective

Thioredoxin (Trx), thioredoxin reductase (TrxR) and NADPH constitute the thioredoxin system. The thioredoxin system plays a key role in DNA synthesis as well as defense against oxidative stress and apoptosis or redox signaling with reference to many diseases¹³¹. Human thioredoxin is a small (12 kDa) redox protein that reduces oxidized cysteine groups in proteins. It has many biological functions including the supply of reducing equivalents to thioredoxin peroxidases and ribonucleotide reductase (DNA replication), the regulation of transcription factor activity, and the regulation of enzyme activity by heterodimer formation¹³². Recent evidence from yeast indicates that members of the thioredoxin family interact with the 20S proteasome, indicating redox regulation of proteasome activity¹³³. However, there is little information about the interrelationship of thioredoxin proteins with the proteasome system in mammalian cells, especially in the nucleus.

A recent study showed that *Salmonella* was able to trigger cell death and inhibit thioredoxin activity in HeLa cells several hours post-infection via the *Salmonella* effector protein, SlrP¹³⁴. This study assigned a functional role to SlrP as a binding partner and an E3 ubiquitin ligase for mammalian thioredoxin¹³⁴.

We set out to determine the effect of ubiquitination on thioredoxin as a model system and study the effect on its structure, redox activity as well as to understand whether the site of ubiquitination on thioredoxin programs its fate.

5.2 Thioredoxin in solution

Thioredoxin (C73S mutant human protein in pQE30, hTrx) plasmid was provided by Prof. Katja Becker (Institute for Nutritional sciences, Germany). The C73S mutation prevents undesirable thioredoxin dimer formation while retaining redox activity^{135,136}. The fusion protein with a 6xHis tag was initially purified using immobilized-metal affinity chromatography (IMAC) followed by gel filtration chromatography. NMR sample of the purified protein was prepared in 20 mM sodium phosphate, pH 6.8. ¹H-¹⁵N SOFAST-HMQC experiment showed well resolved peaks for this protein at 295.4 K. An approximate peaklist for all of the resonances in the spectrum was generated using the BMRB entry 255 for the solution structure of human recombinant thioredoxin¹³⁷.

5.3 Invitro ubiquitination of thioredoxin using an E3 ligase- SlrP

Thioredoxin was enzymatically ubiquitinated using the Ub activating enzyme (E1), Ub conjugating enzyme (E2)-UbcH5b, Ub and the Ub ligase (E3)-SlrP. The Slrp (pGEX) plasmid was provided by Prof. Francisco Ramos-Morales (Universidad de Sevilla, Spain). Ubiquitinated thioredoxin was separated from thioredoxin using gel filtration chromatography (figure 5.2d) and their molecular masses were confirmed by electrospray ionization mass spectrometry (ESI-MS) (12,986.4 Da versus 12,988.7 Da expected for thioredoxin; 21,550 Da versus 21,535.7 Da expected for ubiquitinated thioredoxin) (figure 5.1a,b). The monoubiquitinated thioredoxin sample was subjected to tryptic digestion which indicated that the sample had a mixture comprising of thioredoxin with ubiquitin on multiple lysines, the most predominant ones being Lys8 and Lys96 (figure 5.1c). The yield of ubiquitinated

thioredoxin from enzymatic reactions was minimal (figure 5.2a,b,d). Optimization attempts by varying the enzyme concentrations and setting up ligations at different temperatures did not improve the yield. Chemical methods to attach ubiquitin^{112,138} to thioredoxin were tested. A small-scale ligation reaction with alloc protected Ub-COSR and thioredoxin in DMSO showed multiple monoubiquitination on the different lysine residues in thioredoxin (figure 5.2e). However, stability of thioredoxin to some of the harsher steps in the process is yet to be tested.

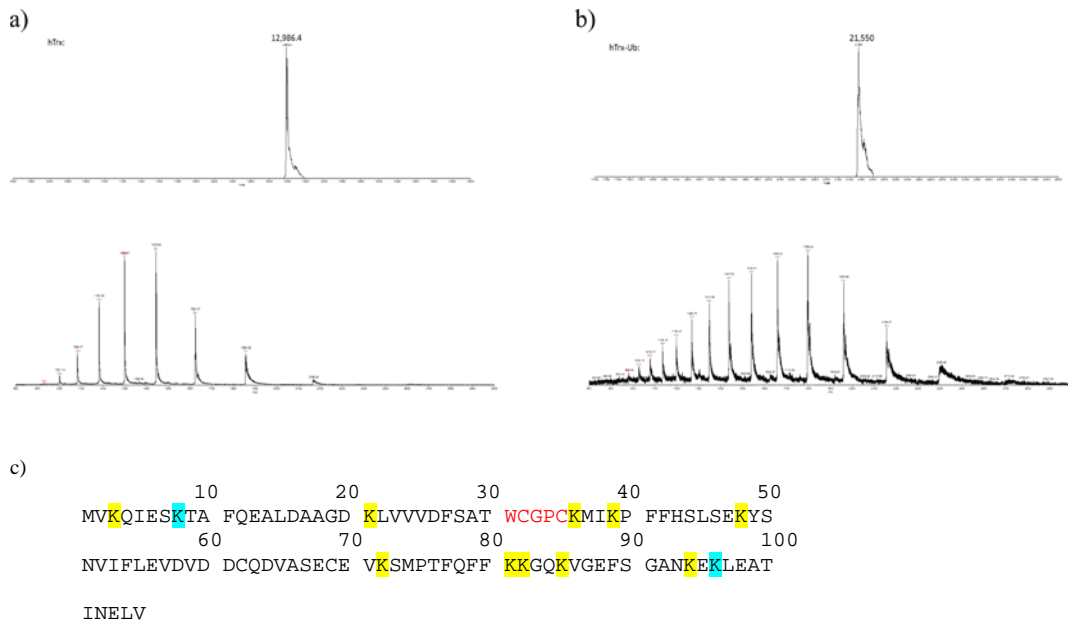


Figure 5.1 Mass chromatograms for thioredoxin- a) The molecular mass of thioredoxin is 12,986.4 Da versus 12,988.7 Da expected; b) the mass of monoubiquitinated thioredoxin is 21,550 Da versus 21,535.7 Da expected; c) Amino acid sequence for human thioredoxin with all of the Lys residues highlighted in yellow while the ubiquitinated Lys residues are highlighted in cyan and the active site is in red.

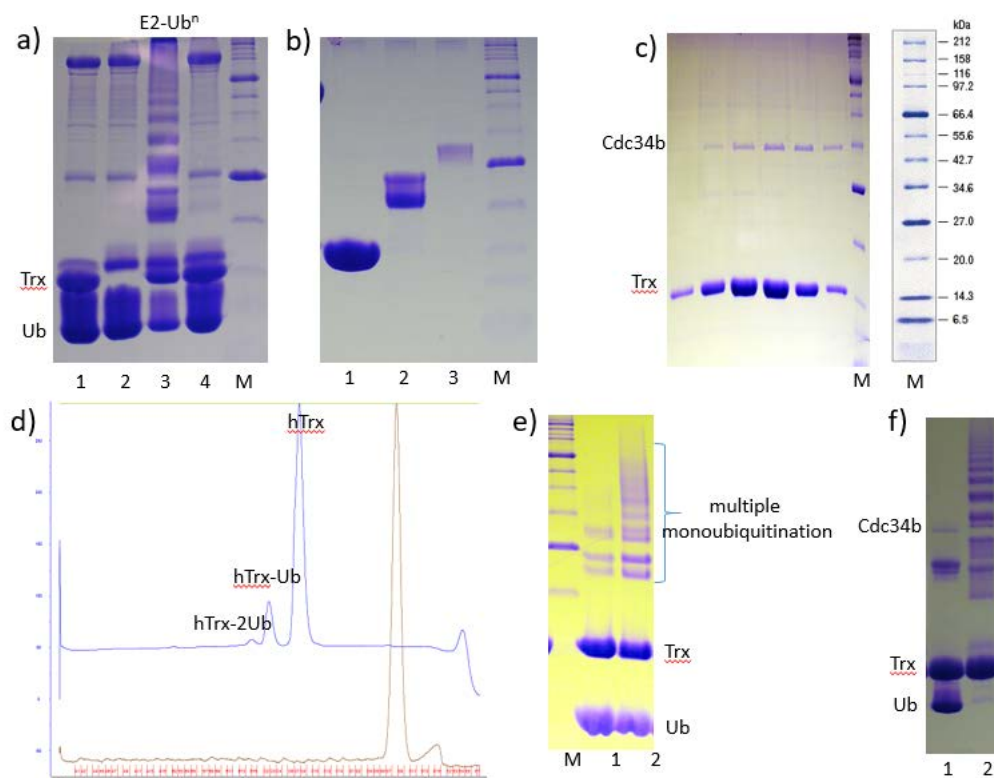


Figure 5.2 Ubiquitination of thioredoxin- **a)** enzymatic reactions to generate ubiquitinated thioredoxin using the E3-SlrP – SDS-PAGE gel shows reaction mixture with 1) no E1, 2) no hTrx, 3) no SlrP, 4) complete reaction mixture after ~20 hrs; **b)** final stock solutions of SEC purified fractions from enzymatic reaction mixture on a 15% SDS-PAGE gel - 1) hTrx, 2) hTrx-Ub, 3) hTrx-2Ub; **c)** the gel depicts various fractions from SEC co-elution of Cdc34b and hTrx; **d)** SEC elution profile for the separation of hTrx from its ubiquitinated counterparts; **e)** Chemical methods to ubiquitinate thioredoxin using alloc protected Ub-COSR – 1) pre-ligation reaction mixture in DMSO, 2) ligation reaction mixture after ~16 hrs of reaction shows higher molecular weight species indicating multiple monoubiquitination on the numerous Lys residues on hTrx; **f)** hTrx ubiquitination with Cdc34b- 1) reaction mixture without E1, 2) complete reaction mixture after ~20 hrs; M- (2-212 kDa) protein marker from NEB.

5.4 Interaction of thioredoxin with Cdc34b

In our attempts to optimize ubiquitination of thioredoxin substituting different E2 enzymes in the ubiquitination assays, it was observed that thioredoxin interacts selectively with human Cdc34b, an E2 which is known for its key role in cell cycle regulation¹³⁹. Cdc34b (pET11b) plasmid was provided by Professor Gary Kleiger (University of Nevada). The interaction between thioredoxin and Cdc34b was

inferred based on co-elution of the two proteins from size exclusion chromatography (figure 5.2c). This finding is very exciting as it could indicate cross-talk between two major signaling pathways in the cell- the ubiquitin proteasome system and redox regulation. The interaction between thioredoxin and Cdc34b was further analyzed using NMR titration experiments.

The average K_d for the interaction between oxidized thioredoxin and Cdc34b was determined to be $40 \pm 7 \mu\text{M}$ from CSP analysis (figure 5.3) based on the assumption that Cdc34b has two binding sites for thioredoxin. A 1:1 binding model fit the data poorly (giving systematic deviations in residuals of all residues) but a 2:1 model fit well. Therefore we assumed that the stoichiometry is 2:1. A future, more detailed analysis will be required to characterize the interaction in detail. Chemical shift perturbations were observed in the ^1H - ^{15}N SOFAST- HMQC spectra of thioredoxin (for both oxidized and reduced states) in the presence of Cdc34b (figure 5.4). This suggests that the oxidation state of thioredoxin may not be important for the interaction with Cdc34b. The high affinity interaction with thioredoxin does not seem to interfere with the enzyme activity of Cdc34 based on *in vitro* ubiquitination assays (figure 5.2f). Although oxidation of Cdc34 occurs under oxidative stress¹⁴⁰, currently there is very little information in the literature suggesting direct interaction between the thioredoxin system and Cdc34. The biological significance of this interaction remains to be elucidated.

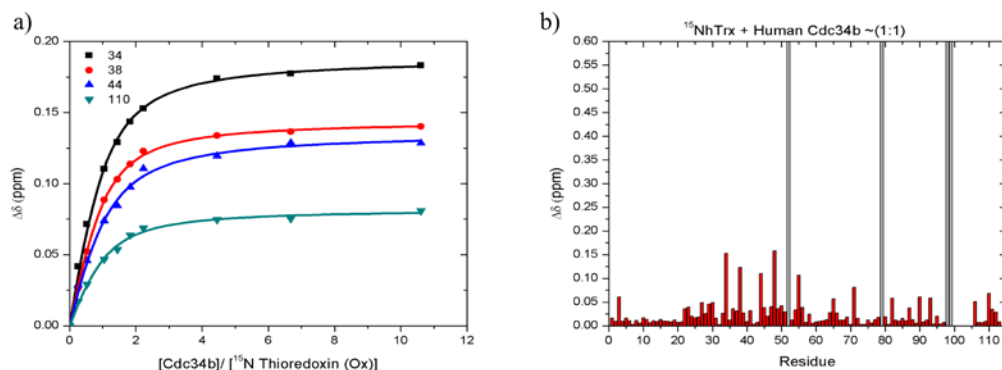


Figure 5.3 Titration curves and CSP plot* for thioredoxin binding to Cdc34b- * the residue assignment is not accurate, and the plots are shown to indicate the overall magnitudes of the CSPs; the grey bars indicate residues that show signal attenuations arising due to binding.

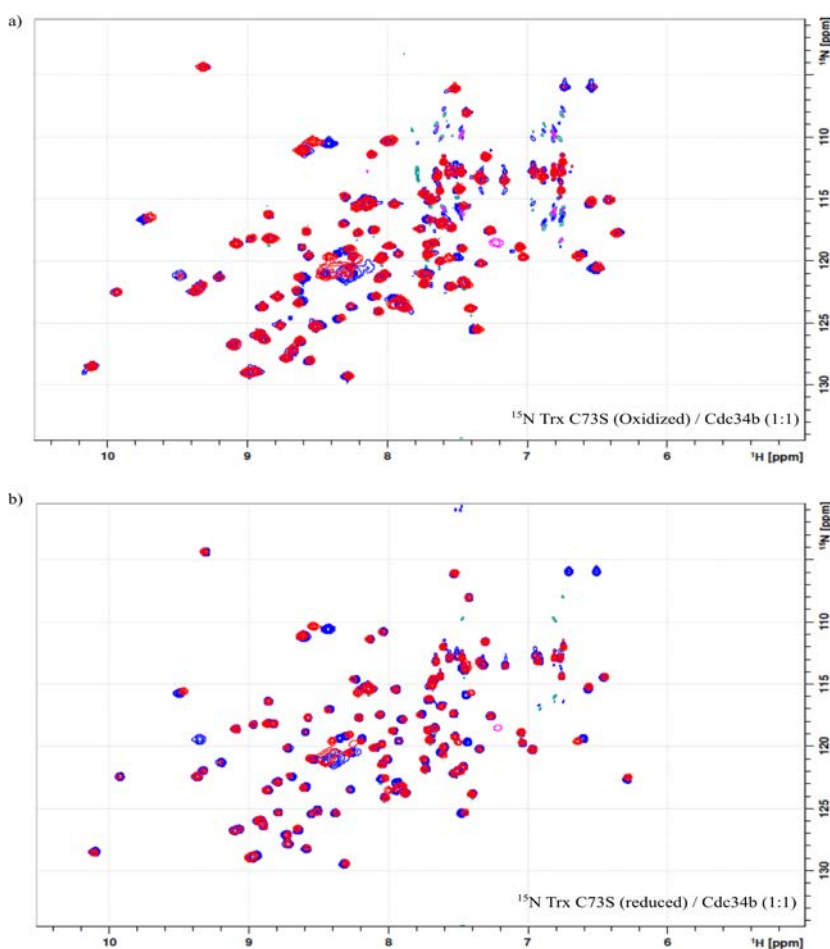


Figure 5.4 ^1H - ^{15}N HMQC SOFAST spectra of thioredoxin binding to Cdc34b- Thioredoxin spectra in blue overlaid with thioredoxin in the presence of Cdc34b (red) at a concentration of 87 μM each - a) Thioredoxin (oxidized) b) Thioredoxin (reduced).

5.5 Summary

Thioredoxin is amenable for solution NMR studies. Enzymatic ubiquitination of thioredoxin resulted in minimal yield, despite efforts to optimize the reaction. Tryptic digestion of monoubiquitinated thioredoxin indicated the possibility of ubiquitination at multiple lysine residues on thioredoxin including Lys8 and Lys96. Our attempts to optimize the enzymatic yield of ubiquitinated thioredoxin by varying the E2 enzymes revealed a novel and unexpected high affinity interaction between thioredoxin and the E2 Cdc34b, implicated in cell cycle regulation. This finding is very exciting as it could indicate cross-talk between two major signaling pathways in the cell- the ubiquitin proteasome system and redox regulation. Currently, there is very little information in the literature suggesting direct interaction between the thioredoxin system and Cdc34. The biological significance of this interaction remains to be elucidated.

Chapter 6: Summary and scope for future studies

6.1 Structural characterization of interaction of K11 and K63 mixed-linkage

polyubiquitin chains with the tandem UIMs of epsin1

Ubiquitylation of membrane surface receptor proteins plays a very important role in regulating receptor-mediated endocytosis as well as endosomal sorting for lysosomal degradation⁹¹. Epsin1 is an endocytic adaptor protein with three tandem UIMs (Ubiquitin Interacting Motifs) which are responsible for the highly specific interaction between epsin and ubiquitylated receptors. Epsin1 is also an oncogenic protein and its expression is upregulated in some types of cancer⁹⁷. Recently it has been shown that novel K11 and K63 mixed-linkage polyubiquitin chains serve as internalization signal for MHC I (Major Histocompatibility Complex I) molecule through their association with the tUIMs of epsin1^{49,98}. However the molecular mode of action and structural details of the interaction between polyubiquitin chains on receptors and tUIMs of epsin1 is yet to be determined. This information is crucial for the development of anticancer therapeutics targeting epsin1.

Our study illustrates that branched K11 and K63 mixed-linkage polyubiquitin chains retain the structural properties of their K11 and K63 components. Epsin1 tUIMs bind monoubiquitin very weakly and they exhibit preferential binding to chains of different linkages, with the strongest affinity for K63-Ub₂, followed by K11-Ub₂ and lastly K48-Ub₂. Epsin1 tUIM-23 binds avidly with a domain-specific orientation across K63-Ub₂, wherein UIM-2 interacts with the proximal domain of K63-Ub₂. Epsin1 tUIM-12 binds both K63-, and K11-Ub₂ with similar affinities with no domain-specific interaction across K11-Ub₂. The linker region between the tUIMs

is critical for linkage-dependent polyubiquitin recognition. Our results support the hypothesis that in addition to the length of the tUIM linker region, its composition also determines the selective recognition of K63-Ub₂. Epsin1 tUIMs do not distinguish between mixed-linkage branched and unbranched polyubiquitin chains. Our NMR binding studies carried out in the absence and presence of NaCl, revealed that in addition to the canonical hydrophobic patch residues of ubiquitin, electrostatic interactions play a major role in the molecular recognition of polyubiquitin by the tUIMs of epsin1. The interdomain dynamics exhibited by polyubiquitin chains of a specific-linkage type could determine the potential for electrostatic interactions with putative binding partners, which might partially explain the different affinities of K11-, and K63-Ub₂ observed for tUIMs of epsin1. These results provide the first glimpse of the mechanism behind specific recognition of complex mixed polyubiquitin signals by a multivalent receptor with three tandem UIMs.

As a precedent for in depth atomic-level analysis of the structural details of the interaction between epsin1 tUIMs and polyubiquitin chains, we collected a series of 3D triple resonance experiments for the tUIMs of epsin1. We also identified a few potential leads for optimizing crystallization conditions for the epsin1 tUIM-K63-Ub₂ complex, in preparation for X-ray crystallography. The resonance assignment for the tUIMs would enable further examination of the specific residues in the tUIMs that form the binding interface with K11-, and K63-Ub₂. This information would prove to be useful for further analysis using site-directed mutagenesis and solution structure studies to determine the role of electrostatics in molecular recognition between the tUIMs and ubiquitin. It would be interesting to analyze the interaction between epsin1

tUIMs and K6-Ub₂, which was shown to have a compact conformation¹⁴¹ along with other atypical polyubiquitin chains to better understand the role of unique interdomain dynamics among polyubiquitin chains of different linkage types.

6.2 Structural studies of K11-linked polyubiquitin chains

K11-linked polyubiquitin chains have been implicated to play an important role in regulating cell cycle^{31,57}. Recently a quantitative MS study has highlighted that K11-linked polyubiquitin chains are as abundant as K48-linked polyubiquitin in the cellular milieu⁸. We set out to determine the solution structure of K11-Ub₂ in order to understand the structural basis for these chains to serve as unique cellular signals.

We determined the three-dimensional solution structure of K11-Ub₂ based on experimental data including CSPs and PREs. These studies revealed unique structural and dynamical properties of K11-Ub₂. There is a marked difference between the solution structure of K11-Ub₂ and the recently published crystal structures (PDB IDs- 3NOB and 2XEW). The interdomain interface observed for K11-Ub₂ is unique. The excellent agreement between back-calculated PRE attenuation profile and experimental data along with structures derived from overall tumbling and molecular alignment suggest that these structures represent the predominant conformations for K11-Ub₂. Our solution structures and the crystal structures together depict the range of conformations possible for this linkage type under varying conditions. The diversity in biological roles observed for K11-linked polyubiquitin chains can be attributed to the range of conformations possible with this chain. However, more work needs to be done in order to understand the underlying relationship between structure and biological function. Studying these chains along with their cognate

receptors may be important to understand the role of interdomain dynamics in the recognition process.

6.3 An attempt to understand the molecular interaction between the anti-oncogenic protein ARF and the oncoprotein Mdm2

Tight regulation of the levels of tumor suppressor protein p53 is essential for normal cellular growth and development¹¹⁵. Overexpression of the RING E3 ligase Mdm2 causes inactivation of p53 leading to cancer. ARF blocks Mdm2 activity thereby promoting p53 stability and its function is lost in over 75% of some tumor types¹¹⁸. We set out to study the details of the interaction between ARF and Mdm2/MdmX from a molecular and structural biology perspective.

We determined the K_d for the noncovalent binding of ubiquitin by UbcH5b as $120 \pm 23 \mu\text{M}$ from a 1:1 binding model. This is twofold stronger compared to the noncovalent interaction of ubiquitin with UbcH5c (a homologue of UbcH5b). The noncovalent binding surface for ubiquitin on UbcH5b is away from both the active site as well as the putative Mdm2 binding site, allowing for the simultaneous interaction with both proteins. Several Mdm2/MdmX protein variants were predominantly in an unfolded conformation (as revealed from NMR studies), after purification from bacterial cell lysates. As a result, we could not detect their interaction with UbcH5b. Expression of intact mammalian proteins in bacterial cells is not always straightforward since bacterial cells are fairly simple and may not have all of the components required for their assembly such as chaperones. The exact requirements for the intact expression of Mdm2/MdmX proteins in bacterial cells remains to be determined. Several constructs of human ARF protein did not

overexpress in bacterial cells. Careful examination of the DNA sequence encoding the protein revealed the presence of a large number of rare codons that cannot be recognized by *E.Coli* tRNAs. Therefore, the plasmid DNA sequence encoding this protein has to be redesigned to include preferred bacterial codons. The structural details of the vital interaction between human UbcH5b, Mdm2/MdmX and ARF proteins remains to be elucidated.

6.4 Thioredoxin and ubiquitin proteasome system

Thioredoxin, thioredoxin reductase and NADPH constitute the thioredoxin system. The thioredoxin system plays a key role in DNA synthesis as well as defense against oxidative stress and apoptosis or redox signaling with reference to many diseases¹³¹. Currently, there is little information about the interrelationship of thioredoxin proteins with the proteasome system in mammalian cells. We set out to determine the effect of ubiquitination on thioredoxin as a model system and study the effect on its structure, redox activity as well as to understand whether the site of ubiquitination on thioredoxin programs its fate.

Thioredoxin is amenable for solution NMR studies. Enzymatic ubiquitination of thioredoxin resulted in minimal yield, despite efforts to optimize the reaction. Tryptic digestion of monoubiquitinated thioredoxin indicated the possibility of ubiquitination at multiple lysine residues on thioredoxin including Lys8 and Lys96. Our attempts to optimize the enzymatic yield of ubiquitinated thioredoxin by varying the E2 enzymes revealed a novel and unexpected high affinity interaction between thioredoxin and the E2 Cdc34b, implicated in cell cycle regulation. This finding is very exciting as it could indicate cross-talk between two major signaling pathways in

the cell- the ubiquitin proteasome system and redox regulation. Currently, there is very little information in the literature suggesting direct interaction between the thioredoxin system and Cdc34. The biological significance of this interaction remains to be elucidated.

Chapter 7: Methods and materials

7.1 Protein expression and purification

All of the constructs used in this work encode human proteins (except for the yeast proteins MMS2 and Ubc13) in commercially available DNA plasmids for expression in *E.Coli* cells. The plasmids were propagated in DH5 α cells and expressed in BL21(DE3) variants. The different protein constructs used in this work are listed in table 7.1. Additional cloning was carried out mostly using site directed mutagenesis and where necessary using restriction digestion and ligation.

The E2 Ube2S (pMAL) plasmid was provided by Professor Michael Rape (University of California, Berkeley). A C-terminal truncation Ube2S Δ C (M1-G156) was cloned to improve the yield of free K11-Ub₂¹⁴² in enzymatic reactions.

The epsin1 fusion proteins comprising tUIMs- GB1 and tUIMs-Cys_at_N-terminus (pET28) plasmids were provided by Professor Robert Cohen (Colorado State University). A Tyr residue was inserted N-terminal to the tUIMs past the thrombin cleavage site adjacent to the 6xHis tag (figure 7.1), to enable quick and reliable determination of protein concentration.

Epsin1 tUIMs with Tyr at N-terminus (pET28):

MPSSHHHHHSSGLVPRGS **MQSSG** **EEELQLQLALAMSKEEADQPPSCGP** **EDDAQLQLALSLSREEHDKEERIRRGDDLRLQMAIEESKRETGGKEES**

Epsin1 tUIMs with Cys at N-terminus (Cohen lab, pET28):

Q **SG** **EEELQLQLALAMSKEEADQPPS** **SG** **PEDDAQLQLALSLSREEHDKEERIRRGDDLRLQMAIEESKRETGGKEES**

Epsin1 tUIM-12 with Cys at N-terminus (pET28):

Q **SG** **EEELQLQLALAMSKEEADQPPS** **SG** **PEDDAQLQLALSLSREEHDKEERIRR**

Epsin1 tUIM-23 with Cys at N-terminus (pET28):

QSSG**PS****C**GP**EDDAQLQLALSLSREEHDKEERIRRGDDLRLQMAIEESKRETGGK**EES

Epsin1 tUIM-23 with Cys at C-terminus (pET28):

QSSG**PS****S**GP**EDDAQLQLALSLSREEHDKEERIRRGDDLRLQMAIEESKRETGGK**EE**C**

Figure 7.1 Amino acid sequences of various epsin1 tUIM constructs- mutations are highlighted in green

Protein	Plasmid	Affinity tag
Ubiquitin (Ub)- wild type	pET3a	-
D77 Ub	pET3a	-
K11R Ub	pET3a	-
K63R Ub	pET3a	-
K11RK63R Ub	pET3a	-
K63RD77 Ub	pET3a	-
K11RD77 Ub	pET3a	-
K11RK63RI36C Ub	pET3a	-
Epsin1 tUIMs-GB1	pET28	6xHis
Epsin1 tUIMs-Cys_at_N-terminus	pET28	6xHis
Epsin1 Y-tUIMs	pET28	6xHis
Epsin1 Y-tUIM-12	pET28	6xHis
Epsin1 Y-tUIM-23	pET28	6xHis
Epsin1 Y-tUIM-13-LR1	pET28	6xHis
Epsin1 Y-tUIM-13-LR2	pET28	6xHis
Epsin1 Y-tUIM-12-Cys_at_N-terminus	pET28	6xHis
Epsin1 Y-tUIM-23-Cys_at_C-terminus	pET28	6xHis
Epsin1 Y-tUIMs-Cys_at_N-terminus	pET28	6xHis
Epsin1 Y-tUIMs-Cys_at_C-terminus	pET28	6xHis
E1	pET15b	6xHis
MMS2	pGEX	GST
Ubc13	pGEX4T2	GST
Ube2S	pMAL	MBP-6xHis
Ube2SΔC	pMAL	MBP-6xHis
E2-25K	pGEX4T2	GST
UbcH5b	pGEX-KG	GST

Table 7.1 Protein constructs used in this work

Ubiquitin and its mutants were expressed in *E.Coli* pJY2 strain. The proteins were expressed and purified as described previously¹¹⁴. Unlabeled epsin1 tUIM variants were expressed in *E.Coli* BL21(DE3) cells in LB media. The cells were induced at OD₆₀₀ ~0.8 with 1 mM IPTG and grown for ~18 hrs overnight at 16 °C. The cells were harvested and resuspended in lysis buffer (Phosphate buffer saline-

PBS, 0.5 M NaCl, 20 mM Imidazole, pH 7.4 along with 0.02 % Triton X-100, 0.4 mg/mL lysozyme, protease inhibitors: 1 mM PMSF, 50 μ M TLCK, 5 μ g/mL STI, 2.5 μ g/mL leupeptin, 20 μ g/mL DNase1). The cell suspension was centrifuged in a preparative ultracentrifuge 45 Ti rotor for 25 minutes at 25,000 rpm. The soluble extract was loaded on a 5 mL HisTrap HP column (GE Lifesciences). Protein was eluted in PBS, 0.5M Imidazole, 0.5 M NaCl, pH 7.4. The purified protein was checked for its apparent molecular weight using a 15% SDS-PAGE gel, concentrated using a 3.5 kDa MWCO Amicon concentrator, exchanged into 20 mM sodium phosphate, pH 6.8 buffer. The protein was further purified using size exclusion chromatography and exchanged into NMR buffer (20 mM sodium phosphate, pH 6.8 with 130 mM NaCl where mentioned) and protein concentration was measured using the NanoDrop 2000c (Thermo Scientific). ^{13}C , ^{15}N enriched epsin1 Y-tUIMs (tUIM-12, tUIM-23 and full length tUIM) for 3D triple resonance NMR experiments were expressed in M9 media in BL21(DE3) cells. The rest of the growth and purification protocol for these proteins is similar to that described above.

His-tagged proteins E1 and Ube2S were expressed and purified using a similar methodology to that of epsin1 tUIMs with the exception of the final storage buffer (50 mM Tris, 1 mM DTT, pH 8). The final stocks were stored in small aliquots at -80°C.

Most of the GST-tagged proteins were expressed in *E.Coli* BL21(DE3) cells using LB media. The growth, induction and harvesting protocol is similar to the method described for epsin1 tUIMs. The exceptions are the differences in loading buffer (PBS, pH 7.4) with the proteins purified using GST columns (GE

LifeSciences) and eluted using 50 mM Tris, 10 mM Glutathione, pH 7.6. The purified GST-MMS2, GST-Ubc13, GST-E2-25K, GST-UbcH5b proteins were concentrated using 10 kDa MWCO Amicon concentrators and stored in 50 mM Tris, pH 8, in small aliquots at -80°C. GST-tag in UbcH5b was cleaved using thrombin protease at 4°C for 4 hrs. UbcH5b was further purified using size exclusion chromatography and exchanged into 50 mM Tris, 120 mM NaCl, pH 7.4 for NMR experiments.

7.2 Synthesis of polyubiquitin chains

K48- and K63-linked polyubiquitin chains were made using controlled-length chain assembly¹⁰² combined with domain-specific ¹⁵N isotope labeling¹⁰³. K11-linked polyubiquitin chains were generated enzymatically using ~15 mg each of the appropriate ¹⁵N enriched ubiquitin chain terminating mutants (example: ¹⁵N K11RK63R and D77, for generating ¹⁵N-distal labeled K11-Ub₂) in a 2 mL reaction in the presence of protein breakdown mix, 2 mM ATP, 3 mM TCEP, 100 nM E1, and 30 μM Ube2S/ Ube2SΔC, for 4 hrs at 37 °C. The reaction was quenched with 5 mM DTT or addition of glacial acetic acid to adjust the pH to 4.5. The efficiency of the reaction was checked on a 15% SDS-PAGE gel. Polyubiquitin chains were separated using cation chromatography on 5 mL HiTrap SPHP columns (GE LifeSciences) using a gradient of 50 mM Ammonium acetate, 1 M NaCl, pH 4.5. The chains were further purified using size exclusion chromatography and finally exchanged into 20 mM sodium phosphate, pH 6.8 for NMR studies.

7.3 Chemical shift perturbation mapping

Most of the NMR experiments were performed on a Bruker 600 MHz (a few experiments were performed on a Bruker 800 MHz) spectrometer equipped with a cryoprobe. Unless otherwise mentioned, most of the samples were prepared at pH 6.8 with 20 mM sodium phosphate buffer, 0.02% NaN₃, and 10% D₂O. CSPs were calculated as follows:

$$\Delta\delta = [(\Delta\delta_H)^2 + (\Delta\delta_N/5)^2]^{1/2}$$

Where $\Delta\delta_H$ and $\Delta\delta_N$ are the differences in the chemical shift for ¹H and ¹⁵N, respectively. Residues with significant CSPs are most likely to be involved in the formation of interdomain interface in the system described.

7.4 Determination of K_d by NMR titration experiments

Binding was monitored through NMR experiments carried out as a series of ¹⁵N SOFAST-HMQC experiments. 0.1-0.25 mM ¹⁵N labeled protein samples were titrated with increasing amounts of unlabeled ligand solution. Binding was monitored through changes in peak positions in ¹H-¹⁵N SOFAST-HMQC spectra and titrations were continued until very little or no chemical shift changes were observed. Combined amide chemical shifts were calculated as mentioned in section 7.3. The signal attenuation for each residue was calculated as a ratio of intensities between HMQC spectra in free and bound states. The apparent dissociation constants were calculated based on CSPs by fitting to different binding models using KDfit¹¹⁴.

7.5 Site-directed MTSL spin labeling experiments

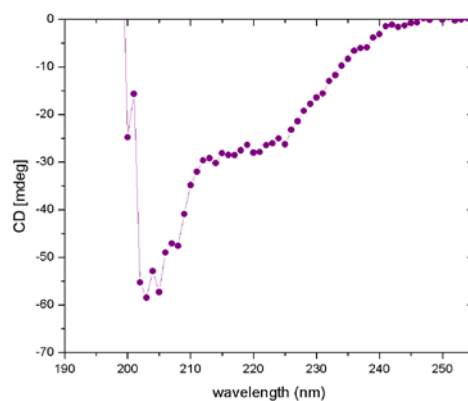
The paramagnetic spin label (1-oxy-2,2,5,5-tetramethyl-3-pyrroline-3-methyl) methane sulfonate (MTSL) was covalently attached to a single Cys residue at the desired position, introduced via site-directed mutagenesis. Spin labeling reactions were carried out at 20 mM sodium phosphate, pH 6.8 in ~3 molar excess of MTSL. MTSL stock is prepared in acetonitrile at 40 mM concentration. The reaction tube was incubated in the dark at 4 °C overnight (~12 hours). Unreacted MTSL was removed by buffer exchanging the protein into 20 mM sodium phosphate, pH 6.8, 5% D₂O and 0.02% NaN₃ for spin-labeling experiments in this study. The paramagnetic relaxation enhancement rate is dependent on the electron-nucleus distance, and therefore can be used to derive distance information. The PRE effects were quantitated as the ratio (I/I_0) of the signal intensities in the HSQC spectra recorded with MTSL in the oxidized and reduced states. The attenuations were used to calculate the location of the unpaired electron in MTSL using SLFIT¹⁰⁹.

Appendix

Table i Dissociation constants of various ubiquitin chains for epsin1 tUIMs
(Determined using NMR titration experiments)

Protein	Ligand	NaCl (mM)	K _d (μM)
¹⁵ N-K11RK63R Ub	epsin1 tUIMs (C-terminal GB1 fusion)	0	222 ± 61
¹⁵ N-D-K63 Ub ₂	epsin1 tUIMs (mutant with Cys at N- terminus)	0	27 ± 9
¹⁵ N-P-K11 Ub ₂	epsin1 tUIMs	130	330 ± 70
¹⁵ N-P-K63 Ub ₂	epsin1 tUIMs	130	197 ± 35
Ub[Ub]- ^{11,63} Ub (¹⁵ N)	epsin1 tUIMs	130	75 ± 30
Ub- ⁶³ Ub- ¹¹ Ub(¹⁵ N)	epsin1 tUIMs	130	229 ± 74

Figure i CD spectrum of epsin1 tUIMs- in 20 mM sodium phosphate, pH 6.8 indicates that the tUIMs have a helical component.



References

- (1) Ordureau, A., Münch, C., and Harper, J. W. (2015) Quantifying Ubiquitin Signaling. *Mol. Cell* 58, 660–676.
- (2) Weissman, A. M. (2001) Themes and variations on ubiquitylation. *Nat. Rev. Mol. Cell Biol.* 2, 169–178.
- (3) Hershko, A., and Ciechanover, A. (1998) The Ubiquitin System. *Annu. Rev. Biochem.* 67, 425–479.
- (4) Pickart, C. M., and Fushman, D. (2004) Polyubiquitin chains: polymeric protein signals. *Curr. Opin. Chem. Biol.* 8, 610–616.
- (5) Fushman, D., and Wilkinson, K. (2011) Structure and recognition of polyubiquitin chains of different lengths and linkage. *F1000 Biol. Rep.* 3.
- (6) Komander, D., and Rape, M. (2012) The Ubiquitin Code. *Annu. Rev. Biochem.* 81, 203–229.
- (7) Peng, J., Schwartz, D., Elias, J. E., Thoreen, C. C., Cheng, D., Marsischky, G., Roelofs, J., Finley, D., and Gygi, S. P. (2003) A proteomics approach to understanding protein ubiquitination. *Nat. Biotechnol.* 21, 921–926.
- (8) Xu, P., Duong, D. M., Seyfried, N. T., Cheng, D., Xie, Y., Robert, J., Rush, J., Hochstrasser, M., Finley, D., and Peng, J. (2009) Quantitative Proteomics Reveals the Function of Unconventional Ubiquitin Chains in Proteasomal Degradation. *Cell* 137, 133–145.
- (9) Dammer, E. B., Na, C. H., Xu, P., Seyfried, N. T., Duong, D. M., Cheng, D., Gearing, M., Rees, H., Lah, J. J., Levey, A. I., Rush, J., and Peng, J. (2011) Polyubiquitin linkage profiles in three models of proteolytic stress suggest the etiology of Alzheimer disease. *J. Biol. Chem.* 286, 10457–10465.
- (10) Castañeda, C. A., Chaturvedi, A., Camara, C. M., Curtis, J. E., Krueger, S., and Fushman, D. (2015) Linkage-specific conformational ensembles of non-canonical polyubiquitin chains. *Phys. Chem. Chem. Phys. PCCP*.
- (11) Scheffner, M., Nuber, U., and Huibregtse, J. M. (1995) Protein ubiquitination involving an E1–E2–E3 enzyme ubiquitin thioester cascade. *Nature* 373, 81–83.
- (12) Ye, Y., and Rape, M. (2009) Building ubiquitin chains: E2 enzymes at work. *Nat. Rev. Mol. Cell Biol.* 10, 755–764.
- (13) Berndsen, C. E., and Wolberger, C. (2014) New insights into ubiquitin E3 ligase mechanism. *Nat. Struct. Mol. Biol.* 21, 301–307.

- (14) Deshaies, R. J., and Joazeiro, C. A. P. (2009) RING Domain E3 Ubiquitin Ligases. *Annu. Rev. Biochem.* 78, 399–434.
- (15) Lipkowitz, S., and Weissman, A. M. (2011) RINGs of good and evil: RING finger ubiquitin ligases at the crossroads of tumour suppression and oncogenesis. *Nat. Rev. Cancer* 11, 629–643.
- (16) Metzger, M. B., Hristova, V. A., and Weissman, A. M. (2012) HECT and RING finger families of E3 ubiquitin ligases at a glance. *J Cell Sci* 125, 531–537.
- (17) Scheffner, M., and Kumar, S. (2014) Mammalian HECT ubiquitin-protein ligases: biological and pathophysiological aspects. *Biochim. Biophys. Acta* 1843, 61–74.
- (18) Spratt, D. E., Walden, H., and Shaw, G. S. (2014) RBR E3 ubiquitin ligases: new structures, new insights, new questions. *Biochem. J.* 458, 421–437.
- (19) Komander, D., Clague, M. J., and Urbé, S. (2009) Breaking the chains: structure and function of the deubiquitinases. *Nat. Rev. Mol. Cell Biol.* 10, 550–563.
- (20) Flotho, A., and Melchior, F. (2013) Sumoylation: A Regulatory Protein Modification in Health and Disease. *Annu. Rev. Biochem.* 82, 357–385.
- (21) Falaschetti, C.A., Mirkin, E.C., Raha, S., Paunesku, T., and Woloschak, G.E., (2011) The Ubiquitin-Proteasome System and DNA Repair, in *DNA Repair - On the Pathways to Fixing DNA Damage and Errors* (Storici, F., Ed.). InTech.
- (22) Hochstrasser, M. (2009) Origin and Function of Ubiquitin-like Protein Conjugation. *Nature* 458, 422.
- (23) Dahlmann, B. (2007) Role of proteasomes in disease. *BMC Biochem.* 8, S3.
- (24) Sun, T., Guo, J., Shallow, H., Yang, T., Xu, J., Li, W., Hanson, C., Wu, J. G., Li, X., Massaeli, H., and Zhang, S. (2011) The Role of Monoubiquitination in Endocytic Degradation of Human Ether-a-go-go-related Gene (hERG) Channels under Low K⁺ Conditions. *J. Biol. Chem.* 286, 6751–6759.
- (25) Haglund, K., Sigismund, S., Polo, S., Szymkiewicz, I., Di Fiore, P. P., and Dikic, I. (2003) Multiple monoubiquitination of RTKs is sufficient for their endocytosis and degradation. *Nat. Cell Biol.* 5, 461–466.
- (26) Chandrasekharan, M. B., Huang, F., and Sun, Z.-W. (2009) Ubiquitination of histone H2B regulates chromatin dynamics by enhancing nucleosome stability. *Proc. Natl. Acad. Sci.* 106, 16686–16691.

- (27) Xia, Z.-P., Sun, L., Chen, X., Pineda, G., Jiang, X., Adhikari, A., Zeng, W., and Chen, Z. J. (2009) Direct activation of protein kinases by unanchored polyubiquitin chains. *Nature* 461, 114–119.
- (28) Zeng, W., Sun, L., Jiang, X., Chen, X., Hou, F., Adhikari, A., Xu, M., and Chen, Z. J. (2010) Reconstitution of the RIG-I Pathway Reveals a Signaling Role of Unanchored Polyubiquitin Chains in Innate Immunity. *Cell* 141, 315–330.
- (29) Wu-Baer, F., Ludwig, T., and Baer, R. (2010) The UBXN1 Protein Associates with Autoubiquitinated Forms of the BRCA1 Tumor Suppressor and Inhibits Its Enzymatic Function. *Mol. Cell. Biol.* 30, 2787–2798.
- (30) Zhang, Z., Lv, X., Yin, W., Zhang, X., Feng, J., Wu, W., Hui, C., Zhang, L., and Zhao, Y. (2013) Ter94 ATPase complex targets k11-linked ubiquitinated ci to proteasomes for partial degradation. *Dev. Cell* 25, 636–644.
- (31) Bremm, A., and Komander, D. (2011) Emerging roles for Lys11-linked polyubiquitin in cellular regulation. *Trends Biochem. Sci.* 36, 355–363.
- (32) Arimoto, K., Funami, K., Saeki, Y., Tanaka, K., Okawa, K., Takeuchi, O., Akira, S., Murakami, Y., and Shimotohno, K. (2010) Polyubiquitin conjugation to NEMO by tripartite motif protein 23 (TRIM23) is critical in antiviral defense. *Proc. Natl. Acad. Sci.* 107, 15856–15861.
- (33) Birsá, N., Norkett, R., Wauer, T., Mevissen, T. E. T., Wu, H.-C., Foltyni, T., Bhatia, K., Hirst, W. D., Komander, D., Plun-Favreau, H., and Kittler, J. T. (2014) K27 ubiquitination of the mitochondrial transport protein Miro is dependent on serine 65 of the Parkin ubiquitin ligase. *J. Biol. Chem.* jbc.M114.563031.
- (34) Koegl, M., Hoppe, T., Schlenker, S., Ulrich, H. D., Mayer, T. U., and Jentsch, S. (1999) A Novel Ubiquitination Factor, E4, Is Involved in Multiubiquitin Chain Assembly. *Cell* 96, 635–644.
- (35) Johnson, E. S., Ma, P. C., Ota, I. M., and Varshavsky, A. (1995) A proteolytic pathway that recognizes ubiquitin as a degradation signal. *J. Biol. Chem.* 270, 17442–17456.
- (36) Fei, C., Li, Z., Li, C., Chen, Y., Chen, Z., He, X., Mao, L., Wang, X., Zeng, R., and Li, L. (2013) Smurf1-Mediated Lys29-Linked Nonproteolytic Polyubiquitination of Axin Negatively Regulates Wnt/ β -Catenin Signaling. *Mol. Cell. Biol.* 33, 4095–4105.
- (37) Zhou, H.-L., Geng, C., Luo, G., and Lou, H. (2013) The p97–UBXD8 complex destabilizes mRNA by promoting release of ubiquitinated HuR from mRNP. *Genes Dev.* 27, 1046–1058.

- (38) Huang, H., Jeon, M., Liao, L., Yang, C., Elly, C., Yates III, J. R., and Liu, Y.-C. (2010) K33-Linked Polyubiquitination of T Cell Receptor- ζ Regulates Proteolysis-Independent T Cell Signaling. *Immunity* 33, 60–70.
- (39) Al-Hakim, A. K., Zagorska, A., Chapman, L., Deak, M., Pegg, M., and Alessi, D. R. (2008) Control of AMPK-related kinases by USP9X and atypical Lys29/Lys33-linked polyubiquitin chains. *Biochem. J.* 411, 249–260.
- (40) Yuan, W.-C., Lee, Y.-R., Lin, S.-Y., Chang, L.-Y., Tan, Y. P., Hung, C.-C., Kuo, J.-C., Liu, C.-H., Lin, M.-Y., Xu, M., Chen, Z. J., and Chen, R.-H. (2014) K33-Linked Polyubiquitination of Coronin 7 by Cul3-KLHL20 Ubiquitin E3 Ligase Regulates Protein Trafficking. *Mol. Cell* 54, 586–600.
- (41) Kristariyanto, Y. A., Choi, S.-Y., Rehman, S. A. A., Ritorto, M. S., Campbell, D. G., Morrice, N. A., Toth, R., and Kulathu, Y. (2015) Assembly and structure of Lys33-linked polyubiquitin reveals distinct conformations. *Biochem. J.* 467, 345–352.
- (42) Chau, V., Tobias, J. W., Bachmair, A., Marriott, D., Ecker, D. J., Gonda, D. K., and Varshavsky, A. (1989) A multiubiquitin chain is confined to specific lysine in a targeted short-lived protein. *Science* 243, 1576–1583.
- (43) Finley, D., Sadis, S., Monia, B. P., Boucher, P., Ecker, D. J., Crooke, S. T., and Chau, V. (1994) Inhibition of proteolysis and cell cycle progression in a multiubiquitination-deficient yeast mutant. *Mol. Cell. Biol.* 14, 5501–5509.
- (44) Hofmann, R. M., and Pickart, C. M. (1999) Noncanonical MMS2-encoded ubiquitin-conjugating enzyme functions in assembly of novel polyubiquitin chains for DNA repair. *Cell* 96, 645–653.
- (45) Deng, L., Wang, C., Spencer, E., Yang, L., Braun, A., You, J., Slaughter, C., Pickart, C., and Chen, Z. J. (2000) Activation of the I κ B kinase complex by TRAF6 requires a dimeric ubiquitin-conjugating enzyme complex and a unique polyubiquitin chain. *Cell* 103, 351–361.
- (46) Chen, Z. J., and Sun, L. J. (2009) Nonproteolytic Functions of Ubiquitin in Cell Signaling. *Mol. Cell* 33, 275–286.
- (47) Tokunaga, F., Sakata, S., Saeki, Y., Satomi, Y., Kirisako, T., Kamei, K., Nakagawa, T., Kato, M., Murata, S., Yamaoka, S., Yamamoto, M., Akira, S., Takao, T., Tanaka, K., and Iwai, K. (2009) Involvement of linear polyubiquitylation of NEMO in NF- κ B activation. *Nat. Cell Biol.* 11, 123–132.
- (48) Dynek, J. N., Goncharov, T., Dueber, E. C., Fedorova, A. V., Izrael-Tomasevic, A., Phu, L., Helgason, E., Fairbrother, W. J., Deshayes, K., Kirkpatrick, D. S., and Vucic, D. (2010) c-IAP1 and UbH5 promote K11-linked polyubiquitination of RIP1 in TNF signalling. *EMBO J.* 29, 4198–4209.

- (49) Boname, J. M., Thomas, M., Stagg, H. R., Xu, P., Peng, J., and Lehner, P. J. (2010) Efficient internalization of MHC I requires lysine-11 and lysine-63 mixed linkage polyubiquitin chains. *Traffic Cph. Den.* 11, 210–220.
- (50) Meyer, H.-J., and Rape, M. (2014) Enhanced Protein Degradation by Branched Ubiquitin Chains. *Cell* 157, 910–921.
- (51) Ciechanover, A., and Ben-Saadon, R. (2004) N-terminal ubiquitination: more protein substrates join in. *Trends Cell Biol.* 14, 103–106.
- (52) Goldberg, A. L., Cascio, P., Saric, T., and Rock, K. L. (2002) The importance of the proteasome and subsequent proteolytic steps in the generation of antigenic peptides. *Mol. Immunol.* 39, 147–164.
- (53) Bhattacharyya, S., Yu, H., Mim, C., and Matouschek, A. (2014) Regulated protein turnover: snapshots of the proteasome in action. *Nat. Rev. Mol. Cell Biol.* 15, 122–133.
- (54) Finley, D. (2009) Recognition and Processing of Ubiquitin-Protein Conjugates by the Proteasome. *Annu. Rev. Biochem.* 78, 477–513.
- (55) Sloper-Mould, K. E., Jemc, J. C., Pickart, C. M., and Hicke, L. (2001) Distinct functional surface regions on ubiquitin. *J. Biol. Chem.* 276, 30483–30489.
- (56) Jin, L., Williamson, A., Banerjee, S., Philipp, I., and Rape, M. (2008) Mechanism of ubiquitin-chain formation by the human anaphase-promoting complex. *Cell* 133, 653–665.
- (57) Matsumoto, M. L., Wickliffe, K. E., Dong, K. C., Yu, C., Bosanac, I., Bustos, D., Phu, L., Kirkpatrick, D. S., Hymowitz, S. G., Rape, M., Kelley, R. F., and Dixit, V. M. (2010) K11-linked polyubiquitination in cell cycle control revealed by a K11 linkage-specific antibody. *Mol. Cell* 39, 477–484.
- (58) Williamson, A., Wickliffe, K. E., Mellone, B. G., Song, L., Karpen, G. H., and Rape, M. (2009) Identification of a physiological E2 module for the human anaphase-promoting complex. *Proc. Natl. Acad. Sci. U. S. A.* 106, 18213–18218.
- (59) Saeki, Y., Kudo, T., Sone, T., Kikuchi, Y., Yokosawa, H., Toh-e, A., and Tanaka, K. (2009) Lysine 63-linked polyubiquitin chain may serve as a targeting signal for the 26S proteasome. *EMBO J.* 28, 359–371.
- (60) Kim, H. T., Kim, K. P., Lledias, F., Kisselev, A. F., Scaglione, K. M., Skowyra, D., Gygi, S. P., and Goldberg, A. L. (2007) Certain pairs of ubiquitin-conjugating enzymes (E2s) and ubiquitin-protein ligases (E3s) synthesize nondegradable forked ubiquitin chains containing all possible isopeptide linkages. *J. Biol. Chem.* 282, 17375–17386.

- (61) Kirkpatrick, D. S., Hathaway, N. A., Hanna, J., Elsasser, S., Rush, J., Finley, D., King, R. W., and Gygi, S. P. (2006) Quantitative analysis of in vitro ubiquitinated cyclin B1 reveals complex chain topology. *Nat. Cell Biol.* 8, 700–710.
- (62) Zhang, D., Chen, T., Ziv, I., Rosenzweig, R., Matiuhin, Y., Bronner, V., Glickman, M. H., and Fushman, D. (2009) Together, Rpn10 and Dsk2 can serve as a polyubiquitin chain-length sensor. *Mol. Cell* 36, 1018–1033.
- (63) Husnjak, K., Elsasser, S., Zhang, N., Chen, X., Randles, L., Shi, Y., Hofmann, K., Walters, K. J., Finley, D., and Dikic, I. (2008) Proteasome subunit Rpn13 is a novel ubiquitin receptor. *Nature* 453, 481–488.
- (64) Mukhopadhyay, D., and Riezman, H. (2007) Proteasome-independent functions of ubiquitin in endocytosis and signaling. *Science* 315, 201–205.
- (65) Bienko, M., Green, C. M., Sabbioneda, S., Crosetto, N., Matic, I., Hibbert, R. G., Begovic, T., Niimi, A., Mann, M., Lehmann, A. R., and Dikic, I. (2010) Regulation of translesion synthesis DNA polymerase η by monoubiquitination. *Mol. Cell* 37, 396–407.
- (66) Mailand, N., Gibbs-Seymour, I., and Bekker-Jensen, S. (2013) Regulation of PCNA-protein interactions for genome stability. *Nat. Rev. Mol. Cell Biol.* 14, 269–282.
- (67) Kim, H., Chen, J., and Yu, X. (2007) Ubiquitin-Binding Protein RAP80 Mediates BRCA1-Dependent DNA Damage Response. *Science* 316, 1202–1205.
- (68) Wang, B., Matsuoka, S., Ballif, B. A., Zhang, D., Smogorzewska, A., Gygi, S. P., and Elledge, S. J. (2007) Abraxas and RAP80 Form a BRCA1 Protein Complex Required for the DNA Damage Response. *Science* 316, 1194–1198.
- (69) Sobhian, B., Shao, G., Lilli, D. R., Culhane, A. C., Moreau, L. A., Xia, B., Livingston, D. M., and Greenberg, R. A. (2007) RAP80 Targets BRCA1 to Specific Ubiquitin Structures at DNA Damage Sites. *Science* 316, 1198–1202.
- (70) Winston, J. T., Strack, P., Beer-Romero, P., Chu, C. Y., Elledge, S. J., and Harper, J. W. (1999) The SCF β -TRCP-ubiquitin ligase complex associates specifically with phosphorylated destruction motifs in I κ B α and β -catenin and stimulates I κ B α ubiquitination in vitro. *Genes Dev.* 13, 270–283.
- (71) Palombella, V. J., Rando, O. J., Goldberg, A. L., and Maniatis, T. (1994) The ubiquitin-proteasome pathway is required for processing the NF- κ B1 precursor protein and the activation of NF- κ B. *Cell* 78, 773–785.

- (72) Plafker, S. M., Plafker, K. S., Weissman, A. M., and Macara, I. G. (2004) Ubiquitin charging of human class III ubiquitin-conjugating enzymes triggers their nuclear import. *J. Cell Biol.* 167, 649–659.
- (73) Li, M., Brooks, C. L., Wu-Baer, F., Chen, D., Baer, R., and Gu, W. (2003) Mono- versus polyubiquitination: differential control of p53 fate by Mdm2. *Science* 302, 1972–1975.
- (74) Beal, R., Deveraux, Q., Xia, G., Rechsteiner, M., and Pickart, C. (1996) Surface hydrophobic residues of multiubiquitin chains essential for proteolytic targeting. *Proc. Natl. Acad. Sci. U. S. A.* 93, 861–866.
- (75) Husnjak, K., and Dikic, I. (2012) Ubiquitin-binding proteins: decoders of ubiquitin-mediated cellular functions. *Annu. Rev. Biochem.* 81, 291–322.
- (76) Nowicka, U., Zhang, D., Walker, O., Krutauz, D., Castañeda, C. A., Chaturvedi, A., Chen, T. Y., Reis, N., Glickman, M. H., and Fushman, D. (2015) DNA-damage-inducible 1 protein (Ddi1) contains an uncharacteristic ubiquitin-like domain that binds ubiquitin. *Structure*, 542–557.
- (77) Kang, R. S., Daniels, C. M., Francis, S. A., Shih, S. C., Salerno, W. J., Hicke, L., and Radhakrishnan, I. (2003) Solution Structure of a CUE-Ubiquitin Complex Reveals a Conserved Mode of Ubiquitin Binding. *Cell* 113, 621–630.
- (78) Fisher, R. D., Wang, B., Alam, S. L., Higginson, D. S., Robinson, H., Sundquist, W. I., and Hill, C. P. (2003) Structure and ubiquitin binding of the ubiquitin-interacting motif. *J. Biol. Chem.* 278, 28976–28984.
- (79) Alam, S. L., Sun, J., Payne, M., Welch, B. D., Blake, B. K., Davis, D. R., Meyer, H. H., Emr, S. D., and Sundquist, W. I. (2004) Ubiquitin interactions of NZF zinc fingers. *EMBO J.* 23, 1411–1421.
- (80) Kaiser, S. E., Riley, B. E., Shaler, T. A., Trevino, R. S., Becker, C. H., Schulman, H., and Kopito, R. R. (2011) Protein standard absolute quantification (PSAQ) method for the measurement of cellular ubiquitin pools. *Nat. Methods* 8, 691–696.
- (81) Di Fiore, P. P., Polo, S., and Hofmann, K. (2003) When ubiquitin meets ubiquitin receptors: a signalling connection. *Nat. Rev. Mol. Cell Biol.* 4, 491–497.
- (82) Does, M. R., Schnell, J. D., Maldonado-Baez, L., Wendland, B., and Hicke, L. (2010) The function of yeast epsin and Ede1 ubiquitin-binding domains during receptor internalization. *Traffic Cph. Den.* 11, 151–160.

- (83) Sigismund, S., Woelk, T., Puri, C., Maspero, E., Tacchetti, C., Transidico, P., Di Fiore, P. P., and Polo, S. (2005) Clathrin-independent endocytosis of ubiquitinated cargos. *Proc. Natl. Acad. Sci. U. S. A.* 102, 2760–2765.
- (84) Sims, J. J., and Cohen, R. E. (2009) Linkage-specific avidity defines the lysine 63-linked polyubiquitin-binding preference of rap80. *Mol. Cell* 33, 775–783.
- (85) Tyrrell, A., Flick, K., Kleiger, G., Zhang, H., Deshaies, R. J., and Kaiser, P. (2010) Physiologically relevant and portable tandem ubiquitin-binding domain stabilizes polyubiquitylated proteins. *Proc. Natl. Acad. Sci. U. S. A.* 107, 19796–19801.
- (86) Kaiser, P., Flick, K., Wittenberg, C., and Reed, S. I. (2000) Regulation of transcription by ubiquitination without proteolysis: Cdc34/SCF(Met30)-mediated inactivation of the transcription factor Met4. *Cell* 102, 303–314.
- (87) Dikic, I., Wakatsuki, S., and Walters, K. J. (2009) Ubiquitin-binding domains — from structures to functions. *Nat. Rev. Mol. Cell Biol.* 10, 659–671.
- (88) Varadan, R., Assfalg, M., Raasi, S., Pickart, C., and Fushman, D. (2005) Structural Determinants for Selective Recognition of a Lys48-Linked Polyubiquitin Chain by a UBA Domain. *Mol. Cell* 18, 687–698.
- (89) Schlessinger, J. (2000) Cell Signaling by Receptor Tyrosine Kinases. *Cell* 103, 211–225.
- (90) Sorkin, A., and von Zastrow, M. (2009) Endocytosis and signalling: intertwining molecular networks. *Nat. Rev. Mol. Cell Biol.* 10, 609–622.
- (91) Haglund, K., and Dikic, I. (2012) The role of ubiquitylation in receptor endocytosis and endosomal sorting. *J Cell Sci* 125, 265–275.
- (92) Raiborg, C., and Stenmark, H. (2009) The ESCRT machinery in endosomal sorting of ubiquitylated membrane proteins. *Nature* 458, 445–452.
- (93) Hurley, J. H., and Hanson, P. I. (2010) Membrane budding and scission by the ESCRT machinery: it's all in the neck. *Nat. Rev. Mol. Cell Biol.* 11, 556–566.
- (94) Tessneer, K. L., Cai, X., Pasula, S., Dong, Y., Liu, X., Chang, B., McManus, J., Hahn, S., Yu, L., and Chen, H. (2013) Epsin Family of Endocytic Adaptor Proteins as Oncogenic Regulators of Cancer Progression. *J. Cancer Res. Updat.* 2, 144–150.
- (95) Mukherjee, D., Coon, B. G., Edwards, D. F., Hanna, C. B., Longhi, S. A., McCaffery, J. M., Wendland, B., Retegui, L. A., Bi, E., and Aguilar, R. C. (2009) The yeast endocytic protein Epsin 2 functions in a cell-division signaling pathway. *J Cell Sci* 122, 2453–2463.

- (96) Hawryluk, M. J., Keyel, P. A., Mishra, S. K., Watkins, S. C., Heuser, J. E., and Traub, L. M. (2006) Epsin 1 is a Polyubiquitin-Selective Clathrin-Associated Sorting Protein. *Traffic* 7, 262–281.
- (97) Tessneer, K. L., Pasula, S., Cai, X., Dong, Y., Liu, X., Yu, L., Hahn, S., McManus, J., Chen, Y., Chang, B., and Chen, H. (2013) Endocytic adaptor protein epsin is elevated in prostate cancer and required for cancer progression. *ISRN Oncol.* 2013, 420597.
- (98) Goto, E., Yamanaka, Y., Ishikawa, A., Aoki-Kawasumi, M., Mito-Yoshida, M., Ohmura-Hoshino, M., Matsuki, Y., Kajikawa, M., Hirano, H., and Ishido, S. (2010) Contribution of Lysine 11-linked Ubiquitination to MIR2-mediated Major Histocompatibility Complex Class I Internalization. *J. Biol. Chem.* 285, 35311–35319.
- (99) Varadan, R. (2004) Dissertation- NMR studies of polyubiquitin chains: insights into structural basis of functional diversity.
- (100) Nakasone, M. A., Livnat-Levanon, N., Glickman, M. H., Cohen, R. E., and Fushman, D. (2013) Mixed-linkage ubiquitin chains send mixed messages. *Structure*, 727–740.
- (101) Ben-Saadon, R., Zaaroor, D., Ziv, T., and Ciechanover, A. (2006) The polycomb protein Ring1B generates self atypical mixed ubiquitin chains required for its in vitro histone H2A ligase activity. *Mol. Cell* 24, 701–711.
- (102) Pickart, C. M., and Raasi, S. (2005) Controlled synthesis of polyubiquitin chains. *Methods Enzymol.* 399, 21–36.
- (103) Varadan, R., Walker, O., Pickart, C., and Fushman, D. (2002) Structural properties of polyubiquitin chains in solution. *J. Mol. Biol.* 324, 637–647.
- (104) Huang, F., Zeng, X., Kim, W., Balasubramani, M., Fortian, A., Gygi, S. P., Yates, N. A., and Sorkin, A. (2013) Lysine 63-linked polyubiquitination is required for EGF receptor degradation. *Proc. Natl. Acad. Sci.* 110, 15722–15727.
- (105) Castañeda, C. A., Kashyap, T. R., Nakasone, M. A., Krueger, S., and Fushman, D. (2013) Unique structural, dynamical, and functional properties of K11-linked polyubiquitin chains. *Structure*, 1168–1181.
- (106) Lange, A., Castañeda, C., Hoeller, D., Lancelin, J.-M., Fushman, D., and Walker, O. (2012) Evidence for cooperative and domain-specific binding of the signal transducing adaptor molecule 2 (STAM2) to Lys63-linked diubiquitin. *J. Biol. Chem.* 287, 18687–18699.

- (107) Sugiyama, S., Kishida, S., Chayama, K., Koyama, S., and Kikuchi, A. (2005) Ubiquitin-Interacting Motifs of Epsin Are Involved in the Regulation of Insulin-Dependent Endocytosis. *J. Biochem. (Tokyo)* 137, 355–364.
- (108) Sato, Y., Yoshikawa, A., Mimura, H., Yamashita, M., Yamagata, A., and Fukai, S. (2009) Structural basis for specific recognition of Lys 63-linked polyubiquitin chains by tandem UIMs of RAP80. *EMBO J.* 28, 2461–2468.
- (109) Ryabov, Y., and Fushman, D. (2006) Interdomain mobility in di-ubiquitin revealed by NMR. *Proteins* 63, 787–796.
- (110) Notredame, C., Higgins, D. G., and Heringa, J. (2000) T-Coffee: A novel method for fast and accurate multiple sequence alignment. *J. Mol. Biol.* 302, 205–217.
- (111) Sinha, N., and Smith-Gill, S. J. (2002) Electrostatics in protein binding and function. *Curr. Protein Pept. Sci.* 3, 601–614.
- (112) Castañeda, C., Liu, J., Chaturvedi, A., Nowicka, U., Cropp, T. A., and Fushman, D. (2011) Nonenzymatic assembly of natural polyubiquitin chains of any linkage composition and isotopic labeling scheme. *J. Am. Chem. Soc.* 133, 17855–17868.
- (113) Bremm, A., Freund, S. M. V., and Komander, D. (2010) Lys11-linked ubiquitin chains adopt compact conformations and are preferentially hydrolyzed by the deubiquitinase Cezanne. *Nat. Struct. Mol. Biol.* 17, 939–947.
- (114) Varadan, R., Assfalg, M., Haririnia, A., Raasi, S., Pickart, C., and Fushman, D. (2004) Solution conformation of Lys63-linked di-ubiquitin chain provides clues to functional diversity of polyubiquitin signaling. *J. Biol. Chem.* 279, 7055–7063.
- (115) Vousden, K. H., and Prives, C. (2009) Blinded by the Light: The Growing Complexity of p53. *Cell* 137, 413–431.
- (116) Marine, J.-C., and Lozano, G. (2010) Mdm2-mediated ubiquitylation: p53 and beyond. *Cell Death Differ.* 17, 93–102.
- (117) Wade, M., and Wahl, G. M. (2009) Targeting Mdm2 and Mdmx in cancer therapy: better living through medicinal chemistry? *Mol. Cancer Res. MCR* 7, 1–11.
- (118) Ozenne, P., Eymin, B., Brambilla, E., and Gazzeri, S. (2010) The ARF tumor suppressor: structure, functions and status in cancer. *Int. J. Cancer J. Int. Cancer* 127, 2239–2247.

- (119) Saporita, A. J., Maggi, L. B., Apicelli, A. J., and Weber, J. D. (2007) Therapeutic targets in the ARF tumor suppressor pathway. *Curr. Med. Chem.* 14, 1815–1827.
- (120) Lohrum, M. A., Ashcroft, M., Kubbutat, M. H., and Vousden, K. H. (2000) Identification of a cryptic nucleolar-localization signal in MDM2. *Nat. Cell Biol.* 2, 179–181.
- (121) Weber, J. D., Kuo, M. L., Bothner, B., DiGiammarino, E. L., Kriwacki, R. W., Roussel, M. F., and Sherr, C. J. (2000) Cooperative signals governing ARF-mdm2 interaction and nucleolar localization of the complex. *Mol. Cell. Biol.* 20, 2517–2528.
- (122) Linke, K., Mace, P. D., Smith, C. A., Vaux, D. L., Silke, J., and Day, C. L. (2008) Structure of the MDM2/MDMX RING domain heterodimer reveals dimerization is required for their ubiquitylation in trans. *Cell Death Differ.* 15, 841–848.
- (123) Jensen, J. P., Bates, P. W., Yang, M., Vierstra, R. D., and Weissman, A. M. (1995) Identification of a Family of Closely Related Human Ubiquitin Conjugating Enzymes. *J. Biol. Chem.* 270, 30408–30414.
- (124) Saville, M. K., Sparks, A., Xirodimas, D. P., Wardrop, J., Stevenson, L. F., Bourdon, J.-C., Woods, Y. L., and Lane, D. P. (2004) Regulation of p53 by the ubiquitin-conjugating enzymes UbcH5B/C in vivo. *J. Biol. Chem.* 279, 42169–42181.
- (125) Haririnia, A., D’Onofrio, M., and Fushman, D. (2007) Mapping the interactions between Lys48 and Lys63-linked di-ubiquitins and a ubiquitin-interacting motif of S5a. *J. Mol. Biol.* 368, 753–766.
- (126) Brzovic, P. S., Lissounov, A., Christensen, D. E., Hoyt, D. W., and Klevit, R. E. (2006) A UbcH5/ubiquitin noncovalent complex is required for processive BRCA1-directed ubiquitination. *Mol. Cell* 21, 873–880.
- (127) Zheng, N., Wang, P., Jeffrey, P. D., and Pavletich, N. P. (2000) Structure of a c-Cbl-UbcH7 Complex: RING Domain Function in Ubiquitin-Protein Ligases. *Cell* 102, 533–539.
- (128) Poyurovsky, M. V., Priest, C., Kentsis, A., Borden, K. L. B., Pan, Z.-Q., Pavletich, N., and Prives, C. (2007) The Mdm2 RING domain C-terminus is required for supramolecular assembly and ubiquitin ligase activity. *EMBO J.* 26, 90–101.
- (129) Wade, M., Li, Y.-C., and Wahl, G. M. (2013) MDM2, MDMX and p53 in oncogenesis and cancer therapy. *Nat. Rev. Cancer* 13, 83–96.

- (130) Kostic, M., Matt, T., Martinez-Yamout, M. A., Dyson, H. J., and Wright, P. E. (2006) Solution structure of the Hdm2 C2H2C4 RING, a domain critical for ubiquitination of p53. *J. Mol. Biol.* 363, 433–450.
- (131) Holmgren, A., and Lu, J. (2010) Thioredoxin and thioredoxin reductase: current research with special reference to human disease. *Biochem. Biophys. Res. Commun.* 396, 120–124.
- (132) Powis, G., and Montfort, W. R. (2001) Properties and biological activities of thioredoxins. *Annu. Rev. Biophys. Biomol. Struct.* 30, 421–455.
- (133) García-Giménez, J. L., Seco-Cervera, M., Aguado, C., Romá-Mateo, C., Dasí, F., Priego, S., Markovic, J., Knecht, E., Sanz, P., and Pallardó, F. V. (2013) Lafora disease fibroblasts exemplify the molecular interdependence between thioredoxin 1 and the proteasome in mammalian cells. *Free Radic. Biol. Med.* 65, 347–359.
- (134) Bernal-Bayard, J., and Ramos-Morales, F. (2009) Salmonella type III secretion effector SlrP is an E3 ubiquitin ligase for mammalian thioredoxin. *J. Biol. Chem.* 284, 27587–27595.
- (135) Fritz-Wolf, K., Kehr, S., Stumpf, M., Rahlfs, S., and Becker, K. (2011) Crystal structure of the human thioredoxin reductase-thioredoxin complex. *Nat. Commun.* 2, 383.
- (136) Gasdaska, J. R., Kirkpatrick, D. L., Montfort, W., Kuperus, M., Hill, S. R., Berggren, M., and Powis, G. (1996) Oxidative inactivation of thioredoxin as a cellular growth factor and protection by a Cys73-->Ser mutation. *Biochem. Pharmacol.* 52, 1741–1747.
- (137) Forman-Kay, J. D., Clore, G. M., Driscoll, P. C., Wingfield, P., Richards, F. M., and Gronenborn, A. M. (1989) A proton nuclear magnetic resonance assignment and secondary structure determination of recombinant human thioredoxin. *Biochemistry (Mosc.)* 28, 7088–7097.
- (138) Singh, R. K., Sundar, A., and Fushman, D. (2014) Nonenzymatic rubylation and ubiquitination of proteins for structural and functional studies. *Angew. Chem. Int. Ed Engl.* 53, 6120–6125.
- (139) Cocklin, R., Heyen, J., Larry, T., Tyers, M., and Goebel, M. (2011) New insight into the role of the Cdc34 ubiquitin-conjugating enzyme in cell cycle regulation via Ace2 and Sic1. *Genetics* 187, 701–715.
- (140) Doris, K. S., Rumsby, E. L., and Morgan, B. A. (2012) Oxidative stress responses involve oxidation of a conserved ubiquitin pathway enzyme. *Mol. Cell. Biol.* 32, 4472–4481.

- (141) Hospenthal, M. K., Freund, S. M. V., and Komander, D. (2013) Assembly, analysis and architecture of atypical ubiquitin chains. *Nat. Struct. Mol. Biol.* 20, 555–565.
- (142) Dong, K. C., Helgason, E., Yu, C., Phu, L., Arnott, D. P., Bosanac, I., Compaan, D. M., Huang, O. W., Fedorova, A. V., Kirkpatrick, D. S., Hymowitz, S. G., and Dueber, E. C. (2011) Preparation of distinct ubiquitin chain reagents of high purity and yield. *Structure*, 1053–1063.